Visualization of Power Systems and Components

Final Project Report

Power Systems Engineering Research Center

A National Science Foundation
Industry/University Cooperative Research Center
since 1996

Power Systems Engineering Research Center

Visualization of Power Systems and Components

Final Report

Thomas. J. Overbye, Project Leader
University of Illinois at Urbana-Champaign (UIUC)

Project Team Members

A. P. Meliopoulos (Georgia Tech)
David. A. Wiegmann (UIUC)
George J. Cokkinides (Georgia Tech)

Research Team Students
Matt Davis, UIUC
George Stefopoulos, Georgia Institute of Technology
Yan Sun, UIUC

PSERC Publication 05-65

November 2005

Information about this Project

For information about this project contact:

Tom Overbye
University of Illinois at Urbana-Champaign
Department of Electrical and Computer Engineering
1406 W. Green St.
Urbana, IL 61801
Phone: 217 333 4463
Fax: 217 333 1162
Email: overbye@ece.uiuc.edu

Power Systems Engineering Research Center

This is a project report from the Power Systems Engineering Research Center (PSERC). PSERC is a multi-university Center conducting research on challenges facing the electric power industry and educating the next generation of power engineers. More information about PSERC can be found at the Center's website: http://www.pserc.org.

For additional information, contact:

Power Systems Engineering Research Center
Cornell University
428 Phillips Hall
Ithaca, New York 14853
Phone: 607-255-5601
Fax: 607-255-8871

Notice Concerning Copyright Material

Acknowledgements

The work described in this report was sponsored by the Power Systems Engineering Research Center (PSERC) and the U.S. DOE through its Consortium for Electric Reliability Technology Solutions (CERTS) program. We express our appreciation for the support provided by PSERC's industrial members, by the National Science Foundation under grant NSF EEC-0120153 received under the Industry/University Cooperative Research Center program, and by the U.S. DOE CERTS program. We also thank the many industrial advisors who helped to contribute to the success of this project, as well as the University of Illinois at Urbana-Champaign students who participated in the human factors experiments.

Executive Summary

The need for enhanced power system visualizations has been increasingly acute over the last decade as the size of power system models has grown. For example, North America planning power flow models can have more than 44,000 buses, and state estimator models can have even more nodes. And with the development of competitive, optimal power flow (OPF) based electricity markets, new study variables (such as locational marginal prices) have increased as well. Finally, large-scale blackouts around the world recent have dramatically demonstrated how a lack of operational "situational awareness" can put millions in the dark. Our research shows that good visualization techniques improves the efficiency of operator response to power system problems.

As the electricity industry becomes increasingly competitive, knowledge concerning the capacity and constraints of the electric system will become a commodity of great value. In an environment where electricity markets can be fast changing, participants can obtain a competitive advantage by understanding the implications of these changes before others. One goal of this project was to develop innovative methods to assist players in the electricity industry to extract and visualize this knowledge from the large set of power system data. The project explored the visualization of data macroscopically and microscopically, i.e., visualization of the power system as a whole as well as individual power system elements.

This report, along with the related publications, present results from the PSERC "Visualization of Power Systems and Components" project. The research focused on (1) the development and/or enhancement of techniques for visualizing power system information, (2) the development of techniques for visualizing power system component information, and (3) performing human factors experiments and analysis on the visualizations developed in the project.

The specific results from the project can be grouped into four areas. First, the project developed enhanced two-dimensional (2D) power system visualizations. A key accomplishment in this area was demonstrating how selective filtering of power system one-lines can be helpful in focusing attention on particular elements of a one-line. The project also demonstrated how gauges could be used on one-lines for reactive power visualization, and how contouring could be used for showing net bus power injections.

Second, the project demonstrated how three-dimensional (3D) visualizations could be used to display contingency analysis bus voltage magnitude information and transmission line/transformer flow information. The desirable functionalities of such visualizations include showing the overall system security status, showing the severity levels of the contingencies in terms of their associated limit violations, and showing the geographic connection between the violated elements and the contingent elements. The traditional EMS display of contingency analysis results is a tabular list of contingencies with their associated limit violations. While this may be sufficient during routine operation, this tabular list can get quite long during system emergencies. The project demonstrated the use of 3D displays to show the geographic relationships between the contingencies causing violations and the violated elements. This allows the overall contingency analysis results for a system to be conveyed "at a glace." Such displays could be used to supplement the traditional tabular displays.

Third, the project demonstrated how system wide overview visualizations could be supplemented with visualizations of the detailed status and operating conditions of important power system devices. The project considered two devices: generators and transformers. For

both the project presents appropriate models for the devices, and then shows how 3D visualizations can be used to show device values. For generators 3D visualized quantities included magnetic fields and temperatures, while the transformer visualizations show temperature.

Last, the project focused on the performance of formal human factor experiments to evaluate the effectiveness of power system visualizations. In particular, the project looked at the use of pie charts to visualize line flow, animated visualization of transmission line flows, animated visualization of power transfer distribution factors (PTDFs), and the use of 3D to show generator real power outputs. The key results were 1) the use of pie charts did not improve overall solution times but did result in solutions with fewer errors, 2) for line violations the use of animated arrows improved solution time and accuracy for contingencies causing multiple violations, 3) the use of pie charts with animated arrows resulted in better results than either alone, 4) the use of animated arrows for PTDF visualization results in quicker and more accurate task completion, and 5) the visualization of 3D generators results in quicker and more accurate task completion compared to comparable 2D visualizations. All experiments were performed using University of Illinois Electrical and Computer Engineering students.

We believe this project has made significant advances in the area of power system visualization. Visualization can also play a crucial role in reducing the risk of future blackouts by helping operators to quickly assess a potentially rapidly changing system state, and by helping them to formulate corrective control actions. This research project has developed several new methods that could be quite useful for the representation of this data both at a system level and at a component level, performed formal human factors experiments to test the effectiveness of several of these techniques, and assisted in the actual implementation of research results in various control centers.

Nevertheless, significant challenges remain. Key challenges include the problem of wide-area visualization of all pertinent system quantities, the incorporation of new system measurements into the visualizations such as those from phasor measurement units and substation IEDs (intelligent electronic devices), the visualization of time-varying system information, the integration of enhanced visualization into existing EMS applications such as alarming, and further work on component level visualization. Hence while we believe we have made significant progress over the course of this research project, more research is certainly needed to develop better methods for visualizing this data, performing human factors assessments on these new techniques, and rapidly transferring the results to industry.

Table of Contents

Table of Contents (continued)

List of Figures

List of Figures (continued)

List of Tables

Visualization of Power Systems and Components

1 Introduction

The rationale for electric power system visualization is found in the saying, "a picture is worth a thousand words." The goal of computer visualization is to use computer generated images to convey information that would otherwise require a thousand or more words, or more germane to electric power systems, a thousand or more numbers. With the visualizations patterns are revealed and underlying relationships exposed. Not that words or numbers are bad. They certainly have their place, and often times it is primary. But so do images, especially when the transmission system is involved.

The need for enhanced power system visualizations has been increasingly acute over the last decade as the size of power system models has grown. Now in North America some planning power flow models have more than 44,000 buses, and some state estimator models even more nodes. And with the development of competitive, optimal power flow (OPF) based electricity markets the number of study variables has increased as well. For example, the bus-based locational marginal prices (LMPs) now needed to be considered in many studies. Finally, around the world the recent large-scale blackouts have dramatically demonstrated how a lack of operational "situational awareness" can put millions in the dark.

While the term "power system visualization" is somewhat generic, a good working definition is "a method for presenting large amounts (10^2 – 10^6) of information (or data) in an interactive, graphical form in which the information is related by an underlying power system." Power system visualization is contained within the general "information visualization" field but is a unique subfield due to the impact of the underlying power system. Most of the research focus in this subfield has been directed towards the display of information associated with many electric substations, a topic known as wide-area-visualization. Usually this information has a geospatial component associated with its location on a one-line diagram. While the one-lines themselves could be drawn in a geographically accurate form usually they are only drawn in a pseudo-geographic form since the areas of most interest (i.e., those with a high concentration of electric facilities) may be geographically quite small. This research project focuses both on system-level wide area visualization, and more detailed visualizations of the components themselves.

This report along with the published publications list in Chapter 7, present results from the PSERC "Visualization of Power Systems and Components" project. The original goals of this project were (1) the development and/or enhancement of techniques for visualizing power system information, (2) the development of techniques for visualizing power system component information, and (3) performing human factors experiments and analysis on the visualizations developed in the project. We believe all three of these goals have been met, with the most germane results presented in this report. Additional results are available in the papers referenced in Chapter 7.

The report is organized as follows. Chapter 2 discusses 2D system-level visualization techniques while Chapter 3 discusses 3D contingency analysis visualization techniques. Power system component visualization techniques are presented in Chapter 4, while the results of the human factors experiments covered in Chapter 5.

2 Two-Dimensional Power System Visualization

As was mentioned in the Introduction, the project focused on developing new methods and enhancing existing methods for both 2D and 3D visualization. This chapter discusses the 2D techniques, integrating the results of this research projects with the key results from previous projects. Two-dimensional visualization has a key advantage in that it is intuitively understandable to essentially all potential viewers. People are just very accustomed to 2D displays through their previous interaction with computer displays and through their familiarity with other techniques for information presentation such as books. Another important advantage is the ability to relatively quickly display 2D computer images.

For the visualization of power system operational information, such as the results of power flow studies or SCADA data, the traditional visualization approach has been to use either tabular displays or substation-based one-line diagrams. In an EMS control center this information is often supplemented with an essentially static mapboard; historically the only dynamic data shown on a mapboard has been the application of different colored lights to indicate the status of various system devices. This section describes some 2D techniques that could be used to supplement, or in some cases replace, such displays. The emphasis in this research was the display of large amounts interrelated information, with the information relationships usually due to either the presence of an underlying electrical gird, or inter-temporal interactions.

2.1 Line Flow Pie Charts

One visualization technique that has proven useful for quickly indicating the location of overloads/outages in a transmission network has been the use of pie charts in which the percent fill of each pie chart is equal to the percentage loading on the line. Optionally, a numeric text could also be superimposed on the pie chart to indicate the exact percentage. For displays with relatively few lines, where each individual line's pie chart can be viewed with sufficient detail, such pie charts can quickly provide an overview of the system loading. If desired, different color shadings could also be used with the pie charts to highlight those devices loaded above some threshold percentage.

However, for larger network overview displays there is insufficient space to show each individual pie chart. Instead, a supplementary technique is to dynamically size the pie-charts based upon the line's percentage loading. In this approach the percentage fill in each pie-chart is still equal to the percentage loading on the line, but the size and color of the pie-chart can be dynamically sized when the loading rises above a specified threshold. By increasing the size and/or changing the color of the pie charts only for the small number of elements loaded above critical thresholds, or on specified open elements, the user's attention can be quickly focused. The overloaded/open elements appear to "pop-out" on the display. Figure 2.1 shows an example of pie charts on a seven bus case in which lines loaded between 80% and 100% are shown using a slightly larger orange pie chart, while open elements are highlighted with a green "X".

From a human factors viewpoint, the underlying mechanism that causes information to pop-out is called preattentive processing. One of the advantages of using visualizations that take advantage of preattentive processing is the time taken to find the desired object on the display is essentially independent of the number of other elements on the display (known as "distractors"). Size, color and motion are three examples of features that are preattentively processed.

Extending the technique to larger cases requires decreasing the size of the "normal" pie charts so they become essentially invisible. As an example Figure 2.2 shows this technique for a case simulating the power flows in Northeast Ohio immediately prior to the first 345 kV line outage on August 14th, 2003. Overall the display shows slightly less than 400 buses (mostly 138 and 345 kV), slightly more than 400 transmission line/transformer pie charts, and the pie chart for a single flowgate. The pie charts are dynamically sized/colored to be substantially larger than their normal size and colored differently (orange on a color display) for a percentage loading above 85% of their emergency limit, and to be even larger and colored red for a loading above 100%. Note that the dynamic sizing immediately draws attention to the single line loaded at 87%.

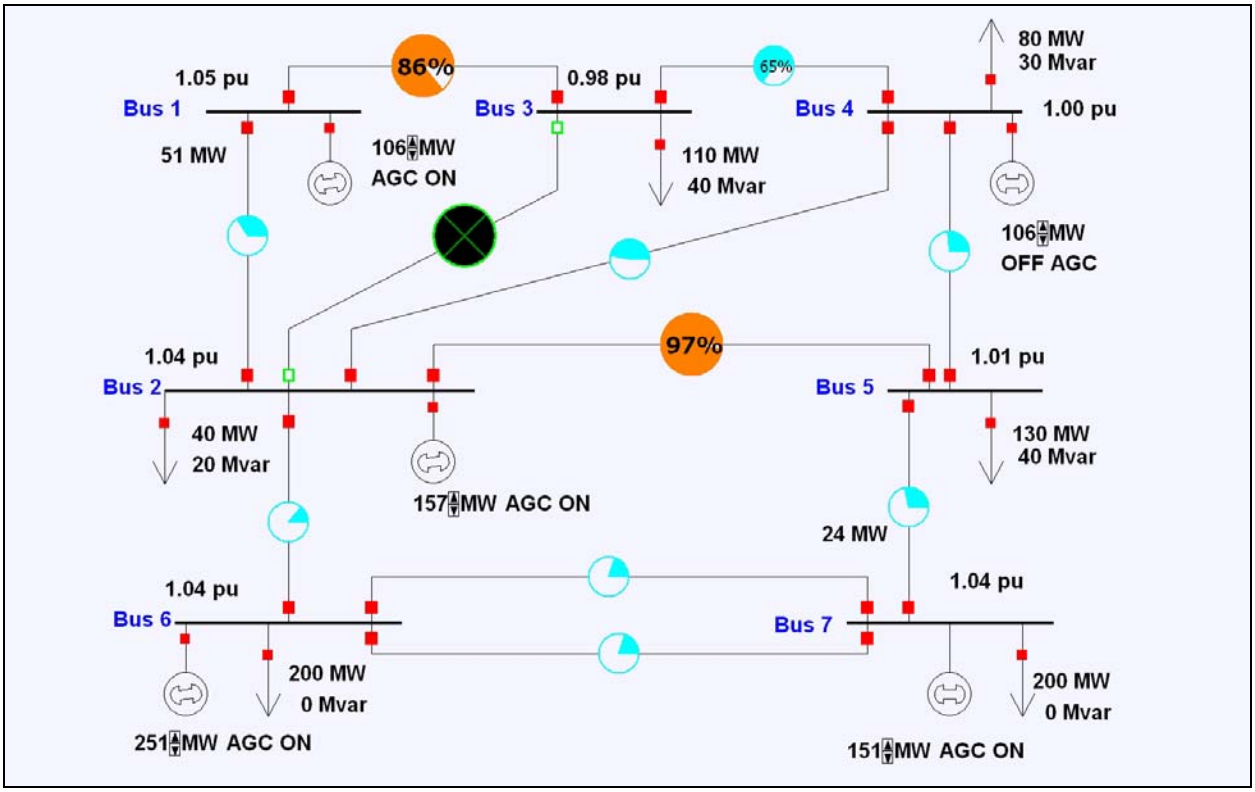

Figure 2.1: Pie Chart Example with a Seven Bus Case

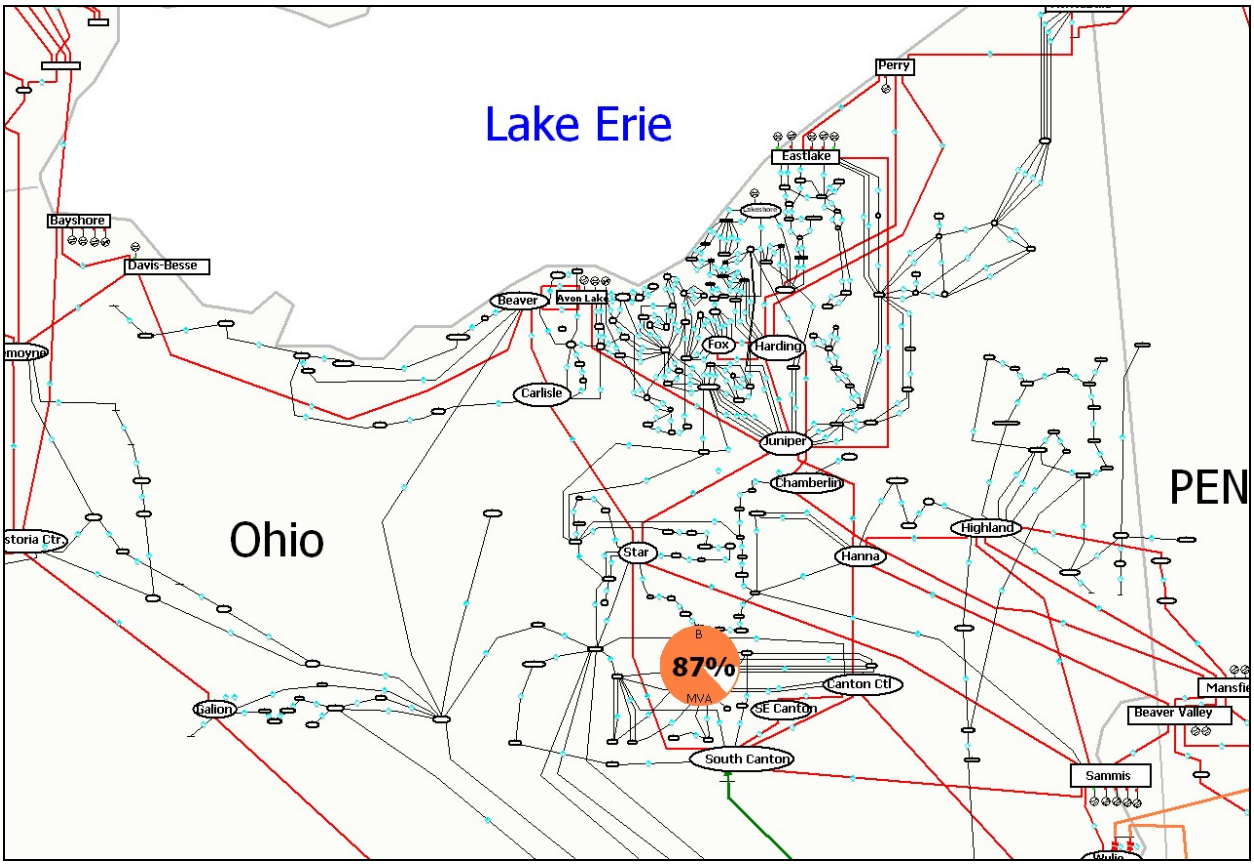

Figure 2.2: Pre-Blackout Northeast Ohio Transmission System Status

There are, however, several potential problems with the pie chart approach. First, care must be taken when applying resizing to devices that are designed to be regularly loaded at a high percentage level. Common examples of this are generator step-up transformers. Such transformers are designed to be regularly loaded at a high percentage of their ratings, but because of their radial connection, they are in no danger of overloading. A straightforward solution to this problem is to either not show pie charts on such devices or to specify that the pie charts should not be dynamically resized.

Second, the use of dynamically sized pie charts involves a tradeoff between making the pie charts large enough to draw attention, yet not too large so as to obscure other important one-line elements. This is illustrated in Figure 2.3, which shows the August 14th system at 15:51 EDT after three 345 kV lines and a number of 138 kV lines have opened. Note, the open transmission lines' pie charts can also be dynamically sized and can have their color/symbol changed to draw attention. As with Figure 2.1, the open lines are indicated by the large pie charts drawn with an "X" symbol.

The large number of overloads/line outages would make it much more difficult for the operator to rapidly locate the most crucially overloaded devices. Of course, this is a characteristic of any approach that uses dynamically sized one-line elements. One solution for this problem is to filter the display to highlight certain lines, and attenuate the display of other lines. Algorithmically the filtering is accomplished by selectively blending portions of the image with the background with a method known as alpha-blending (alpha-blending can also be used in computer visualization to create the effect of transparency).

As an example of filtering Figure 2.4 repeats the Figure 2.3 display except now the lower voltage lines are blended into the background, helping to focus attention just on the more critical 345 kV lines. Now it becomes clear that the Sammis-Star 345 kV line is overloaded, and that four 345 kV devices are open. Yet the lower voltage lines are still partially visible, helping both to provide context for the higher voltage lines and to allow continued monitoring of these lines.

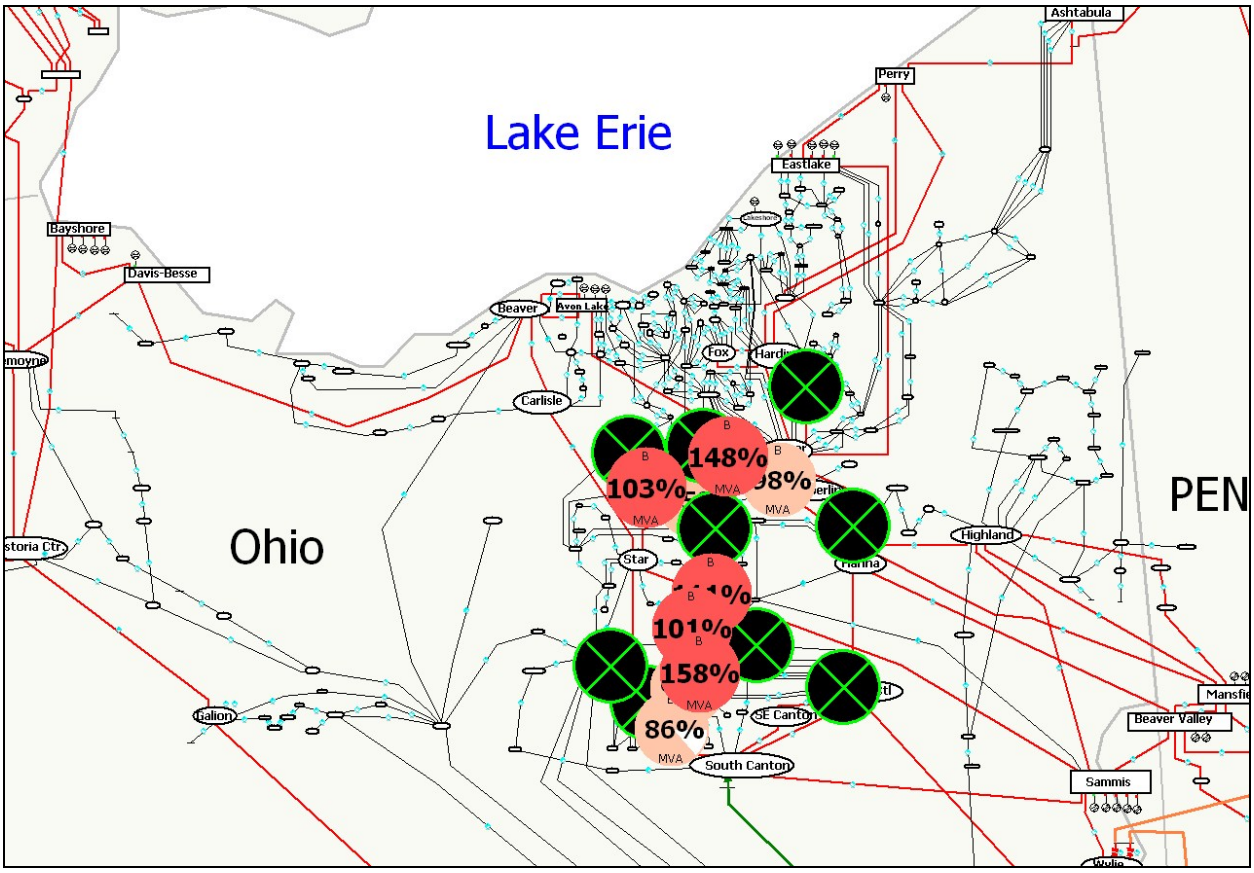

Figure 2.3: Transmission System at 15:51 EDT

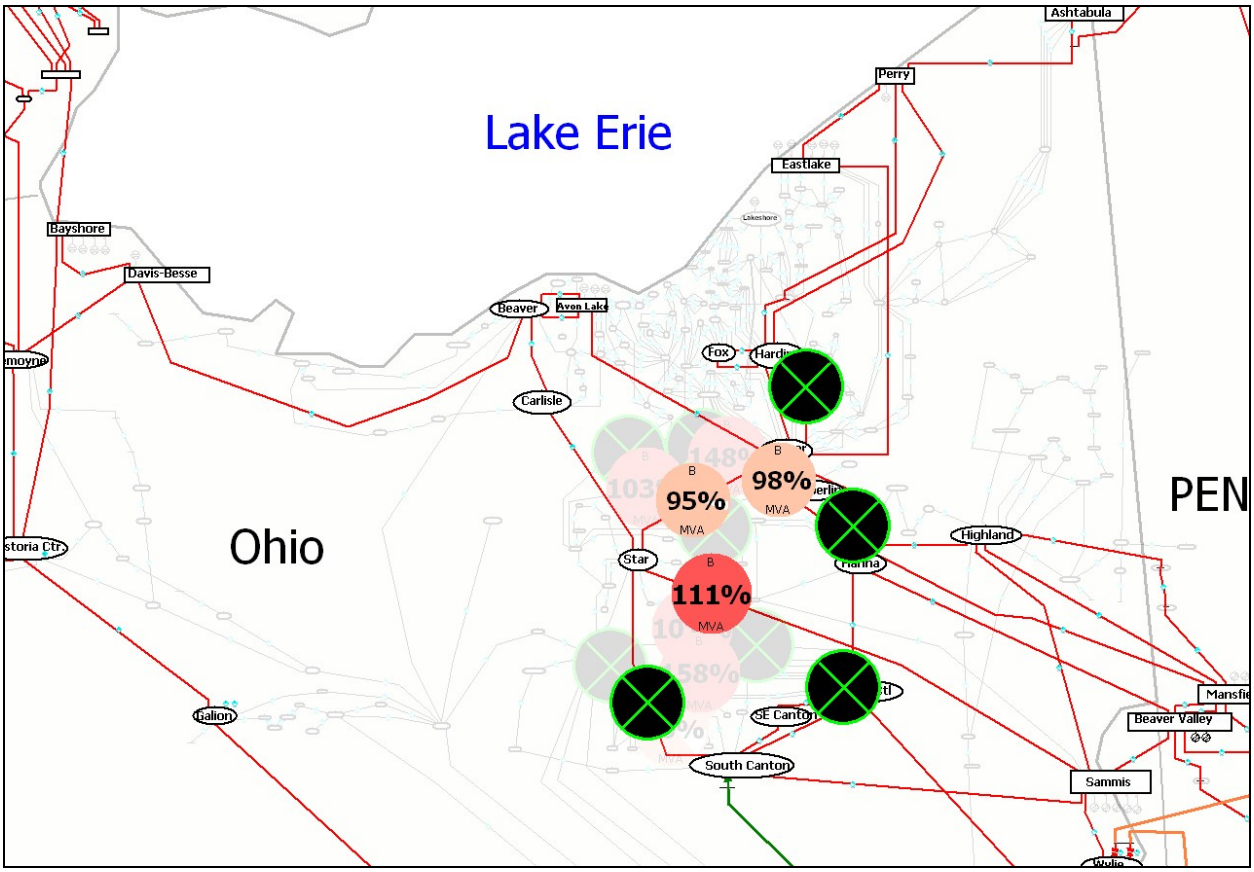

Figure 2.4: Filtered Figure 2.3 Display Highlight just the 345 kV Values

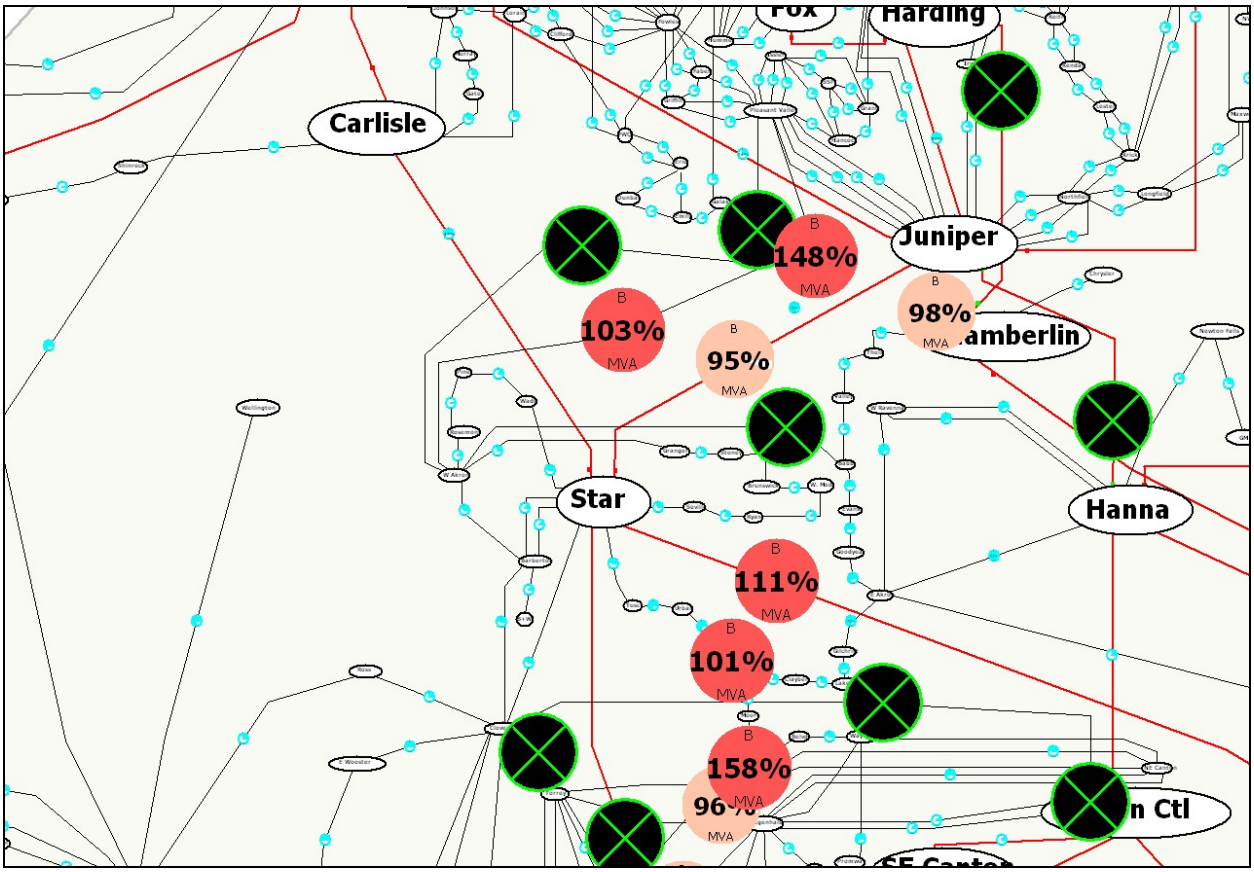

Figure 2.5: Zoomed View of Figure 2.4 with Dynamic Pie Chart Zoom Control

A second potential solution would be to proportionally reduce the amount of resizing as the display is zoomed. For example, a maximum zoom value for full resizing could be specified. Once the display is zoomed past this value the amount of pie chart resizing could be dynamically reduced until reaching some threshold value, such as the size of a normal pie chart. The visual effect during zooming is the resized pie chart remains the same size on the screen causing the overlap to eventually vanish. Figure 2.5 shows a zoomed view of the central portion of Figure 2.3using this technique. The technique could also be used with filtering.

2.2 Animated Flows

Useful as the pie charts may be, they still do not provide any indication of the direction of flow. During emergency operation, in which historical flows may have reversed, quickly conveying this information could prove to be crucial. One technique for displaying line flows is to superimpose small arrows on the lines, with the arrow pointing in the direction of the MW flow, and the size of the arrow proportional to either the MW or MVA flow on the line. The size and color of these arrows can also be used to provide a visual reinforcement with respect to severity of the problem. Figure 2.6 shows the seven bus case with this enhancement, while Figure 2.7 demonstrates flow arrows using the Figure 2.4 case with the arrows on the overloaded Sammis-Star line colored red. The direction of the power flow arrows (into the Cleveland-Akron area) indicates a potential problem in that area.

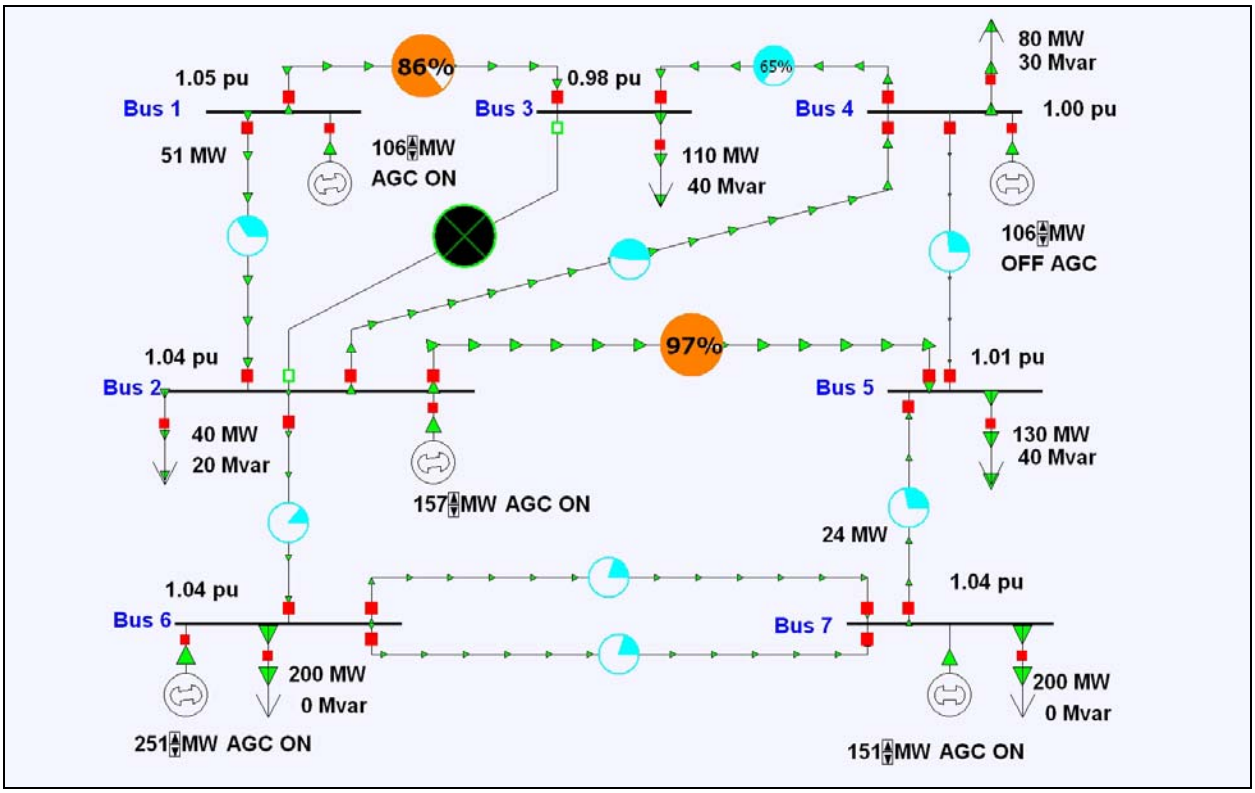

Figure 2.6: Figure 2.1 with Flow Arrows

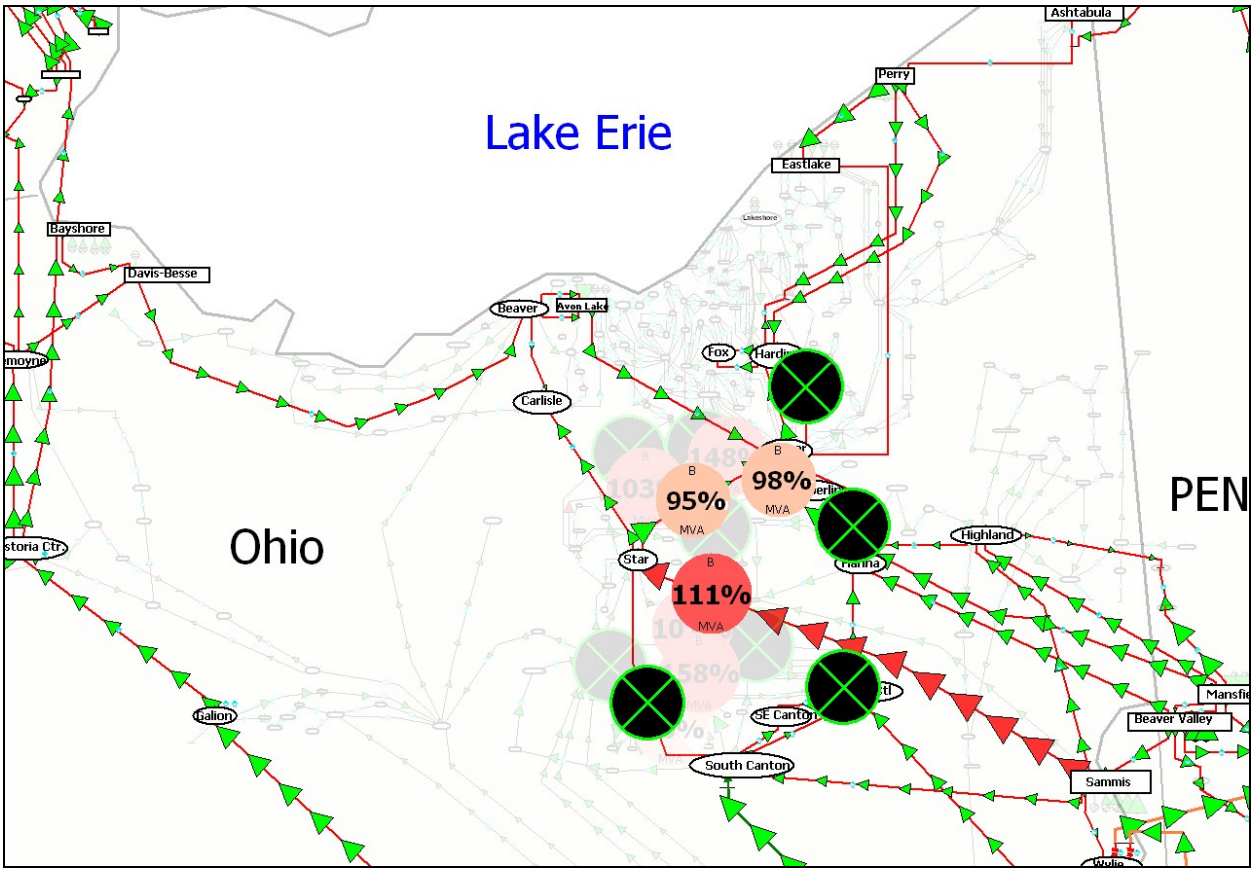

Figure 2.7: Transmission System at 15:51 EDT with Flow Arrows

However a much more dramatic affect is achieved when the flows are animated. With modern computer equipment, animation rates of greater than ten times per second have been achieved when using a relatively fast PC, even on relatively large systems. Smooth, almost continuous, animation is achieved by updating the display using bitmap copies. The effect of the animation is to make the system appear to "come to life". Our experience has been that at a glance a user can gain deep insight into the actual flows occurring on the system. The use of panning and zooming with conditional display of objects gives the user the ability to easily study the flows in a large system.

However, the application of such animated flows to larger systems has to be done with some care. It is certainly possible to create one-lines in which the presence of the flow arrows results in more clutter than insight. For example, Figure 2.8 shows a one-line diagram of the TVA 500/161 kV transmission system (with a few 345/230 kV buses as well). Overall the display shows slightly more than 800 buses and about 1000 transmission lines and transformers. From just viewing the static representation shown in the figure it is relatively difficult to detect flow patterns since the flows from the different voltage levels tend to intermingle. When the display is animated this intermingling is less apparent, but it is still a challenging display to interpret.

But if the view is restricted to just a particular voltage level (such as through highlighting), or zooming is utilized to focus on a particular portion of the grid, then the animated flow arrows can again be quite helpful. As examples, Figure 2.9 shows just the flows on approximately 75 of the 345/500 kV transmission lines, while Figure 2.10 shows a zoomed view of all the transmission

line flows in southwest Kentucky. Animated flows could also be used to show other line quantities, such as reactive power flow or power transfer distribution factors (PTDFs).

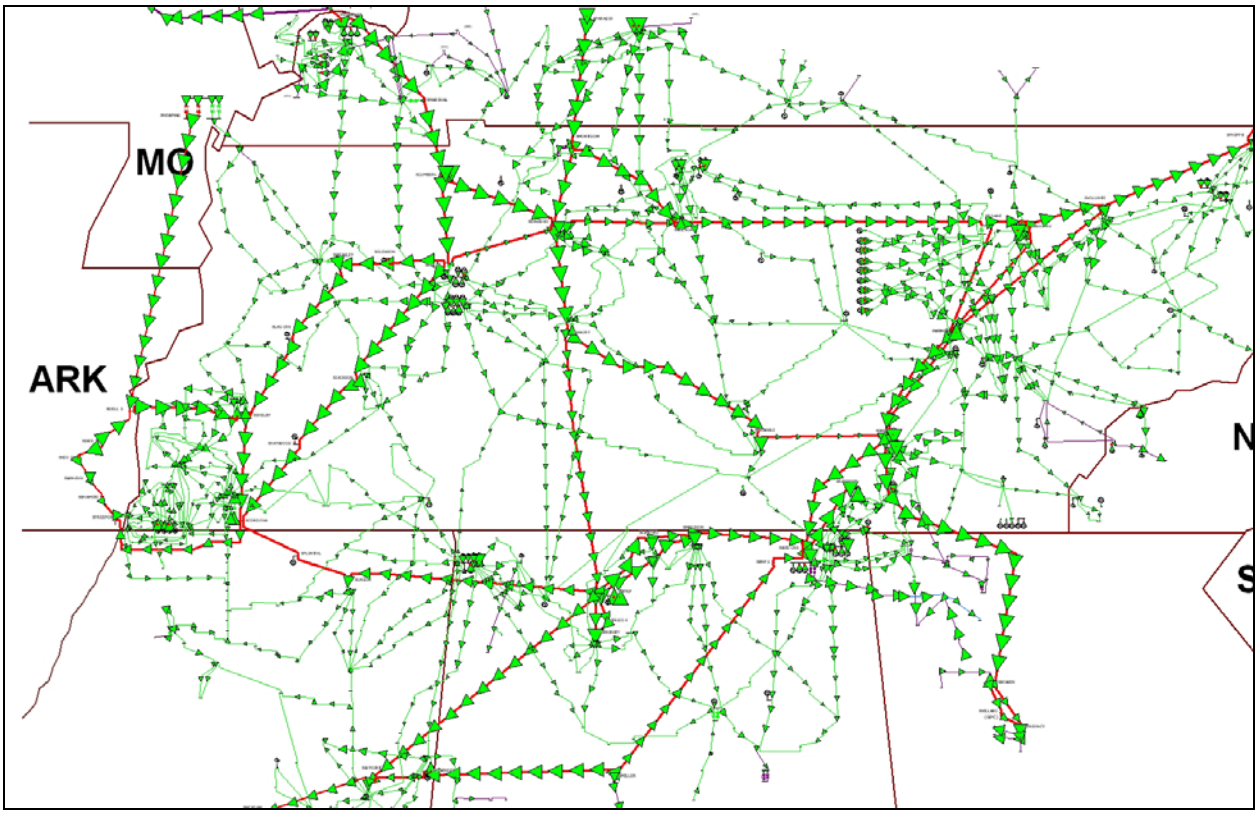

Figure 2.8: TVA 500/161 kV Transmission Grid

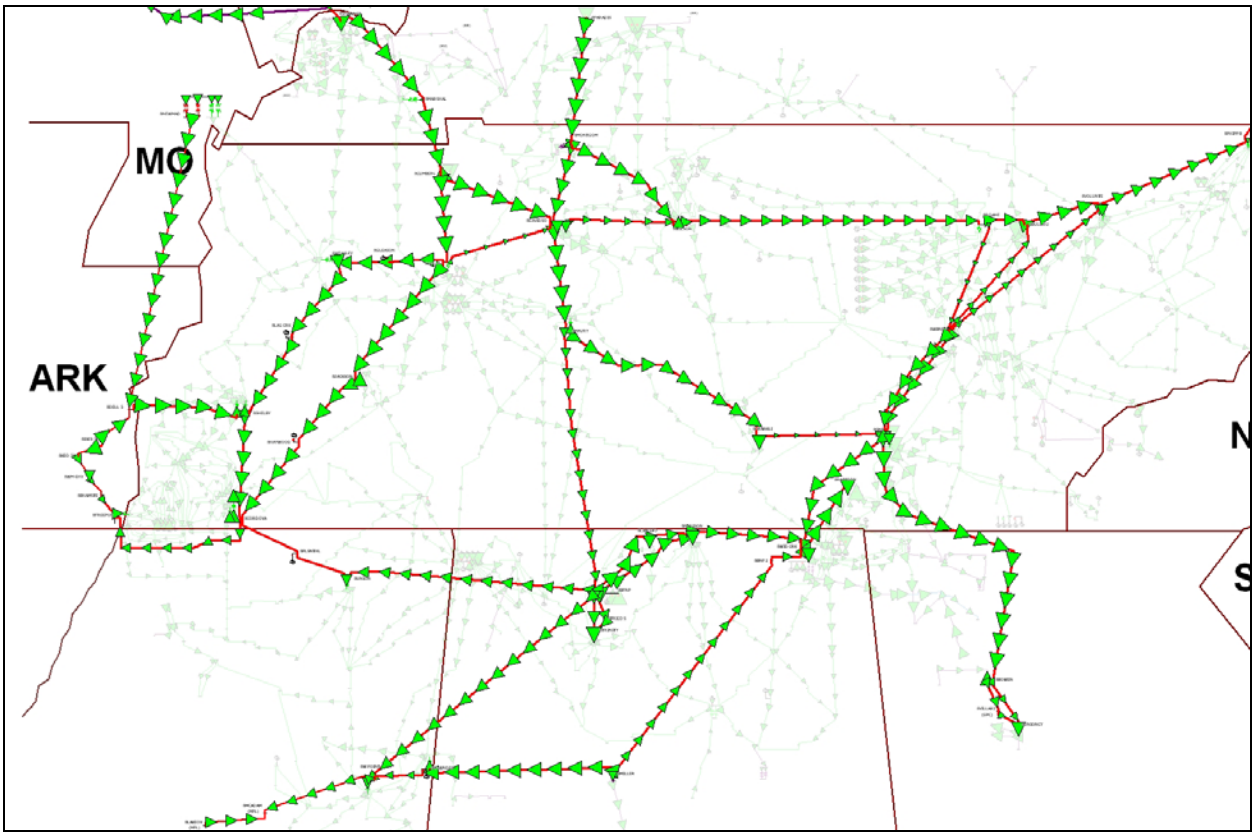

Figure 2.9: TVA 500/161 kV Transmission Grid

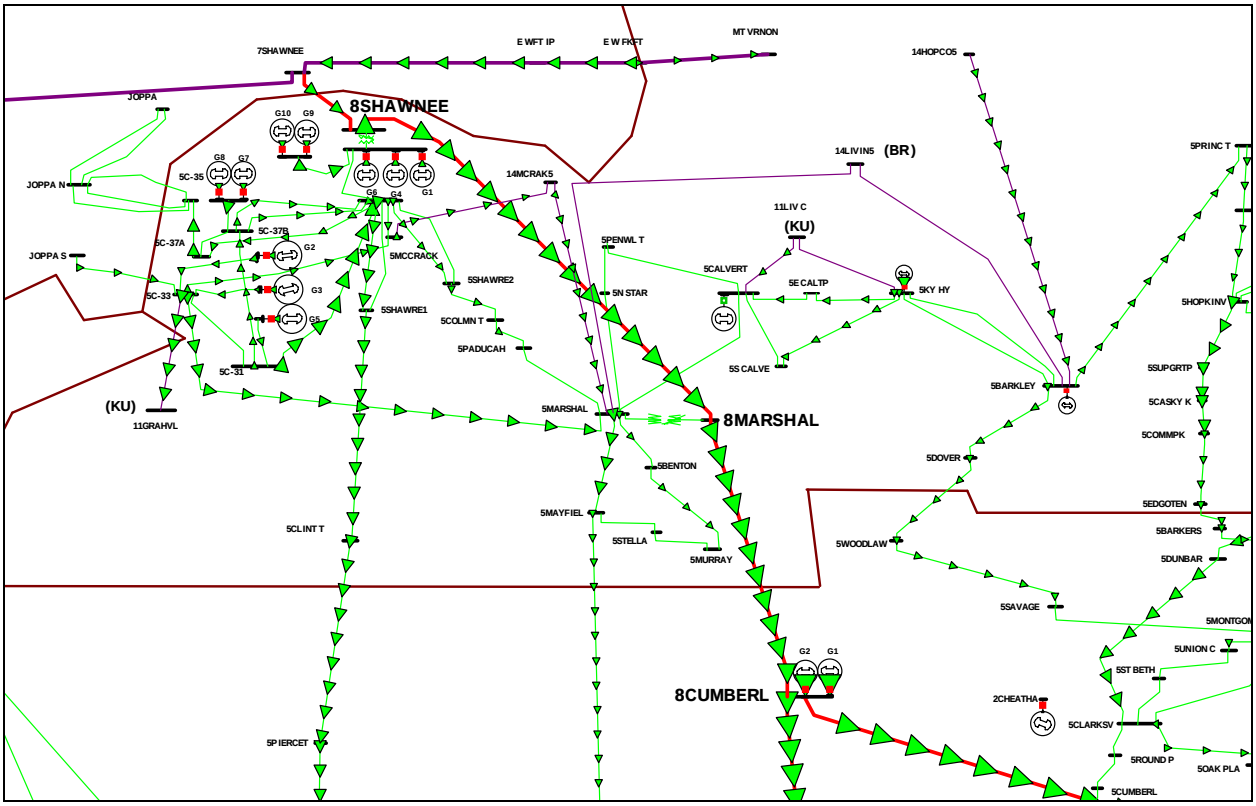

Figure 2.10: Zoomed view of Southwest Kentucky Transmission

2.3 Application of Gauges to Display Power System Values

The generic power system visualization question is how best to show a fairly large number of geospatially distributed real and occasionally complex values. Power system one-line examples of such values are numerous. These may be measured quantities such as bus voltage magnitudes and angles, generator values, LTC tap position, and switch shunt reactive power output. Or they may be derived quantities such as bus locational marginal prices (LMPs), or a host of sensitivity values. If the number of values on a particular display is small then numeric fields by themselves could be used. But for wide-area-visualization symbolic displays of numeric values can have a significant advantage, particularly if adjacent values are somehow related, something that is quite common in power visualizations in which the values are related through the underlying power system.

For the symbolic display of real values there are several common techniques. For example, if the numeric value is a normalized quantity, such as a percentage loading, one could use a pie chart approach, perhaps dynamically sized, in which the amount of fill is used to indicate a percentage. Another technique is to use gauges in which a rectangular bar is filled to graphically indicate a value's position within a range. This approach is illustrated in Figure 2.11 where a bottom-filled gauge is used to indicate the relative voltage level at a bus, with the actual value shown within the gauge. In this example the gauge's limits were set to show the range from 0.9 to 1.1 p.u. Of course, the limits could be shown next to the gauge, but this might cause a display to become excessively cluttered.

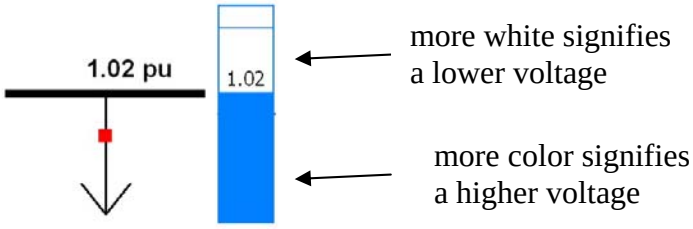

Figure 2.11: Gauge Symbol Used to Show Bus Voltage

Bottom-filled gauges are particularly useful when the primary concern is to determine how close a value is to an upper limit, such as would occur with line flows or generator real power limits. For quantities with both upper and lower limits, such as bus voltage magnitudes, transformer tap positions, and generator reactive power output, an alternative is to use a center-filled gauge in which the fill extends up or down from a center, potentially nonzero deadband. An example of such a gauge is shown in Figure 2.12 which again shows a bus voltage magnitude, except now the gauge has a deadband such that values between 0.98 and 1.02 p.u. would have no fill. Figure 2.13 demonstrates the application of the Figure 2.12 gauges (minus the numeric display of limits) on a 37 bus system. The advantage of using a deadband is it allows attention to be focused on those values that have deviated from their normal range.

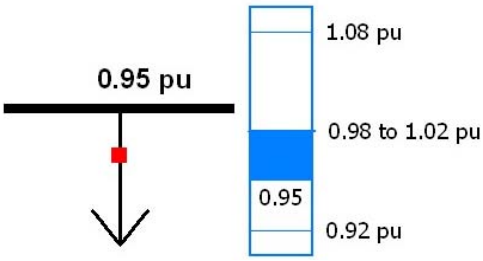

Figure 2.12: Center Filled Gauge with Center Deadband between 0.98 and 1.02 p.u.

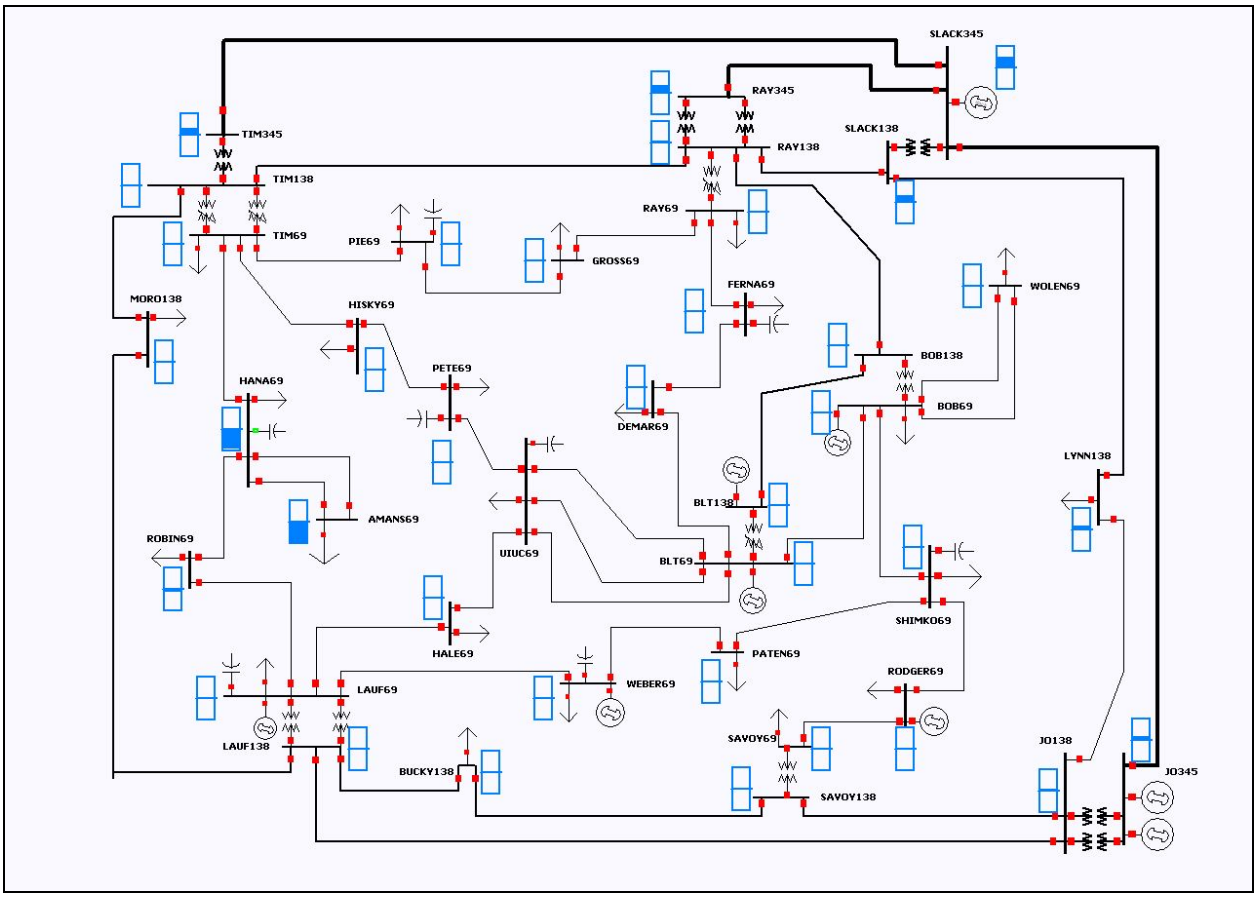

Figure 2.13: Voltage Gauges used with a 37 Bus Case

Dynamic sizing and/or coloring can also be used to further focus attention on values that are either exceeding their limits or are approaching their limits. This is demonstrated in Figure 2.14 where the gauges are set to change their fill color to orange if the voltage is less than 0.935 p.u., change their color to red and increase their size if it is less than 0.92 p.u., and to be drawn at half their normal size otherwise.

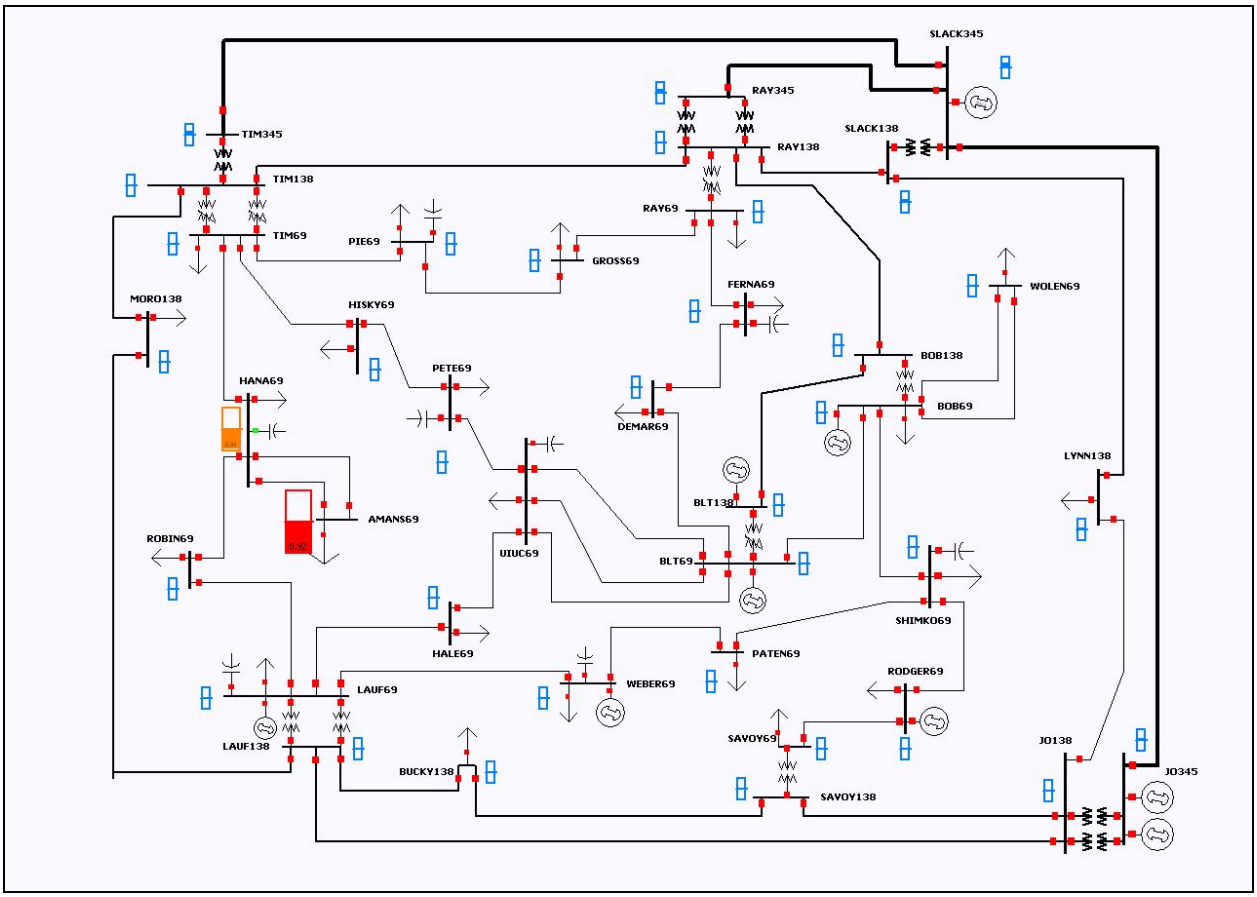

Figure 2.14: Dynamically Sized Voltage Gauges on 37 Bus Case

Of course, gauges and pie charts can be used to show other power system quantities as well. For example, Figure 2.15 demonstrates the use of pie charts to show the percentage reactive power output of the major generating stations in the TVA area. In the figure each pie chart shows the net reactive power produced at each of the substations with significant generation. The reason for showing pie charts on a substation basis rather than an individual generator basis was to minimize display clutter. When visualizing reactive power, which can be either negative or positive, one needs to determine how to display negative numbers. One approach would be to indicate negative values by filling the pie chart with a different color. This has the advantage of making it readily apparent which generators are supplying reactive power and which are absorbing reactive power. However, since the negative reactive limits often have small absolute values than the positive, one needs to carefully consider the scale when calculating the negative percentage fill. Using the negative limit could be confusing since one pie chart would then be showing values using two different scales. Using the positive limit would result in the pie chart not being completely filled when it is at its negative reactive power limit. This approach also does not work well if the generator has a positive minimum reactive power limit.

An alternative approach (used in this example) was to define the minimum reactive power output of the substation generators as zero percent. The pie chart then fills normally, reaching 100% when all the generators are at their maximum reactive power limits. The advantage of this approach is the available reactive reserves at a generator become readily apparent. Also the approach works well with generators with positive minimum reactive power limits. A potential

disadvantage of this approach is it is no longer readily apparent which generators are absorbing reactive power. Also, special symbols need to be used to show the off-line generators since otherwise they might appear as partially filled since zero could be a midpoint in its range. The Figure 2.15 case has a single open substation (in west central Tennessee) which is drawn as a circle with a green "X" in its interior.

Of course gauges could be used instead of pie charts. This wasn't done in the Figure 2.15 case because gauges were already being used at the top of the display to summarize the amount of reactive power supplied by the generators and the switched shunts in each of the three TVA zones modeled in the power flow case. The generator reactive power gauges are shown with a yellow background, while the switched shunt gauges are shown as unfilled.

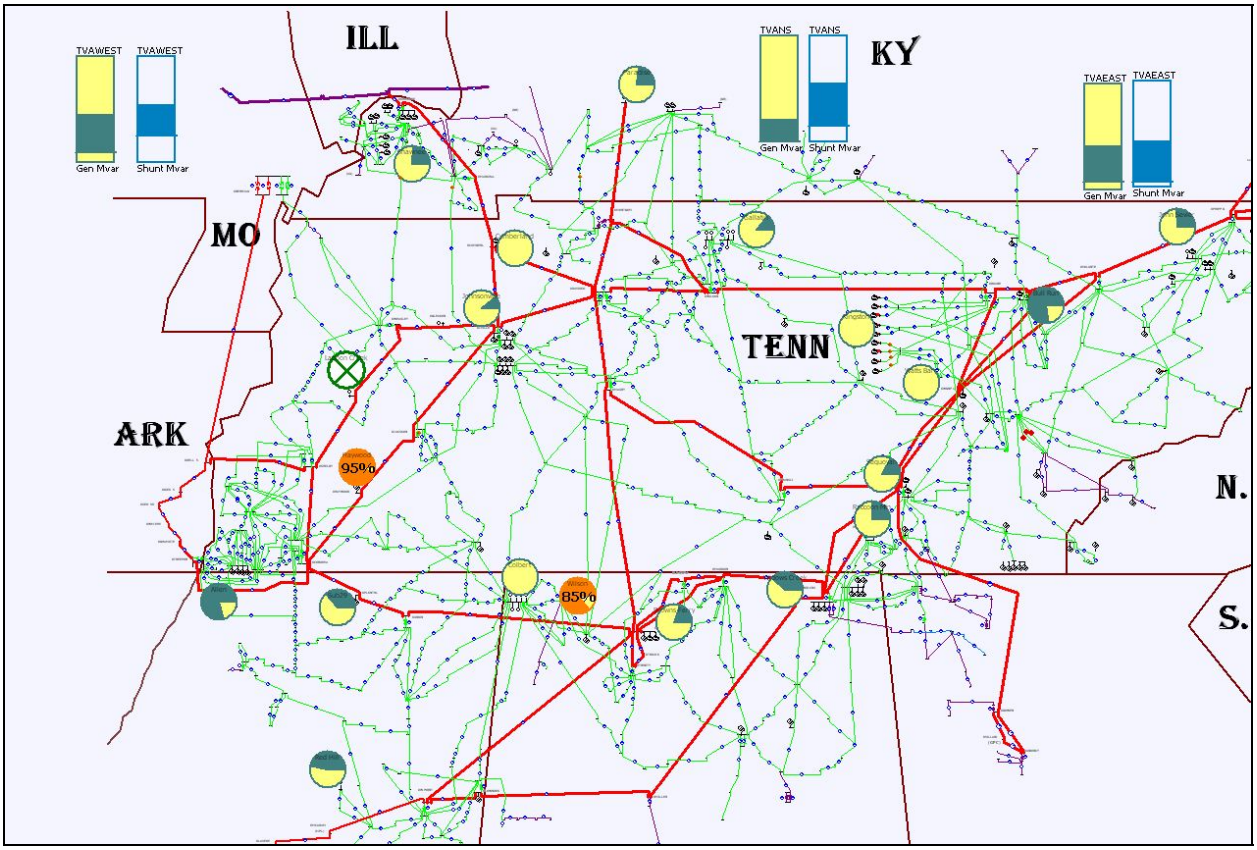

Figure 2.15: Combined Pie Chart/Gauge Display Showing TVA's Reactive Power

While the Figure 2.15 display does a good job of showing the percentage reactive power output of the generators, what is not apparent from the display is the absolute amount of reactive power available at the different substations. This problem can be solved by scaling the size of the pie charts so the pie charts total area is proportional to the total reactive power output of the on-line generators at the various substations. This is done in Figure 2.16 which presents a better overall summary of the true reactive power situation in the system. A similar scaling was done with the zone reactive power summary gauges. Note, dynamic coloring was also used in both Figure 2.15 andFigure 2.16.

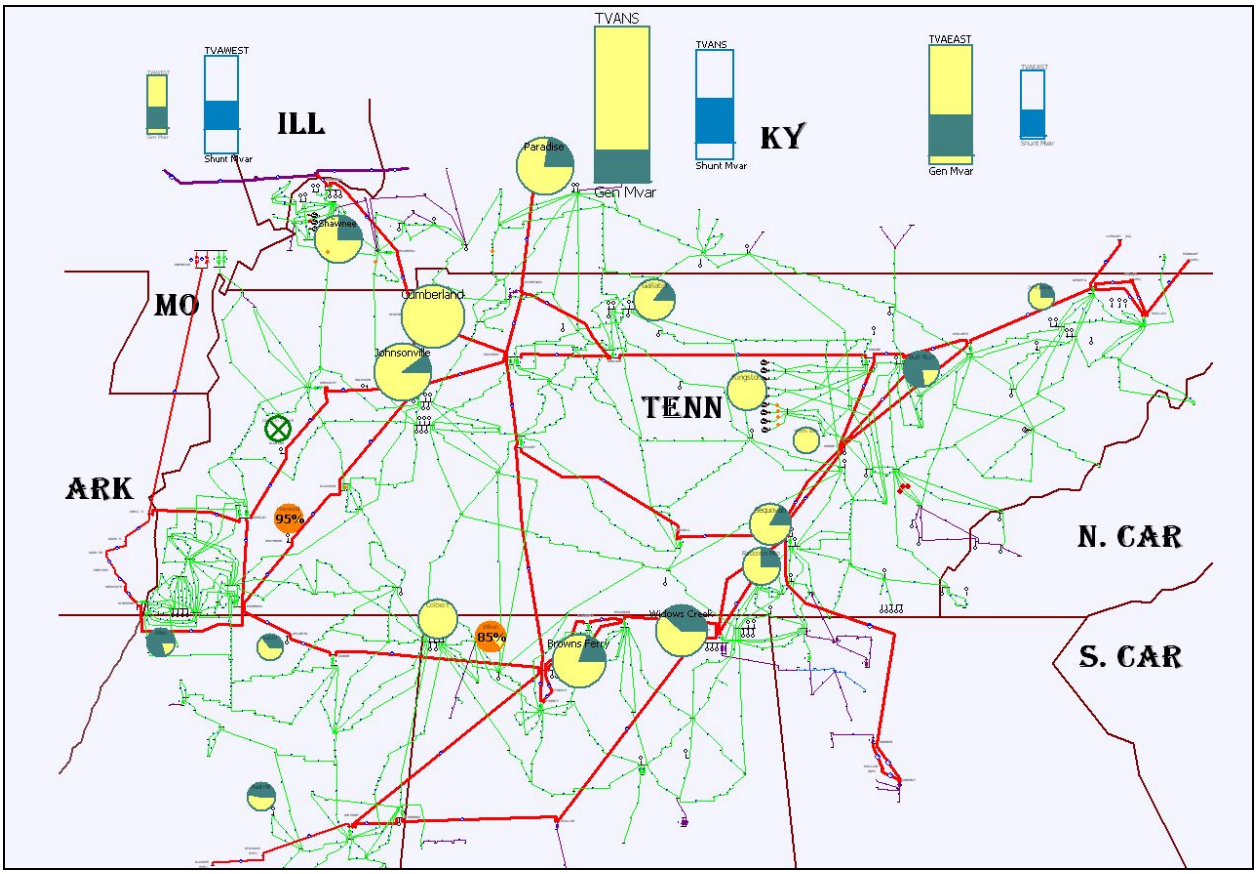

Figure 2.16: TVA Reactive Power Display using Pie Charts with Sizes Proportional to Substation Reactive Power Capability

With dynamic sizing and coloring gauges and pie charts can probably be used on single monitor displays to show up to several hundred quantities. The application of gauges/pie charts to displays with more values depends upon the type of values being displayed, and how likely they are to violate their limits, and hence be dynamically sized. As was shown in the previous section pie charts (or gauges) can be used successfully to show line flow violations on displays containing thousands of values. This works because usually there will only be a handful of violations, and hence dynamically sized values. For example, in Figure 2.7 there are only about 20 lines that are either violating their limits or are open. In contrast, in using gauges to show bus voltages during a severe disturbance there may be a large number of buses in a concentrated area with low voltages. In the case illustrated in Figure 2.7 there were about 100 buses with voltages below 0.92 p.u. For such values the use of dynamically sized gauges could quickly result in an extremely cluttered display. Highlighting could help, but the display would still likely be difficult to read. For bus-based displays with more than several hundred values the use of color contouring is probably more appropriate.

2.4 Contouring Bus Data

Contours have been used extensively for the display of spatially distributed continuous data in many other fields. However, there are three main issues with applying contouring to the display

of bus-based power system information such as voltage magnitudes and angles and generator data. First, the buses themselves are not spatially continuous – bus data values only exist at the distinct, individual buses with no values in between. To address this issue virtual values must be created to span the entire two-dimensional contour region. The virtual value is a weighted average of nearby data points, with different averaging functions providing different results. Second, tap-changing transformers may introduce discrete changes in bus voltage magnitude values. Contour plots normally imply a continuous variation in value. However, this issue can be addressed by setting up a contour in which only bus values within a particular nominal voltage range (say only 138 kV) are contoured. Third, voltages that are near one another on a one-line diagram may not be "near" one another electrically. This issue can also be addressed by only contouring particular voltage range, and perhaps by judicious construction of the contouring diagram. If a strictly geographical layout is used, normally buses of the same nominal voltage that are near each other geographically are also near electrically.

Once these virtual values are calculated, a color-map is used to relate the numeric virtual value to a color for display on the screen. A wide variety of different color maps are possible, utilizing either a continuous or discrete scaling. One common mapping is to use red for lower voltage values and blue for higher values, while another common mapping is the exact opposite. Standardization of contour color mappings, both within a control center and between control centers, could be beneficial.

Perceptually, contouring works well because the human visual system is well designed for detecting patterns. For example, Figure 2.17 shows a voltage contour of about 5600 bus voltages in the Mid-Atlantic portion of North America at about 15:00 EDT on August 14 using a discrete red-blue color mapping. Notice that at a glance the relatively low initial voltages in Ohio and Indiana are visible, with the extremely low voltages in Southern Indiana due to line outages that occurred at about noon on August 14th.

Human factors testing of power system voltage contours indicates that it is useful both for increased speed and accuracy in problem diagnosis, particularly for situations with many voltage violations. This occurs because color serves as an effective highlighting feature that attracts attention to an area of a display and reduces the size of the search space, thus allowing for the rapid localization of problem areas. In addition, the use of color contouring has the ability to create global or holistic properties in the display, which are in contrast to the local or component parts that exist. Global properties of objects depend on the interrelations between the component parts and generally refers to the Gestalt concept that the "whole is greater than the sum of its parts." Hence, color contouring may allow operators to assess the overall state of the system more readily (gain better situation awareness or develop a more accurate mental model) and therefore facilitate the choice of a more appropriate and timely corrective action.

Another advantage of contouring, which is impossible to show here, is the images can be readily animated to quickly show the progression of the system over time (similar to what is done with animated weather maps). During an emergency this information could be used to rapidly convey the direction of the system state, and could also be used to rapidly bring late arriving people to the control room (such as engineers and management) up-to-speed on what is going on. However, one does need to be careful about trying to convey too much information in a single display. For example Figure 2.18 combines transmission system information (pie charts and flow arrows) with the contour. While this may be tolerable if there are just a few problems, as more problems develop it would become increasingly cluttered.

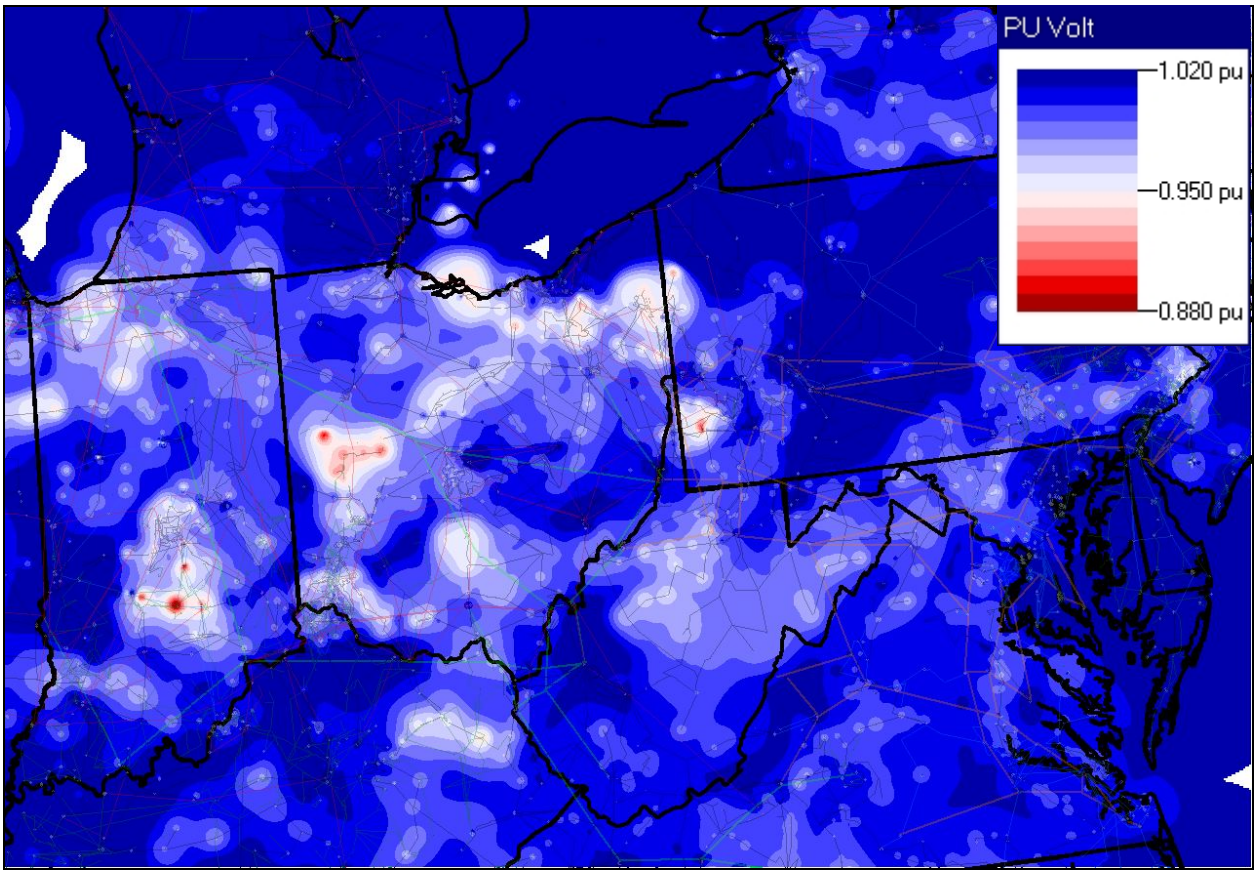

Figure 2.17: Pre-Blackout Ohio Region 115-230 kV Voltage Contour

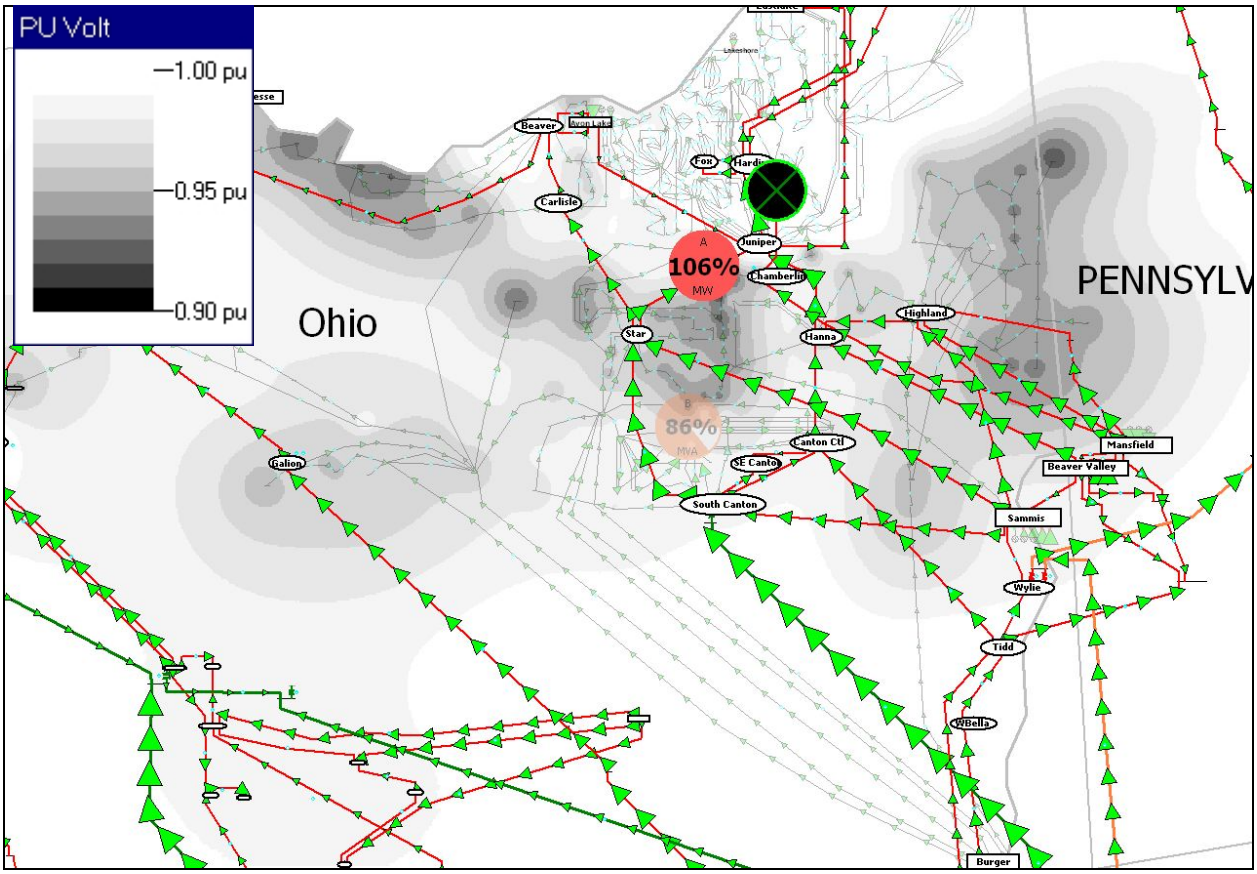

Figure 2.18: Northeast Ohio Voltage Contour at 15:05 EDT

As was discussed in previous PSERC reports [12] contouring can also be applied to many other types of power system information and is still an area of active research. For example, consider the problem of rapidly showing the overall loading of a large power system. Figure 2.19 presents an initial example of how contouring could be useful for this problem. The contour uses a red-blue color mapping to show the density of the power injections across a portion of the Southeast, with red used to indicate sources of generation and blue sources of load. Since this is a density contour both the size and intensity of the color is used to indicate the injection values. Whether such a contour would be useful in an operations setting is not yet clear. It would be interesting to see how such a contour changes over time (such as a day), and to see whether an experienced operator/engineer would find the display useful for quickly determining if there were problems with the system.

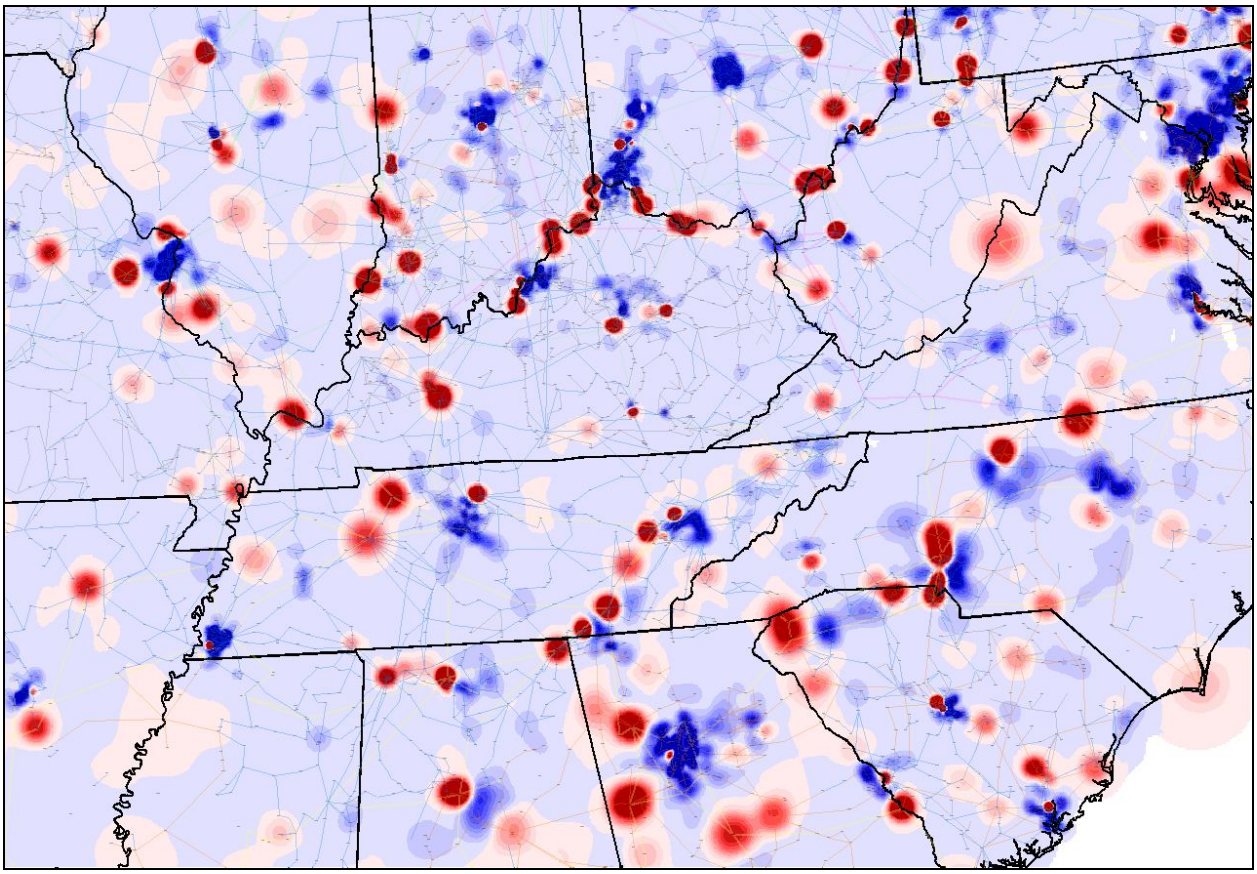

Figure 2.19: Contour of Net Power Injections in Southeast US

3 Contingency Analysis Visualization

In addition to just considering the visualization of base case power system information this research project also considered the visualization of contingency analysis results. Note, many of the results presented in this section were presented earlier in [1]. Contingency analysis (CA), as a part of static security analysis, is critical in many routine power system and power market analyses, such as ATC evaluation, security assessment and transaction arrangement. A typical CA models single element outages (one transmission line or one generator outage), multiple-element outages (two transmission line outage, one transmission line and one generator outage, etc.), and sequential outages (one outage after another). Limit checking is done for each contingency to determine whether the system is secure.

With the global trend towards deregulation in the power system industry, the volume and the complexity of the CA results in the daily operation and system studies have been increasing. Not only has deregulation resulted in much larger system model sizes, but also CA is computed more frequently in the restructured power markets to monitor the states of the system under "what if" situations in order to accommodate the maximum number of power transfers. The net impact of these changes is a need for more effective and efficient visualizations for CA results to help with the comprehension of the essential security information, information which could be buried in the enormous and complex CA data sets.

The traditional display for CA results in an EMS is often a tabular list showing the violated buses and transmission elements, along with the corresponding contingency name, element value, limit and perhaps the percentage violation. However, when the number of elements in the list becomes excessive it can be difficult to build a mental connection between the violated elements and the contingencies causing the violations, or to understand the underlying problems in the system. Thus, better schemes to visualize the data computed by CA are needed.

3.1 Previous Work on Contingency Data Visualization

Surprisingly few visualization techniques have been presented in the technical literature aimed at assisting power system operators and engineers with contingency data visualization. The techniques that have been presented fall mainly in three categories: 2D visualizations based on the traditional one-line diagram, 2D visualizations not based on the geographic network and 3D visualizations without geographic environment.

The 2D visualizations based on one-line diagrams have been relatively popular due to the familiarity of power operators with one-line diagrams and the importance of geographic information in power system operation and control. Example schemes include encoding the width [2, 3, 4, 5, 6], color [4, 5, 6] and arrow size [4] of transmission lines according to line performance indices (PIs) or post contingency loadings; augmenting the one-lines with the thermometers [2,3] showing bus PIs and the pie charts [7] for contingent voltage angles.

In contrast to the one-line diagram based visualizations, the presentation of contingency data in a 2D matrix [5, 6, 8, 9] or bar charts [10] gives a clear overview of the system severity status, but at the expense of the loss of geographic information. Other 2D visualizations not based on the geographical network can be found in [7] where high-level security risk levels were displayed by rectangular and oval meters and 2D iso-risk curves displayed security level as a function of operating conditions.

In addition to the 2D visualization techniques listed, 3D visualization without geographic

background has been applied into power system CA results. In [5] a third dimension was added to represent time, allowing the display to show the time variation in contingency severity. Similarly, in [11] a 3D manifold was used to display the percentage overload of the monitored transmission lines under each contingency by scaling the z axis in terms of percentage overload, assigning each point on the y axis a contingency and each point on the x axis a monitored line.

This literature review indicates that power system CA visualization is still in its infantry, with a pressing need for better techniques. This section of the report first discusses possible 2D visualization techniques for CA data and their drawbacks, and then presents a geographic 3D approach.

3.2 From 2D To 3D

The entirety of the CA results can be conceptualized as a set of 2D matrices, perhaps one matrix for voltage results, and one for transmission element loading results. The loading matrix could have the columns correspond to the transmission elements while the rows correspond to the contingencies. The matrix entries are then the percentage loading of each transmission element for each contingency. Similarly, the columns of the voltage matrix may correspond to the buses and the rows correspond to the contingencies, with the p.u. voltage values being the matrix entries.

To aid in the interpretation of the results, a discrete color contour could be added to the background of the matrices, with the cell color based on the corresponding percentage loading or p.u. voltage value. This visualization technique has been applied to show the variation of bus marginal prices over time in [12]. If applied to contingency data, it gives a clear overview of the system static security status in terms of post contingency voltages and loadings.

Of course, if one is just concerned with the element/contingency pairs which resulted in limit violations, the size of the matrices could be reduced by limiting the columns to the set of elements with violations, and the rows to the set of contingencies causing limit violations. The disadvantage of this matrix approach is the absence of geographic information either for the power system elements (buses, transmission lines and transformers) or for the contingencies.

To add geographic information one might consider somehow displaying CA results using a 2D one-line diagram. The one-line has the ability to at least approximate a geographic location and is certainly familiar to power system operators and engineers. To incorporate various kinds of power system data into one-line diagrams, the 2D color contour technique has been found to be intuitive and effective. Contouring has been used to visualize base case voltage magnitudes [13], LMPs [14] and line flow information [15]. However, the application of contouring to CA results has a significant disadvantage – the color for each power system element on the one-line contour can only be mapped to a single data point.

Nevertheless, 2D color contouring still has some applicability within the CA context. For example, for contingency loading data, one could map the color of a transmission element according to some contingency related criteria, such as the worst overloading on the line for the entire contingency set, or the total number of possible contingent overloads on the line, or some more advanced contingency related PI. This approach can also be used to visualize bus information by contouring buses according to some contingency criteria associated with buses. But visualizing transmission element and bus information at the same time using 2D color contoured one-line is problematic and would probably cause confusion. Moreover, in such approach the transmission element/bus information (i.e., the columns from the above

loading/voltage matrix) is being displayed geographically, while the contingency information (i.e., the rows) is not.

An alternative 2D approach would be to present the contingency information geographically while presenting the transmission element loading and/or bus voltage information in an aggregate form. For example, if one only considers single device contingencies then we could contour the contingent device itself with information related to that particular device outage, such as the number of limit violations caused by the contingent loss of that line.

In order to simultaneously display geographic information associated with both the power system elements and the contingencies, we propose expanding the display space from 2D to 3D. The goal in going to a 3D visualization is the potential to include information of more dimensions within a display without creating excessive display clutter and confusion [16]. This property of 3D visualization fits the CA requirement to effectively show the vast volume of multi-dimensional data. Due to widespread industry familiarity with one-line diagrams, the 3D visualizations presented here are based on the one-line diagram, with the one-line drawn in the x-y plane.

3.3 Organization of Data

Because of the potential for CA to create a large amount of data, effective data organization is a prerequisite to the visualization of CA. The goals of CA results visualization include helping to extract the following essential information: (1) the extent of the limit violations in terms of low voltages (defined as voltage magnitudes lower than the voltage lower limit) and transmission element overloads (defined here as loadings above the limit of the corresponding transmission element) for the whole examined contingency set, (2) the identification of contingencies imposing loading and/or voltage violations, and (3) the set of power system elements inclined to contingent limit violations.

To better visualize the CA results geographically one needs to differentiate between two different concepts: (1) the *severity* of each contingency and (2) the *vulnerability* of each power system element. The 3D one-lines that primarily use geographic information based on the contingent element itself will be called contingency severity displays. The 3D one-lines that primarily use geographic information based on the monitored elements will be called element vulnerability displays. Also, given the potentially large amount of CA data to display, the approach described here presents an interactive, hierarchical approach, with the data grouped into three levels: overview, middle and detail level, based upon the desired degree of detail.

In visualizing contingency analysis information it is also important to have the ability to simultaneously display different types of limit violations. In the research presented here we consider the simultaneous display of contingency voltage violations and contingency branch violations. However, doing so presents two challenges: (1) How to differentiate the data sets and avoid interference? (2) With possibly many more limit violations than in the separate voltage/loading visualizations, how to avoid overwhelming users with too much information?

Inasmuch as people are sensitive to clusters and patterns created by colors [17], the approach proposed here is to distinguish voltage data from loading data using color. For example, the objects associated with voltage data could be shaded blue, while objects representing loading data could be shaded red. A solution to the second issue could be the application of transparency – the most severe/vulnerable contingencies/elements are made more solid, and hence more prominent. Less severe violations are still shown, but with varying degrees of transparency. This

focuses attention on the more severe violations, but also provides context by still showing all the violations.

3.4 Contingency Severity Visualization

The first type of displays, the contingency severity one-lines, show information about the severity of the contingencies in terms of the power flow loadings on the monitored transmission elements and voltage magnitudes at the monitored buses. Three categories of this display type are presented. First, the overview display summarizes the loading and voltage limit violations caused by each contingency by showing the number of violations and the approximate worst percentage overload and/or the lowest p.u. voltage in the system. Second, the middle-level display augments the overview display to also show the location of the violations. Third, the detailed display shows the location and magnitudes of the violations for a single, specified contingency. Each of these categories is described in detail below.

In the contingency severity overview display the one-line is used to show the location of the contingent devices, along with an indication of the violations caused by each contingency. An example of this visualization is shown in Figure 3.1 for the IEEE 118 bus system. Overall the display shows results for 187 single line/transformer contingencies and 54 single generator contingencies. A total of 29 contingencies resulted in bus voltage and/or transmission element violations.

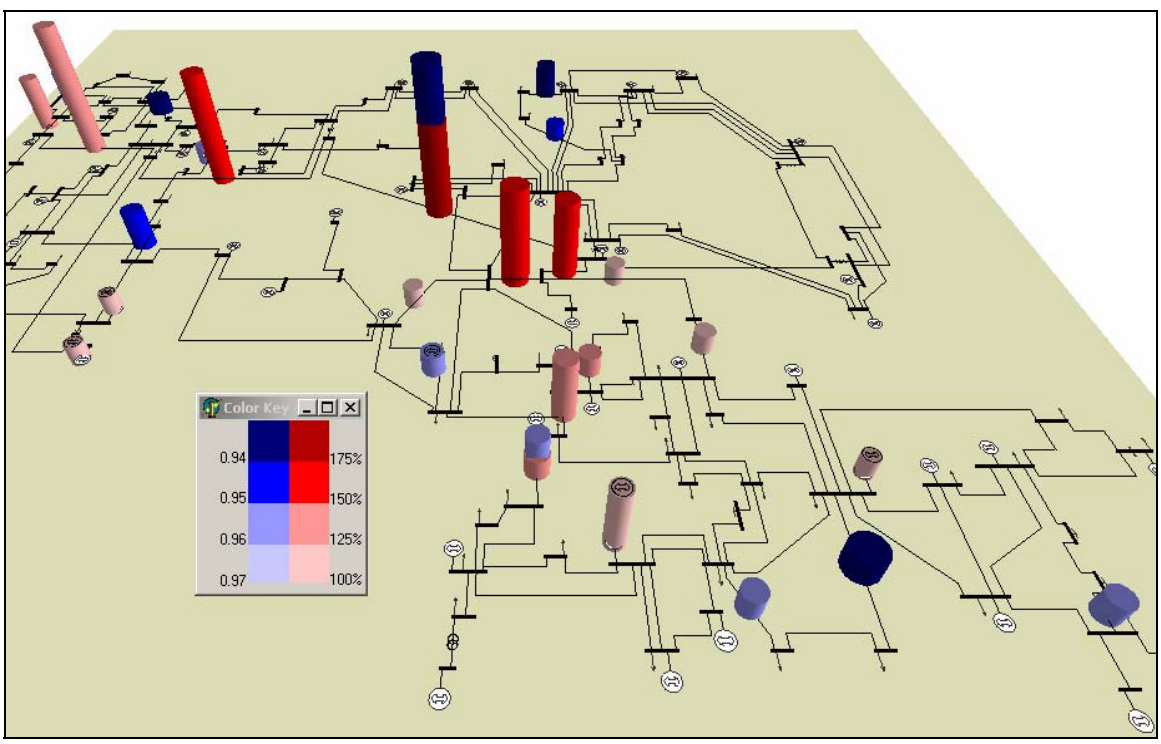

Figure 3.1: Contingency Severity Overview Visualization

In the visualization 3D cylinders are located on the contingent devices that cause violations, with the cylinder shaded blue for low voltage violations and shaded red for transmission violations. The height of each cylinder is proportional to the number of violations caused by the contingency, while the shading and radius of the cylinders are proportional to the magnitude of

the worst violation. The voltage cylinder is stacked on top of the transmission cylinder if a contingency causes both low voltages and overloads (which is the case for two of the contingencies shown in the figure). The doubling coding of the magnitudes of the worst contingent violations by color shade and cylinder radius helps to focus attention on these contingencies. A discrete color mapping is adopted from the consideration of its ease in distinguishing values in different small ranges over continuous color coding. The correspondence between the value ranges and the colors is shown by the color key.

Since only those problem contingencies that cause limit violations have associated cylinders, the overall static security status of the system is obvious at a glance. In case of insecure status with contingent limit violations, viewer's attention can be drawn to problem contingencies quickly with the geographic location of the contingency encoded by the display. Furthermore, one can quickly tell which kind of violations (low voltage or overload) each contingency would cause. The severity of the problem contingencies can be compared through the heights and radii of the cylinders. The encoded color of the cylinders would help to overcome the potential vagueness due to the perspective effect in 3D visualization where a distant cylinder with larger width/height may seem thinner/shorter than another one closer but with smaller width/height. With the help of the color key the p.u. or percentage range, in which the lowest voltage or the worst overloading lies under each problem contingency, can be read out from the color of the cylinders.

The take-away message from Figure 3.1 is the visualization is presenting a significant amount of information, the results of 241 contingencies, in a single display. This same amount of information could not be presented as concisely using the traditional tabular approach, especially the spatial relationships between the various contingencies on the one-line. Of course, the new visualizations presented here could be used in tandem with existing methods. Furthermore, the approach could easily be extended to larger one-lines, with the key concern being the density of the 3D symbols. Computationally, even displays with many hundreds of buses can be rendered quite quickly, allowing for highly interactive displays. For example, results from [18] indicate a 3D one-line with 1600 buses can be rendered at around seven frames per second using a 2.8 GHz Pentium machine.

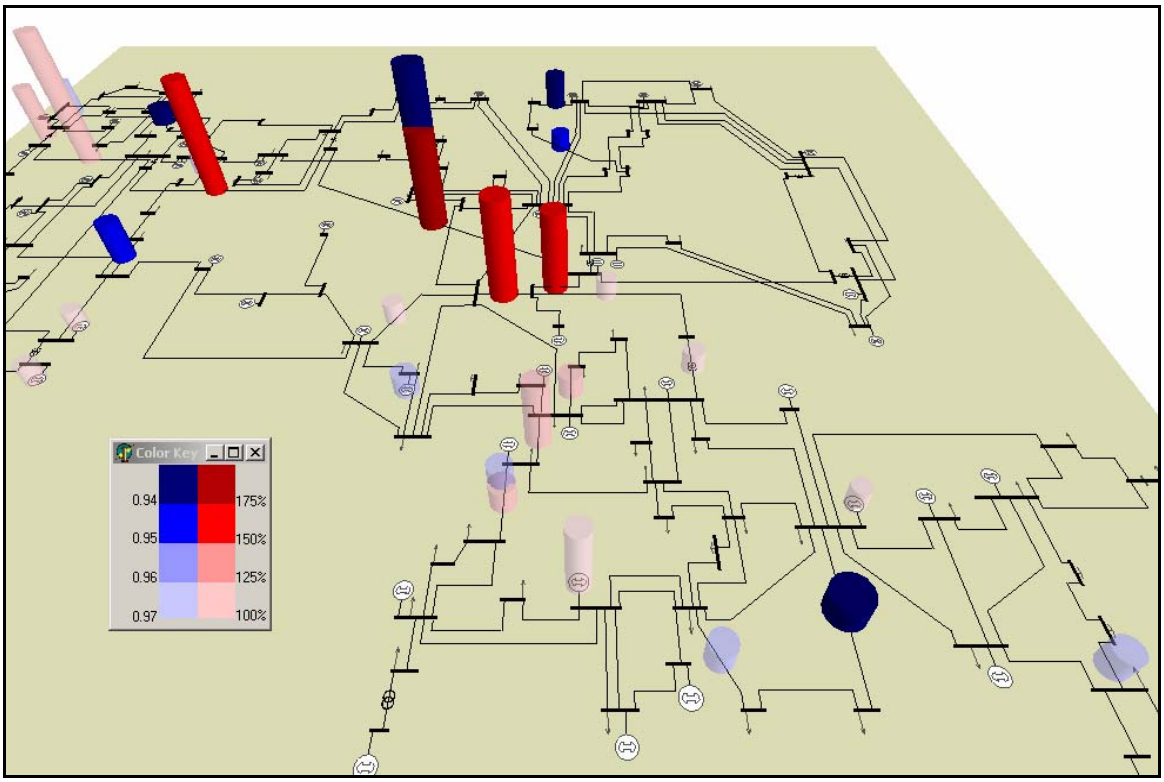

Figure 3.2: Contingency Severity Overview Visualization with Coded Transparency

The color mapping of Figure 3.1 was designed so more severe violations (lower voltage or higher loading) have darker or brighter colors while less severe violations have lighter colors. This helps to focus attention on the more severe contingencies. To further bring attention to the most severe contingencies one could also modify the transparency of the 3D objects, according to the worst violation or some other severity index. Figure 3.2 shows the severity overview visualization with transparency coded for the same IEEE 118 bus example system as in Figure 3.1. The voltage cylinders representing a lowest voltage above 0.95 p.u. are transparent, while the low voltage cylinders representing a lowest voltage below 0.95 p.u. are solid. For overload cylinders, those with loadings above 150% are solid, while loadings below 150% are transparent. Of course, any number of different transparency mappings are possible.

While the top-level display shows only two pieces of information per contingency violation type (i.e., worst violation and total number of violations), through an interactive extension the geographic relationships between the contingent elements and the power system elements suffering violations could be displayed. One approach, designated here as the middle level severity visualization, draws “link lines” between each contingency’s cylinder and the violated elements from that contingency. To avoid excessive clutter link lines might only be displayed for an interactively selected set of contingencies. This approach is illustrated in Figure 3.3, with more detailed results shown for three of the more severe contingencies. Blue lines are used for bus voltage violations while red lines are used for flow violations. To highlight the starting points of the link lines, we designed to have all the link lines associated with a contingency radiating from the top cylinder of the corresponding contingency. In a one-line diagram of a system with multiple voltage levels, the transmission lines are traditionally color coded according to their nominal voltage levels. In this case, the colors used by the link lines could be

modified to avoid using the same colors as those used on the one-line itself.

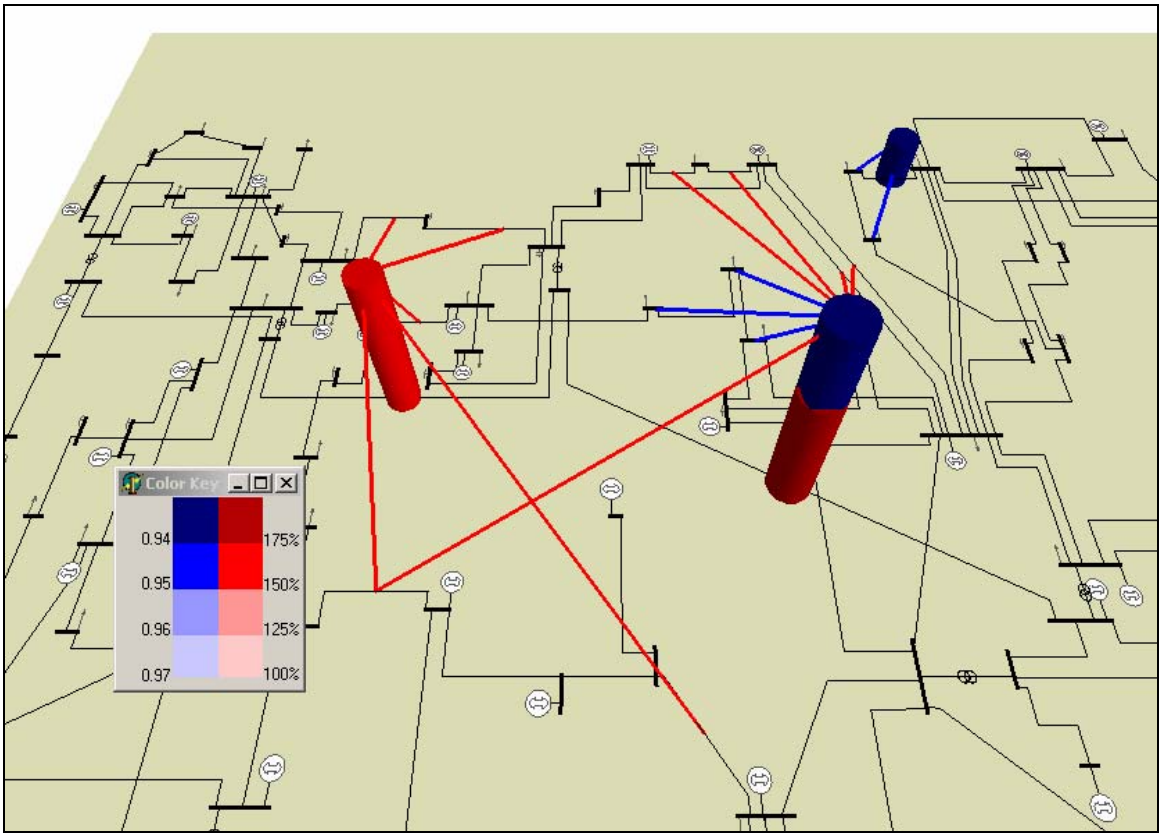

Figure 3.3: Contingency Severity Middle-Level Visualization

When contingency voltage and loading results are visualized separately, detailed severity information for a specific contingency can be displayed using a 2D color contour described in [13] and [15]. For voltage results, the one-line diagram could be contoured according to the post-contingency voltage at every bus under the selected contingency. For loading results, line contouring suffices by contouring transmission lines and transformers according to their post-contingency percentage loadings.

To integrate the voltage and loading results for a single selected contingency in the same display, we propose to supplement the 2D bus color contour of post-contingency voltages with 3D "transmission element terrains" to better show the post-contingency loadings. An illustrative example of this design is shown in Figure 3.4. The one-line diagram in the x-y plane is contoured only for the buses with low voltages under the selected contingency, with the contingent line indicated by its severity cylinder.

The overloaded transmission elements under this contingency are drawn as "terrains" – triangular prisms along the length of the line, with the height and color both coded for the percentage loading on the corresponding element. The width of the prisms has not been coded here in recognition that in medium to large systems there is often insufficient space on the one-line for significant variation in line thickness (see in [19] for a 118 bus system example of such transmission line width variation).

It is noteworthy that the 3D line terrain presented here enhances the 2D line color contour in that the loading of a transmission element is double coded by the height of the triangular prism in

addition to its color. Thus, a severely overloaded short line will stand out in this 3D visualization while it might be hard to perceive in a 2D color contoured one-line. By looking for a dark blue contour and a tall dark red prism in the contingency severity detail visualization illustrated by Figure 3.4 one can easily identify the bus with the lowest voltage and the transmission element with the worst overload, under the contingency highlighted by its severity overview cylinder.

The similar color contour enhancement could also be applied to bus voltage contour, thus resulting in an alternative contingency severity detail visualization as shown in Figure 3.5. The bus contour enhancement is achieved by extruding the color contour of buses along the z-axis in cone shape with their height proportional to the difference between the nominal voltage and the actual voltage. From a comparison between Figure 3.4 and Figure 3.5 it is apparent that the buses with low voltages look more prominent with 3D cones, designated here as “bus terrain”.

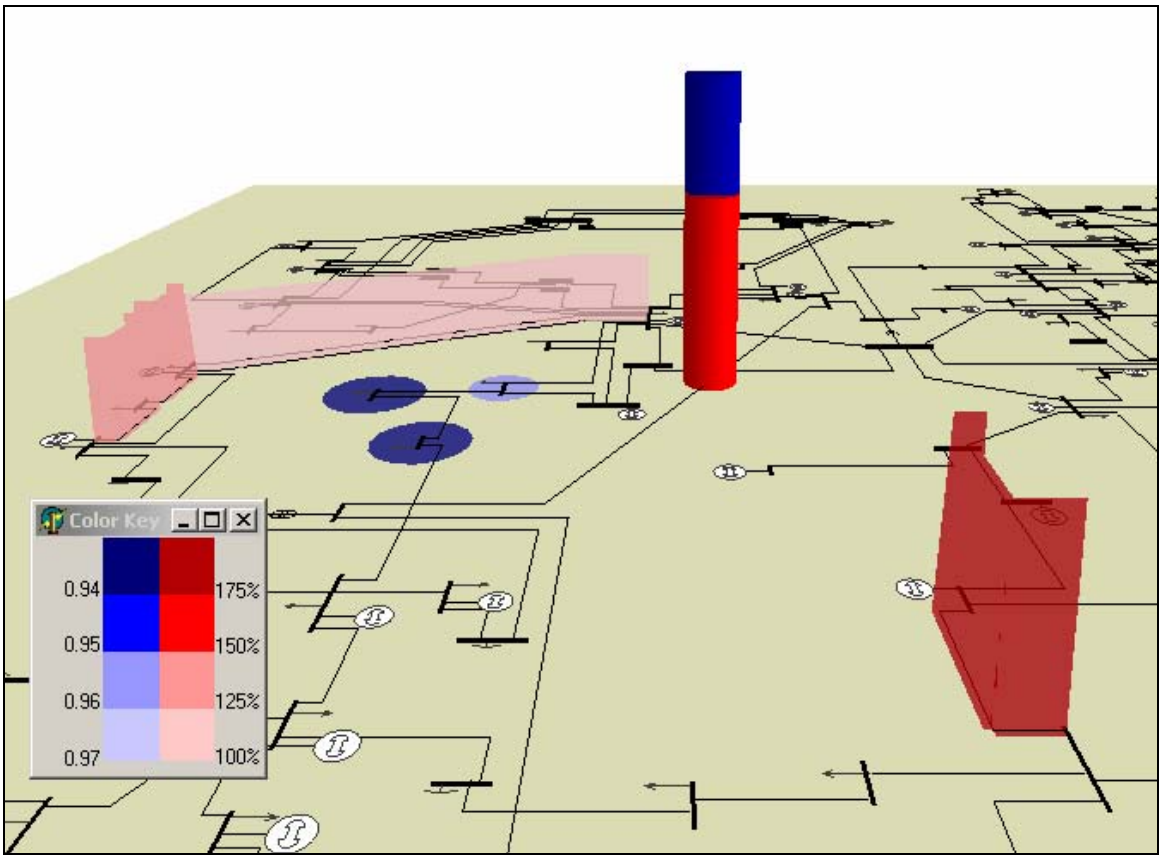

Figure 3.4: Contingency Severity Detail Visualization

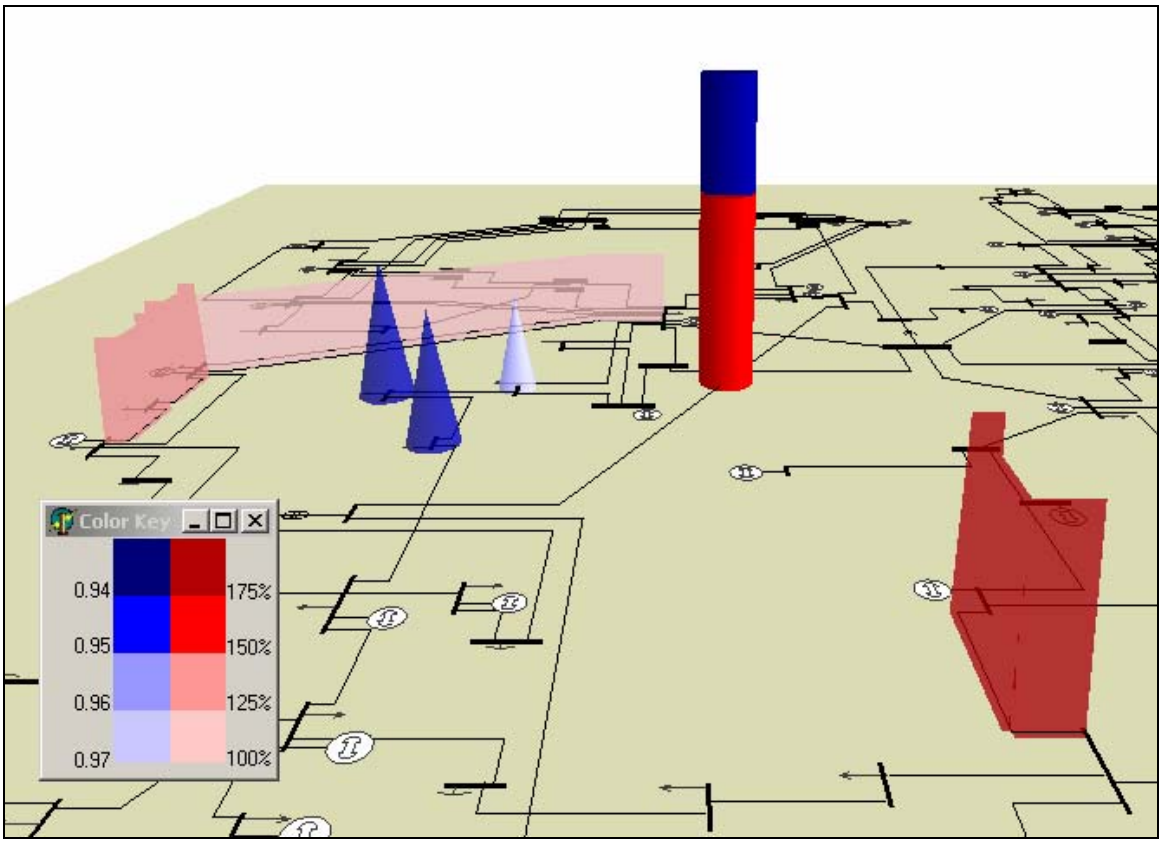

Figure 3.5: Contingency Severity Detail Alternative Visualization

Such prominence not only provides valuable information in contingency data analysis, but also has the potential to aid with corrective controls. Corrective actions for voltage limit violations are often localized because reactive power does not travel well. The search for controllable equipments could be outward from the location of limit violations. Available controls, such as capacitors, could even be highlighted on the one-line. For example, in Figure 3.5 capacitors could be shown using gray cylinders with heights proportional to the available reactive capacities.

3.5 Power System Element Vulnerability Visualization

In contrast to contingency severity information, power system element vulnerability describes the vulnerability of buses and transmission elements in face of contingencies in terms of their post-contingency voltages or loadings. Hence here the primary focus is on the violated element itself, with the different categories of visualizations showing sequentially more detail about the contingencies which cause violations on the element. Again, three different categories are presented: overview, middle-level, and detail.

The power system element vulnerability overview display is similar to the contingency severity overview display, with the following important change. Instead of severity cylinders for contingent elements, reversed cones are now drawn on buses and transmission elements to represent the information extracted from the voltage magnitudes at a bus or the loadings on a transmission element under all single failure contingencies examined. An advantage of using a reversed cone is it takes less one-line space compared to a cylinder. This can be important since

the number of violated elements could be substantially greater than the number of problem contingencies shown in the last section on the contingency severity displays. Another advantage of reversed cones is their footprint on the one-line is much smaller; hence they do not cover their one-line elements, making it easier to see the association between the 3D symbol and the one-line elements. Finally, by using a different symbol the element vulnerability displays and the contingency severity displays are readily distinguishable. Of course, other 3D shapes could certainly be used.

To preserve consistency with the contingency severity displays the coding of the size, color and transparency is the same as from the previous section. That is, the upper radius and the hue of a reversed cone for buses (or transmission elements) convey the lowest voltage (or worst overload) the bus (or transmission element) will undergo under all contingencies while the height of each reversed cone is encoded to show the number of contingencies imposing voltage (or loading) limit violations on the bus (or the transmission element). The same discrete color mapping has also been used with the bus vulnerability cones colored blue and the transmission element vulnerability cones shaded red. A top-level vulnerability display is shown in Figure 3.6, in which the transparency of the reversed cones is again coded according to the corresponding worst limit violation (lowest voltage for buses and worst overload for transmission lines or transformers) to accentuate the most vulnerable elements in the system.

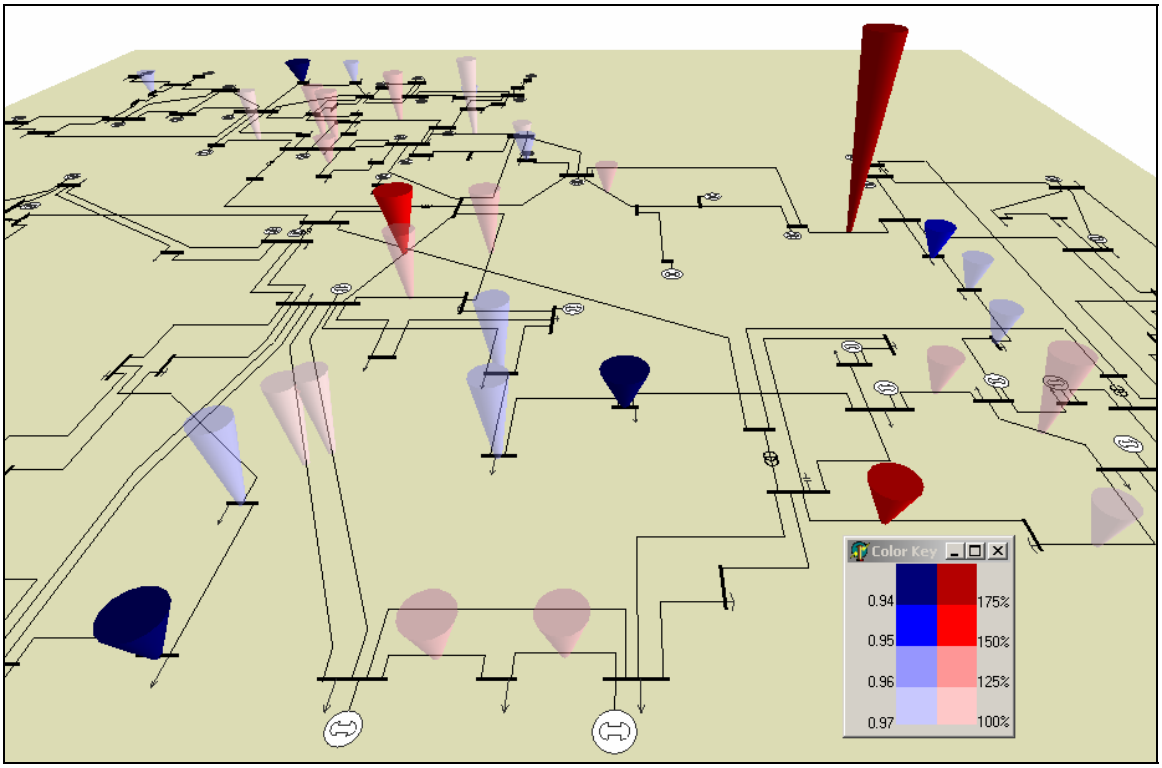

Figure 3.6: Element Vulnerability Overview Visualization

As seen in Figure 3.6, the vulnerable buses and transmission elements, which would suffer contingent limit violations, are highlighted by the reversed cones. The widest and highest dark blue cones pinpoint the most vulnerable buses in the system, while the widest and tallest dark red cones mark the most overloaded transmission elements. Moreover, the pattern formed by the

color of the cones reveals the regions where low voltages and/or overloading are of most concern.

As was the case with the middle-level contingency severity displays, the vulnerability middle-level visualizations use link lines to visualize the geographic connection between the violated elements and the associated contingencies. Again, an interactive process could be used to display the link lines for just a single selected violated element, or a set of violated elements. Such a display is shown in Figure 3.7 for four selected elements. Here, the blue link lines connect the selected low voltage buses with the single element contingencies that cause low voltages at those buses, while the red link lines connect the overloaded transmission elements.

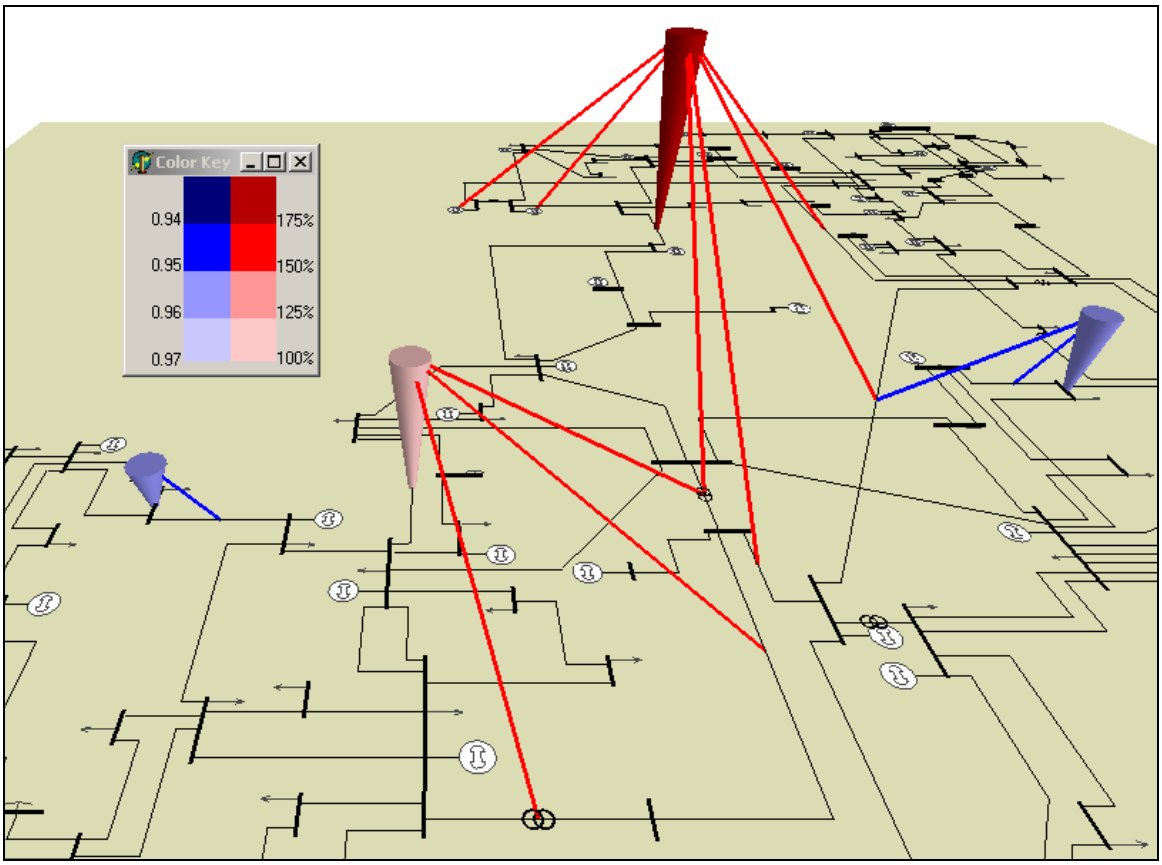

Figure 3.7: Element Middle-Level Visualization

The vulnerability detail category visualizations can be used to provide more detailed information about a single specified bus or transmission element. The approach again uses the 3D "terrain" visualization to show information about the device for each contingency causing a violation. Figure 3.8 demonstrates the vulnerability detail display for a selected transmission line flagged by its red vulnerability cone. Each single-element outage which would impose overloads on the selected line has a terrain visualization (i.e., a triangular prism along the length of the contingent line or transformer, or a cone extruding from the contingent generator). The height, as well as the color of a prism or cone are encoded according to the percentage loading on the flagged line.

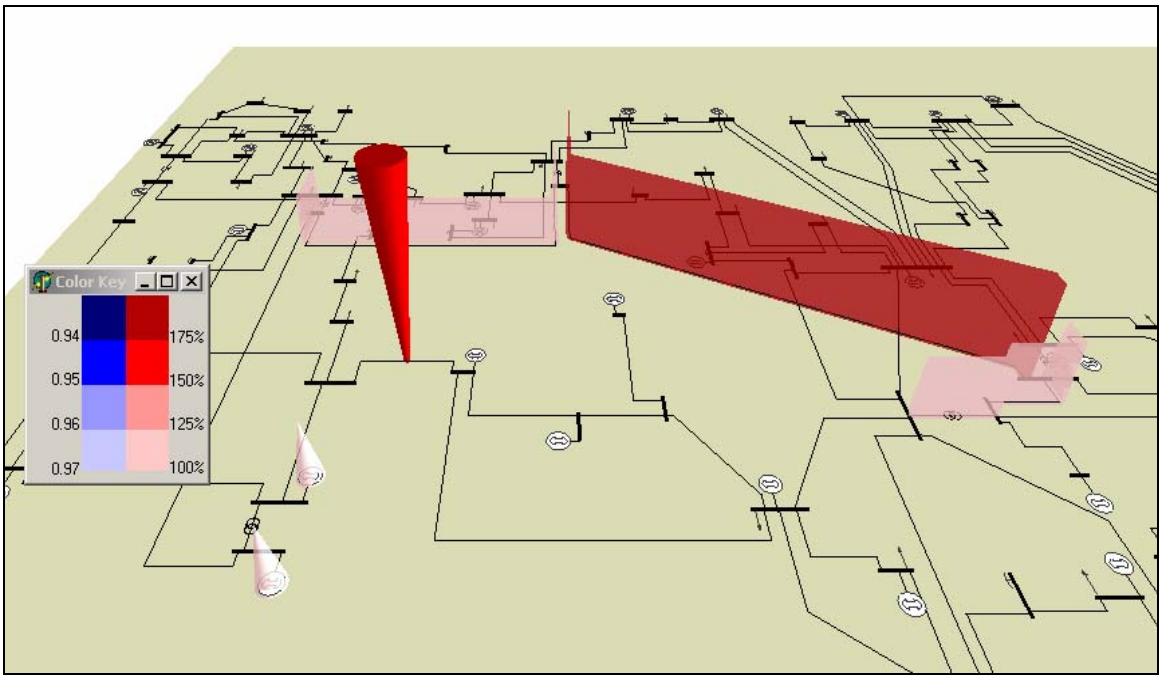

Figure 3.8: Transmission Element Vulnerability Detail Display

Such visualization can also display vulnerability detail information for a bus as illustrated by Figure 3.8. Here, the blue reversed cone signalizes the bus of concern and the blue terrains are associated with the contingent elements which would cause low voltages on the bus when outaged. The height as well as the color of each terrain are mapped to reveal the p.u. voltage at the selected bus for the terrain element contingency. By looking for tall terrains with the colors indicating severe limit violation in the vulnerability detail visualization illustrated by Figure 3.8 and Figure 3.9 one can readily identify the contingency resulting in the worst limit violation on the selected element signaled by the reversed cone.

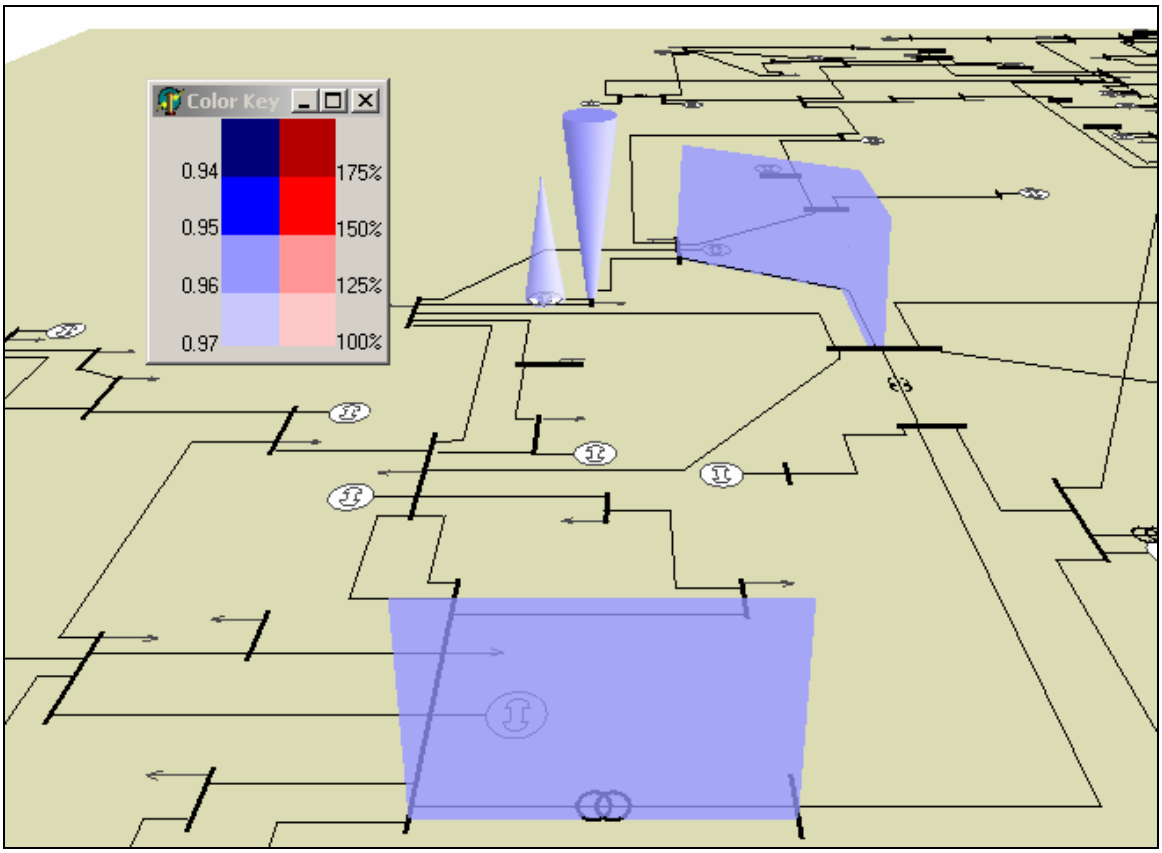

Figure 3.9: Bus Vulnerability Detail Display

3.6 Discussion of Switching among Different Visualizations

Separation of the contingency severity visualizations and the power system element vulnerability visualizations, along with the three-level hierarchy displays, necessitate an interactive interface to move between different displays of different detail levels. Typically two different visualizations would be shown in different windows. However, there is no reason to preclude combining the two.

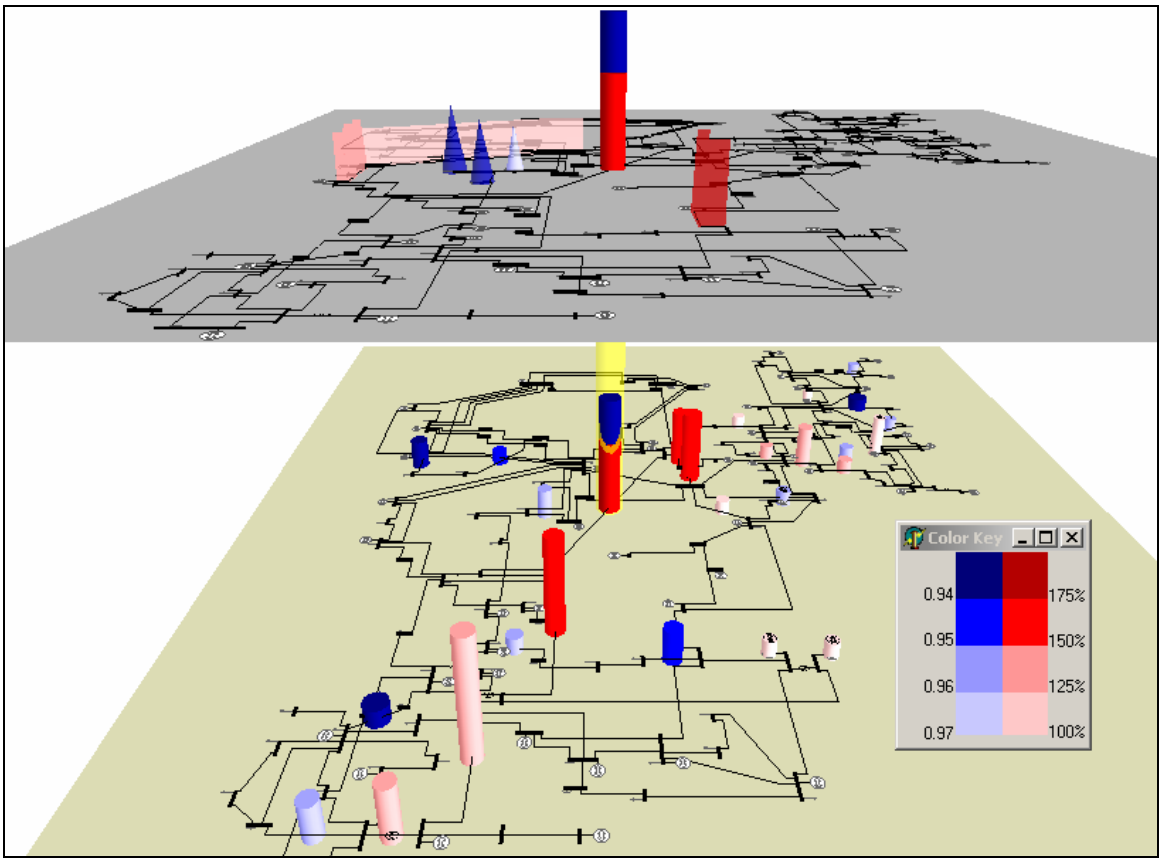

Figure 3.10: Two-Layer Contingency Severity Visualization

Figure 3.10 shows an example of such a two-layer mechanism for a contingency severity display, where the lower layer visualizes contingency severity overview information, and the upper layer displays the detailed severity information of the selected contingency highlighted by the transparent yellow cylinder stretching from the lower layer to the upper layer. Similarly, in Figure 3.11 the two-layer mechanism is used for power system element vulnerability visualization. The lower layer visualizes the vulnerability overview information and the upper layer shows the vulnerability middle-level display for the selected monitored elements again signified by the yellow cylinders.

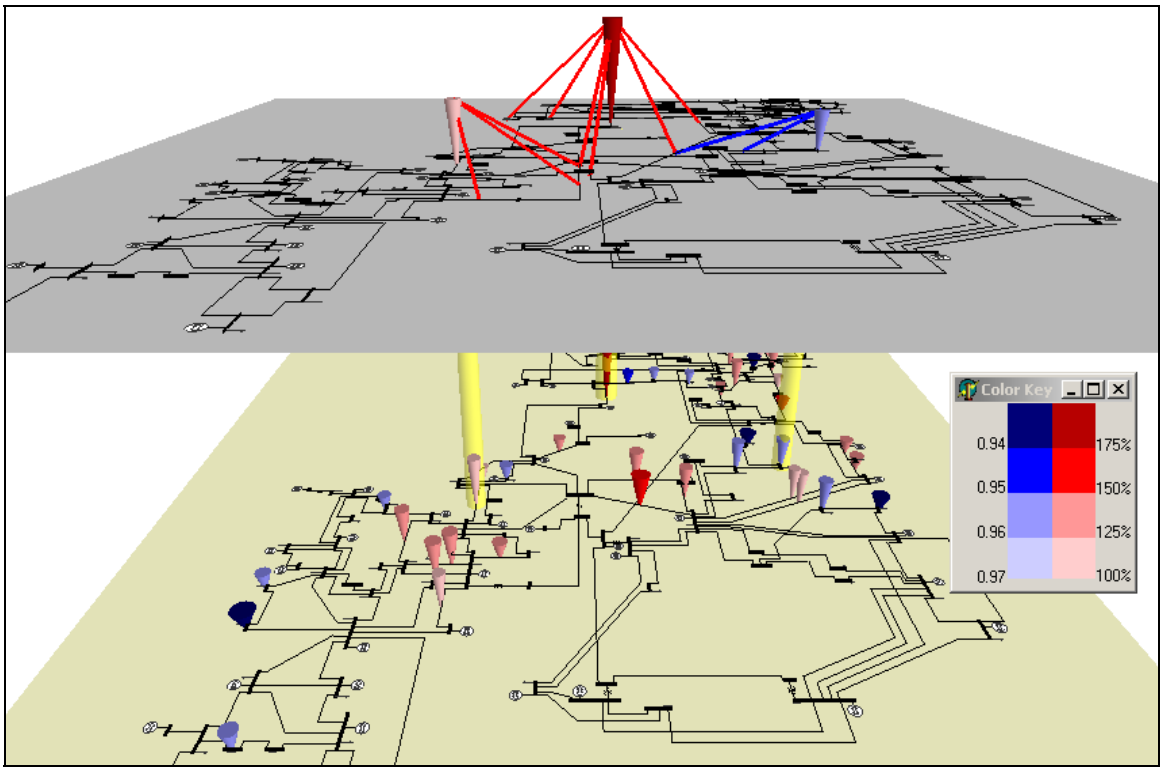

Figure 3.11: Two-Layer Power System Element Vulnerability Visualization

3.7 Conclusions and Future Work

Additional CA result visualizations are needed to help power system engineers and operators more quickly understand the potentially overwhelming amount of data created by a CA study. The research described here has presented several innovative 3D visualizations to provide critical information in different detail levels. This information includes a global view of the system static security level in terms of the CA voltage magnitudes at buses and loadings on the monitored transmission elements, the locations of vulnerable power system elements and the severe contingencies, and the geographical relationships between contingent limit violations and the contingencies themselves.

The voltage violations visualized here have only been for low voltages. Of course, high voltage violations could be displayed using the same approach. In situations where both high and low voltage violations are of concern, they could be distinguished by different colors, for example, blue for low voltages and violet for high voltages. The worst voltage violation for each contingency or each bus, as conveyed by the cylinder in contingency severity displays and the reversed cone for the bus in power system element vulnerability displays, could be defined as the voltage magnitude deviating from the nominal level the most for the contingency or at the bus.

It is worth noting that the visualizations presented here are certainly not intended to completely replace the traditional tabular displays for contingency analysis results, but rather to supplement such lists. Moreover, tabular displays can be integrated into these visualizations when numerical values are needed. For instance, one design could be through the use of popup dialogs showing the matrices discussed in section III in the contingency severity or power system element vulnerability overview display. In middle-level or detail-level displays, the matrices

could be reduced to only keep the rows corresponding to the selected contingencies or contingency, or the columns corresponding to the selected power system element(s).

Concerning directions for future research, one promising approach would be to augment the visualizations to include information about the location of candidate controls to correct the contingent limit violations. For voltage violations, candidate controls could be the reactive power reserve of generators, LTC transformers, and available switched shunts of SVC devices. Example controls for overload correction could include generators with controllable real output, phase shifters and other power electronics devices such as UPFC and IPFC.

A second extension would be the consideration of multiple device and sequential outage contingencies. One potential approach would be to just define additional one-line “elements” representing the multiple device contingencies. For example, if a contingency involves opening three lines sharing a single right-of-way, the new contingency element could be shown on the one-line parallel to the three lines.

Finally, the performance of these candidate visualizations needs to be assessed by formal human factor experiments and, of course, through implementation in actual power system software.

4 Visualization of Power System Components

The system wide visualizations can be nicely supplemented with visualization of the detailed status and operating conditions of important power system devices such as major generators and major transformers. At the device level, system operators would like detailed information that may include the real time capability of the device and/or information as to how much for how long they can overload the device (dynamic rating). Such device specific visualizations can be realized from the available real time data with appropriate processing of this information. We describe here the approach towards this goal and the application of the proposed approach to two important components of the electric power system, i.e., the generator and the transformer.

The technology of intelligent electronic equipment (IED) has advanced to the point that is changing the legacy SCADA systems of electric power systems. The trend has resulted in an explosion of information that is available in real time. This information is available locally (at the substation) or most times it is communicated to the control center. While the amount of available information has exploded, the efficient utilization of this information by operators has been lagging. It is clear that new methods of manipulating the available information and presenting this information to the operator in a meaningful way are needed. Extensive efforts are under way towards this goal. One particular approach is to present this information to the operator with animated visualization techniques. In this approach, the visualized information can be raw information collected by legacy SCADA systems and/or supplemented by IEDs or it can be filtered data via the traditional state estimator. The results presented here are an attempt to push this approach a little bit further. Specifically, it is possible to utilize available real time data for extracting more detailed operational models of power system components. For example, the combined SCADA and IED data can be used to extract a real time electro-thermal model of a transformer, of a generator, etc. The advantage of this approach is that the real time electro-thermal model can be used to determine a multiplicity of useful information, for example, transformer hot spot temperature, loss of life of the transformer, dynamic loading limits, etc. This information can be presented to operators in an animated visualization. Since today's electric power systems are operated ever closer to limits, this approach can be quite useful to operators.

The overall approach is illustrated in Figure 4.1. The figure illustrates the present SCADA structure of an electric power system. The SCADA data are collected at a central location, the control center or the Energy Management System, for processing, state estimation, displays etc. The present approach is to estimate bus voltages and circuit flows and display this information to system operators. We propose that this data can be used for extracting additional information and providing additional useful information of system operators. For example, system operators are very much interested in dynamic loading of various components of the system. What we propose can achieve the objective of providing dynamic loading information to system operators in an animated fashion. The approach is straightforward. Consider a specific power system apparatus, for example a transformer. One can extract from the SCADA database all the information pertinent to this device. It is also important to point out that when we speak of SCADA data here, we mean all available information that exists. This will be traditional SCADA data and additional data from intelligent electronic devices in a substation. Now consider a transformer model that is suitable for advanced applications such as dynamic loading. In this particular case, an electro-thermal model of the transformer is suitable. Using the existing data and the selected model of the device, a state estimation problem is defined for the purpose of extracting the real time model of the device from the existing data. This is a specialized state estimation problem. Once this procedure has been completed the electro-thermal model of the transformer is

available for utilization in real time. The model is subsequently utilized for visualization of the component status, prediction of dynamic loading, etc.

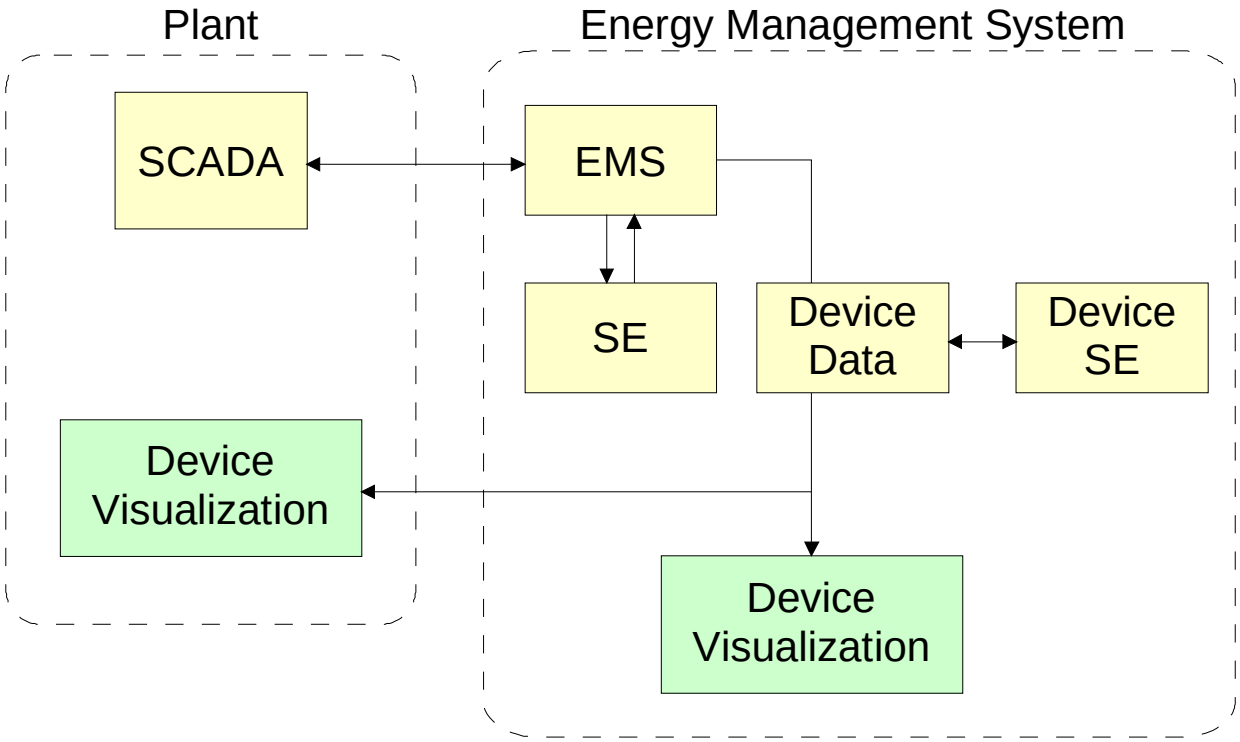

Figure 4.1: Illustration of the Overall Approach for Power Component Visualization and Animation

During this project we have applied this basic approach to two major components of the system: (a) generators and (b) transformers. In subsequent paragraphs the generator and transformer models are presented, their extraction from real time data and visualization applications of these components are demonstrated.

4.1 Generators

Generators are very important components of the system and their status affects operating procedures. Knowledge of the exact operating condition and margins of generators in real time is very important information to operators. This section presents the basic approach for visualization and animation of a generator. We have selected to use a simplified electro-thermal model for the specific purpose of predicting generator thermal status and operational margin in real time. The complete electro-thermal model of a generator is very complex. In this project we used a simplified model to simply demonstrate the ideas. The simple model can be replaced with more sophisticated models for actual implementation of the method. We describe the extraction of the electro-thermal model of a generator from real time data and its utilization to determine operating status and margins from limits. The model is subsequently visualized and animated so that the operator can have a “revealing” picture of the operating condition and limitations in one simple glance. The approach is demonstrated with the aid of a power system simulator. The

power system simulator uses a time function electric load model. As time progresses, the electric load varies and drives the operation of the system. At each instant of time the overall system operating conditions are determined via a power flow solution for the specific load level at that instant. The SCADA system is simulated by extracting data from the power flow solution and providing inputs to the estimators that extract the real time generator model. The estimated electro-thermal models are presented via animation and visualization techniques. The overall approach is demonstrated on an example electric power system, the IEEE RTS system. The system has been modified to include a time function electric load model. Snapshot displays of the animations are also presented in this report. Live demonstrations of the animations have been given in various PSERC meetings.

4.1.1 Generator Electro-Thermal Model

Generator terminal voltages and currents, stator winding temperatures and possibly tank temperature, ambient temperature, etc. may be monitored via a variety of devices, for example, SCADA, relays, metering devices, etc. We assume that this data is available at the control center via the available communication channels. This data is streaming into the control center at regular time intervals determined by the SCADA scanning rate. We utilize this data to extract the real time model of the generating unit. The structure of the model is described next following by the computational procedure to identify the parameters of the model.

The selected generator model is illustrated in Figure 4.2. It is a two-axes model. The electric power model of this generator is expressed with:

$$\begin{aligned}
\tilde{V}_a &= -r(\tilde{I}_d + \tilde{I}_q) - jx_d\tilde{I}_d - jx_q\tilde{I}_q + \tilde{E} \\
\tilde{V}_b &= -r(\tilde{I}_d + \tilde{I}_q)e^{-j\frac{2\pi}{3}} - jx_d\tilde{I}_d e^{-j\frac{2\pi}{3}} - jx_q\tilde{I}_q e^{-j\frac{2\pi}{3}} + \tilde{E}e^{-j\frac{2\pi}{3}} \\
\tilde{V}_c &= -r(\tilde{I}_d + \tilde{I}_q)e^{-j\frac{4\pi}{3}} - jx_d\tilde{I}_d e^{-j\frac{4\pi}{3}} - jx_q\tilde{I}_q e^{-j\frac{4\pi}{3}} + \tilde{E}e^{-j\frac{4\pi}{3}} \\
\tilde{I}_a &= \tilde{I}_d + \tilde{I}_q \\
\tilde{A} &= \tilde{V}_a + r\tilde{I}_a + jx_q\tilde{I}_a \qquad \text{q-axis vector}
\end{aligned} \tag{4.1}$$

In addition to the above electrical model, the thermal model of the generator (very simplified, only two states, the stator temperature and rotor temperature) is:

$$C\frac{d}{dt}T = -GT + Q \tag{4.2}$$

where:

C is the thermal capacitance matrix,
G is the thermal conductance matrix,
T is the temperature vector, consisting of the rotor and stator temperatures, and
Q is the heat source vector.

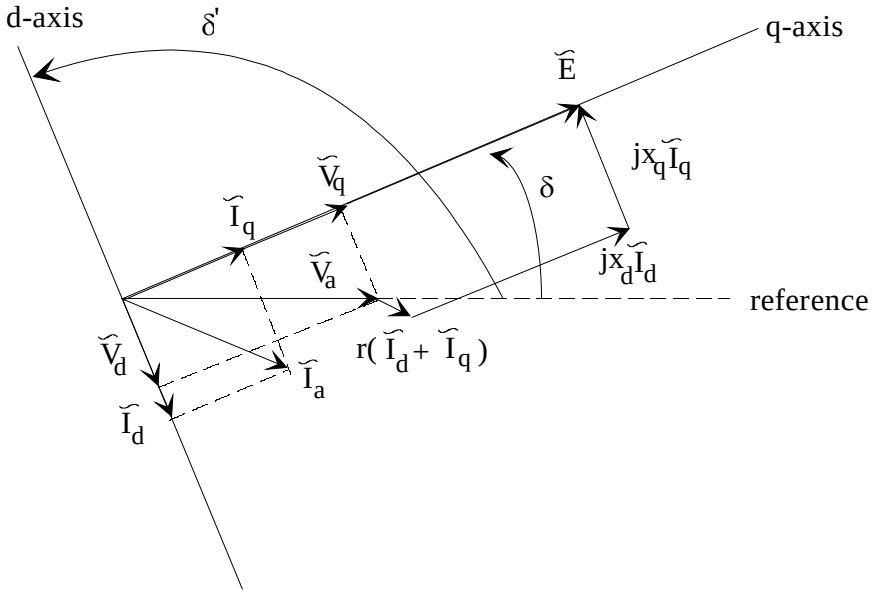

Figure 4.2: Phasor Diagram of Phase A of a Synchronous Machine

While one can use real time model to perform a state estimation procedure to derive the real time model of the generator, we elected to use a simpler procedure for extracting the real time model. A graphical solution for extracting the real time model is utilized as it is illustrated in Figure 4.3. The steps of the graphical construction are as follows (assuming that the terminal voltage and current of the generator have been extracted from the SCADA data). Step 1: From the tip of the phasor $\tilde{V}_a$ draw the phasor $r\tilde{I}_a$. Step 2: Draw the phasor $jx_q\tilde{I}_a$. The line OA defines the q-axis, i.e., the angle δ. Step 3: Compute $\tilde{I}_d$, $\tilde{I}_q$ as projections of $\tilde{I}_a$ on the d and q-axes and complete the diagram.

The generator thermal model is estimated from measurements of ambient temperature and stator temperatures (which are readily available) with a procedure identical to the one used for the transformer model (see next section).

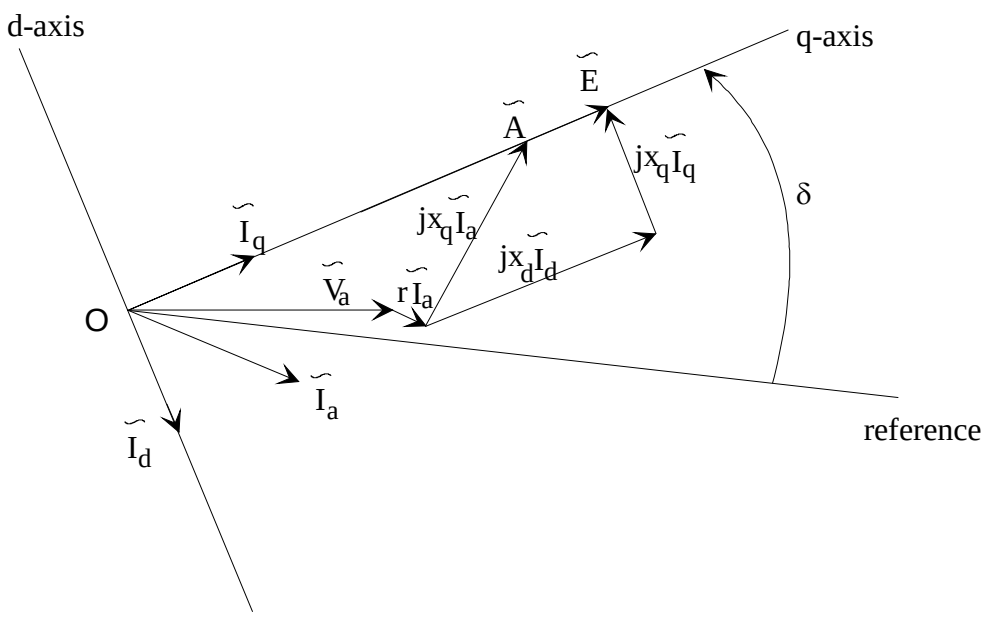

Figure 4.3: Graphical Solution for Determining the Position of the q-Axis

Once the real time electro-thermal model of the generator is obtained from above procedure, the model is utilized to make projections. Examples are: (a) using equations (4.2) with initial conditions the present real time model, one can predict what will be the evolution of generator temperatures over the next 30 minutes, (b) assuming a step change in power and using equations (4.2) with initial conditions the present real time model, one can predict what will be the evolution of generator temperatures over the next 30 minutes, (c) from the real time model one can compute the capability region of the generating unit and then superimpose the present operating point so that the operator can observe at a glance what are the operating margins, (d) the operation of the generating unit can be visualized in terms of generated voltage, magnetic fluxes, etc. Note that the possibilities are many. In the next section, few of these possibilities are discussed with the specific objective of generating useful visualizations.

4.1.2 Generator Visualization and Animation

The computed real time generator electro-thermal model, temperatures and dynamic loading can be effectively visualized using 2D and 3D graphics. Using the generator electro-thermal model within a time domain simulation of a power system, we compute the capability curve of the generator, and plot it along with the generator operating state, as illustrated in Figure 4.4. The figure also includes a phasor diagram indicating the generator voltage and current phasors. Both terminal and internal voltages are displayed. The phasor and capability diagrams are dynamically updated each time the corresponding quantities are estimated from real time data. This results in an animated display that provides the generator dynamic loading capability at a glance. As generator power output changes, a trace is plotted (blue line) while the current state is represented by the circled cross symbol.

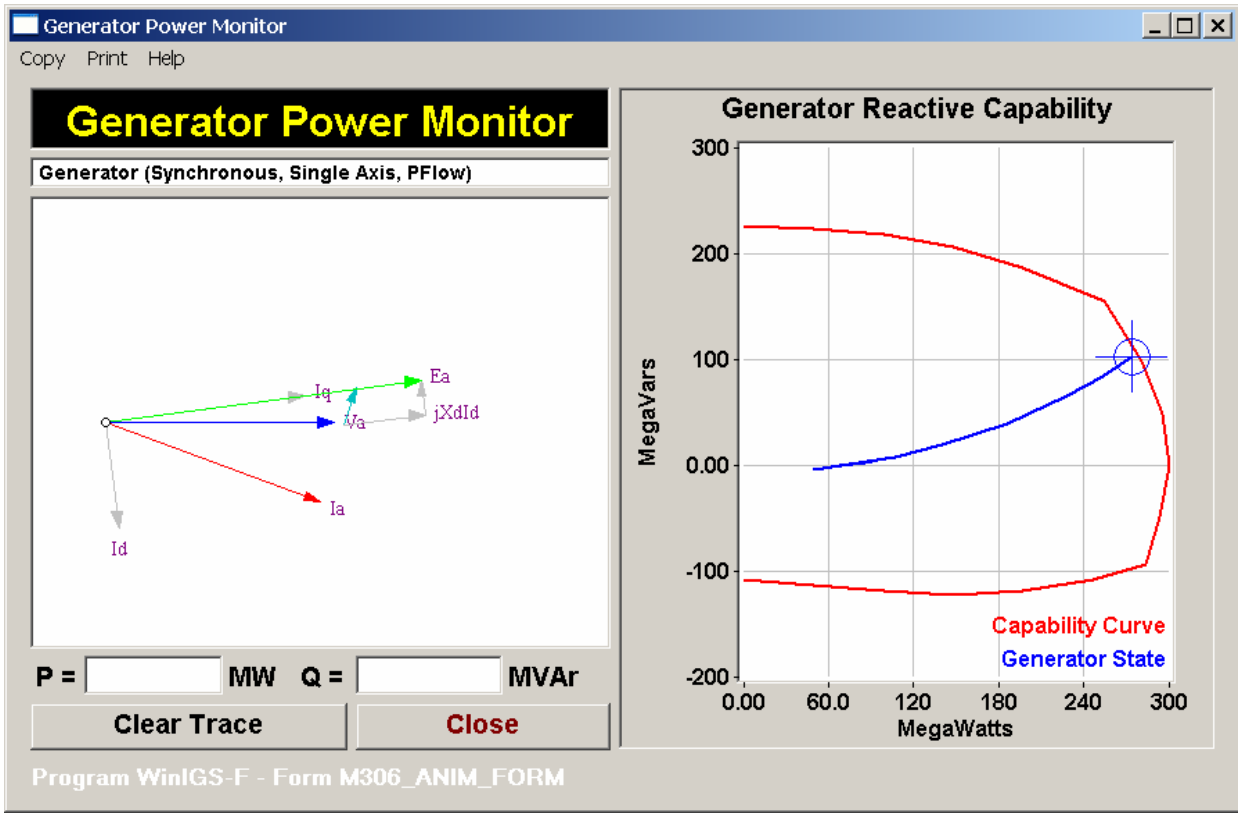

Figure 4.4: Animated Generator Power Monitor

In order to provide a more detailed generator operating state display, an animated 3D model is used. The 3D model is constructed using 3D CAD software. It includes the generator and exciter case, armature, rotor and corresponding windings, as it is illustrated in Figure 4.1. The model is exported from the CAD software in a standard file format (ASE). The file contains the component geometry in the form of quadrilateral elements, with associated material visual properties (color, shininess, texture etc) for appropriate image rendering. The quadrilateral vertex coordinates, and material properties are hierarchically organized so that major components can be readily identified and associated with appropriate temperatures, fields, or motions in real time. Figure 4.2 illustrates a fragment of an example ASE file.

The described 3D generator image is used to facilitate visualization of generator parameters that are distributed over the various components, such as magnetic fields, and temperature distributions. Fields can be displayed as translucent plots or clouds, superimposed over the generator image, and animated along with the corresponding rotor motion. Temperature distributions can be represented by color coded gradients painted over the corresponding components (case, armature, windings etc). At any time, the user can rotate, zoom and pan the displayed model, in order to examine the displayed fields and temperatures from any desired point of view. The generated image is updated as time progresses providing an animated view of the generator operating state.

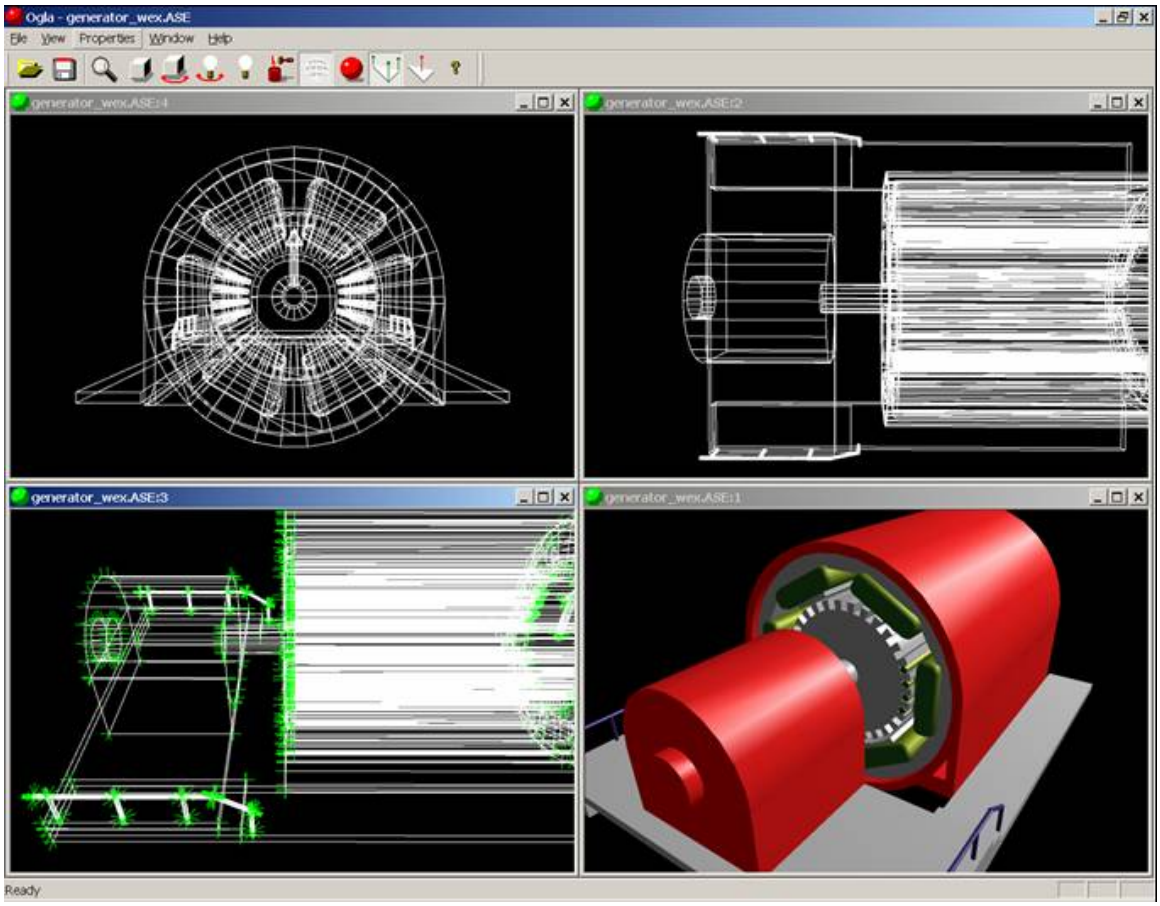

Figure 4.5: Examples of Generator 3D Images

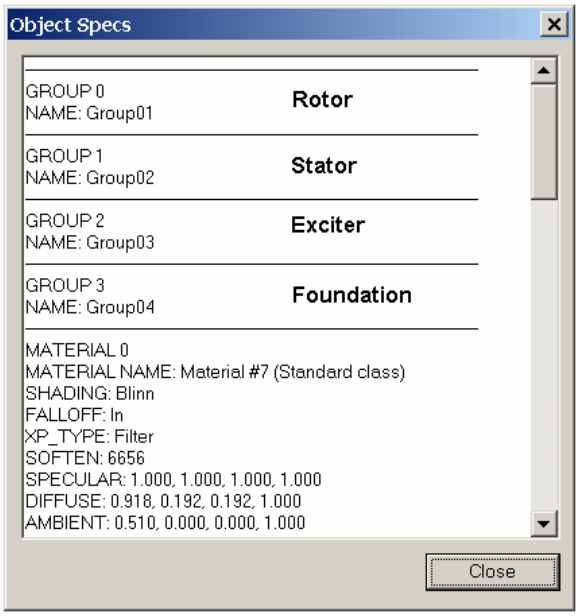

Figure 4.6: Example fragment of a standard file format (ASE)

4.1.3 Generator Simulated Demonstration

The proposed approach for generator monitoring has been demonstrated using time domain simulation. The simulated system is the 24 bus IEEE RTS. This system is loaded with a time varying electric load. At pre-specified intervals, the computed generator terminal voltages and currents are passed to the generator electro-thermal model. This model estimates the generator temperature distribution, and the dynamic loading capability of the generator. The results of these analyses are fed into the generator visualization module.

4.2 Transformers

This section presents the basic approach for visualization and animation of a power transformer. For the transformer we have selected to use its electro-thermal model for the specific purpose of predicting transformer temperatures and loading capability of the transformer in real time. We describe the extraction of the electro-thermal model of a power transformer from real time data and its utilization to determine (a) hot spot temperature, (b) loss of life and (c) transformer dynamic loading. The electro-thermal model is subsequently visualized and animated so that the operator can have a "revealing" picture of the operating condition and limitations in one simple glance. The approach is demonstrated with the aid of a power system simulator. The power system simulator uses a time function electric load model. As time progresses, the electric load varies and drives the operation of the system. At each instant of time the overall system operating conditions are determined via a power flow solution for the specific load level at that instant. The SCADA system is simulated by extracting data from the power flow solution and providing inputs to the estimators that extract the real time transformer and generator models. The estimated electro-thermal models are presented via animation and visualization techniques. The overall approach is demonstrated on an example electric power system, the IEEE 24 bus RTS system. The system has been modified to include a time function electric load model. Snapshot displays of the animations are given here. Live demonstrations of the animations have been given in various PSERC meetings.

Subsequent paragraphs present the transformer electro-thermal model, the estimation of the real time electro-thermal model from SCADA data and additional real time data and specific results from the real time electro-thermal model, such as hot spot temperature, loss of life and transformer dynamic loading. All of this information is visualized and animated. We also describe the simulation environment for the demonstration of these ideas and provide snapshots of the visualizations.

4.2.1 Estimation of Transformer Electro-Thermal Model

Transformer terminal voltages and currents, tap position and possibly tank temperature, ambient temperature, top of oil temperature may be monitored via a variety of devices, for example, SCADA, relays, metering devices, etc. We assume that this data is available at the control center via the available communication channels. The collected data is illustrated in Figure 4.3. This data is streaming into the control center at regular time intervals determined by the SCADA scanning rate.

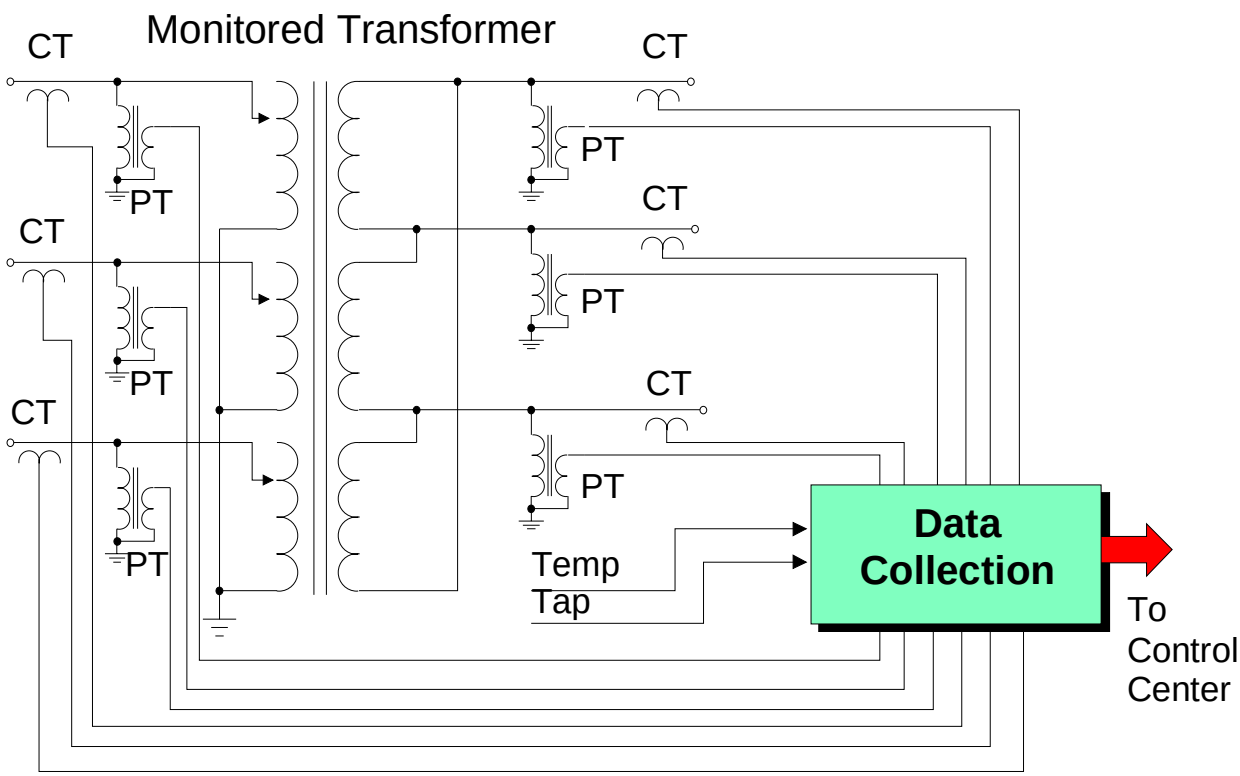

Figure 4.7: Transformer Monitoring System Configuration

This data is utilized to determine a real time electro-thermal model of the transformer. Subsequently the real time model is utilized to compute the loss of life of the transformer and the available dynamic loading margin. The three computational procedures will be described next.

4.2.2 Real-Time Electro-Thermal Model

The electro-thermal model estimates the internal transformer temperature distribution from the measured quantities, i.e., the transformer terminal voltages and currents, top oil temperature, tank temperature, load tap changer position, and ambient temperature.

Figure 4.4 illustrates the equivalent circuit of the transformer electro-thermal model. It consists of 12 temperature nodes corresponding to six coil temperatures, three magnetic core temperatures, oil, tank, and ambient temperature. A capacitor is connected at the coil, core, oil, and tank nodes, representing the thermal capacity of the corresponding components. A resistive network links the 12 nodes. This network represents the thermal conductances among the various components. A higher order model can be used for increased precision.

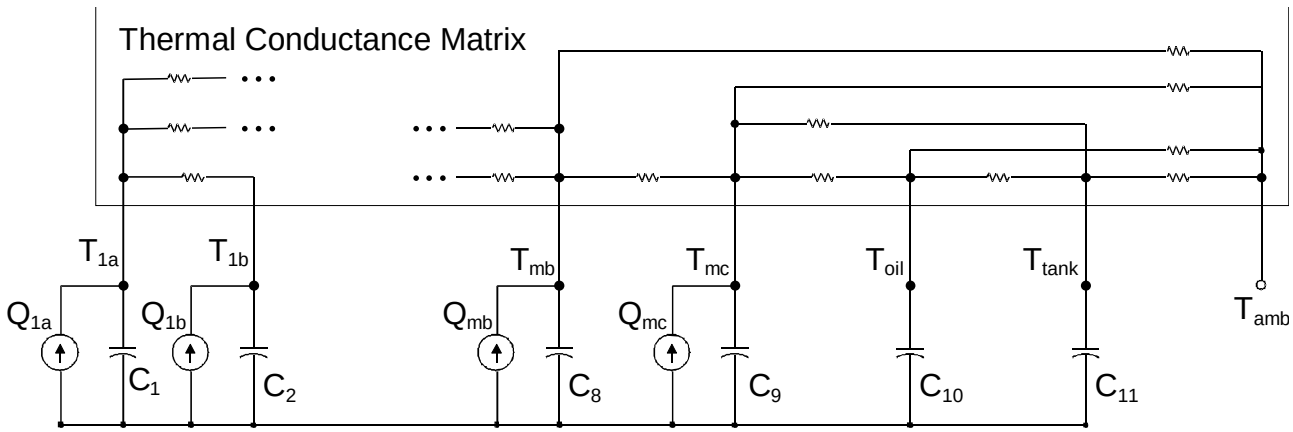

Figure 4.8: Transformer Thermal Model Equivalent Circuit

The dynamics of the above network are described by the following differential equation:

$$C\frac{d}{dt}T = -GT + Q \tag{4.3}$$

where:

C is the thermal capacitance matrix,
G is the thermal conductance matrix,
T is the temperature vector, and
Q is the heat source vector.

The thermal capacitances are computed from the volume and the specific heat constant of the corresponding components. The thermal conductances are estimated from known temperature gradients between coils, oil, tank, and the environment.

The transformer losses are computed from the measured voltage and current waveforms at the transformer terminals. Computed losses include winding ohmic losses as well as magnetic core losses. These losses are treated as heat sources in the electro-thermal model (Q1a, Q1b,…,Qmc). For a three-phase transformer (delta-wye or autotransformer) a total of nine heat sources are computed: six winding ohmic losses and three magnetic core losses (one for each magnetic core leg). These heat sources are shown in Figure 4.4.

Coil losses are computed by multiplying the coil resistance by the squared value of the RMS winding currents. For a three-phase transformer (delta-wye or autotransformer) a total of six winding heat sources are computed. Core loss is a function of the core magnetic flux. The model estimates the flux from measurements and then the core loss is computed. The end result of the estimation module is the state of the electro-thermal model in real time. This model is used to compute the loss of life and the dynamic loading of the transformer.

4.2.3 Transformer Loss of Life

The real-time model of the transformer provides an estimate of the hot spot of the transformer in real time. Specifically, the hot spot temperature is defined as the highest temperature anywhere along the coils of the transformer. Then, the loss of life of the transformer is computed

per IEEE-ANSI standard 57 using the hot spot temperature.

This calculation is based on the ANSI/IEEE C57.91-1981. Specifically, the per unit loss of life, (LOL), of the transformer in the time interval (t-h,t) is computed with the formula:

$$LOL = \exp(-(A + \frac{B}{\tilde{T}}))h \tag{4.4}$$

where:

$\tilde{T}$ is the average hot spot temperature over the time interval (t-h,t) in degrees Kelvin

A, B are constants dependent on transformer design

The above equation is integrated over time to provide the loss of life over this time. The loss of life result can be better appreciated when normalized. The normalization is provided with the following equation.

$$LOL_{pu} = \frac{\int_0^T e^{-\left(A+\frac{B}{\tilde{T}}\right)} dt}{T} \tag{4.5}$$

where T is the elapsed time.

It is known from the standard that if the transformer operates under constant hot spot temperature equal to the permissible value, the normalized LOL will be exactly 1.0. Therefore the above index provides the information that the transformer is losing its life faster than normal if greater than 1.0 and its life is being extended if less than 1.0.

4.2.4 Transformer Dynamic Loading

The objective of the transformer dynamic loading capability is to answer the following question: if the transformer loading is suddenly increased to P, how long it will take until the hot spot temperature of the transformer reaches the maximum permissible value? This information is useful in an emergency since it will let us know for how long we can overload the transformer without exceeding manufacturer's specifications.

The dynamic loading pairs (P,t) are computed via time domain simulation of the transformer operation. The initial conditions are determined by the present operating conditions. The voltages applied to the transformer are assumed constant. The load of the transformer is assumed to be P. Then the differential equations describing the electro-thermal model (1) of the transformer are numerically integrated. Specifically, using trapezoidal integration over the time interval (t-h,t) on equation (4.3) yields:

$$T(t) = \left(\frac{2C}{h} + G\right)^{-1} \left(\left(\frac{2C}{h} - G\right) T(t-h) + 2\tilde{Q}\right) \tag{4.6}$$

where:
C is the thermal capacitance matrix,
G is the thermal conductance matrix, and
$\tilde{Q}$ is the average value of the heat sources over the time interval h

By repeatedly evaluating equation (4.6), the transformer temperatures are computed as a function of time. From the temperatures T(t), the hot spot of the transformer is extracted. When the permissible hot spot temperature is reached, the time t is recorded, yielding the pair (P,t). This procedure is repeated for different values of transformer loading P, yielding a number of pairs (P,t). This data is plotted providing the dynamic loading curve of the transformer.

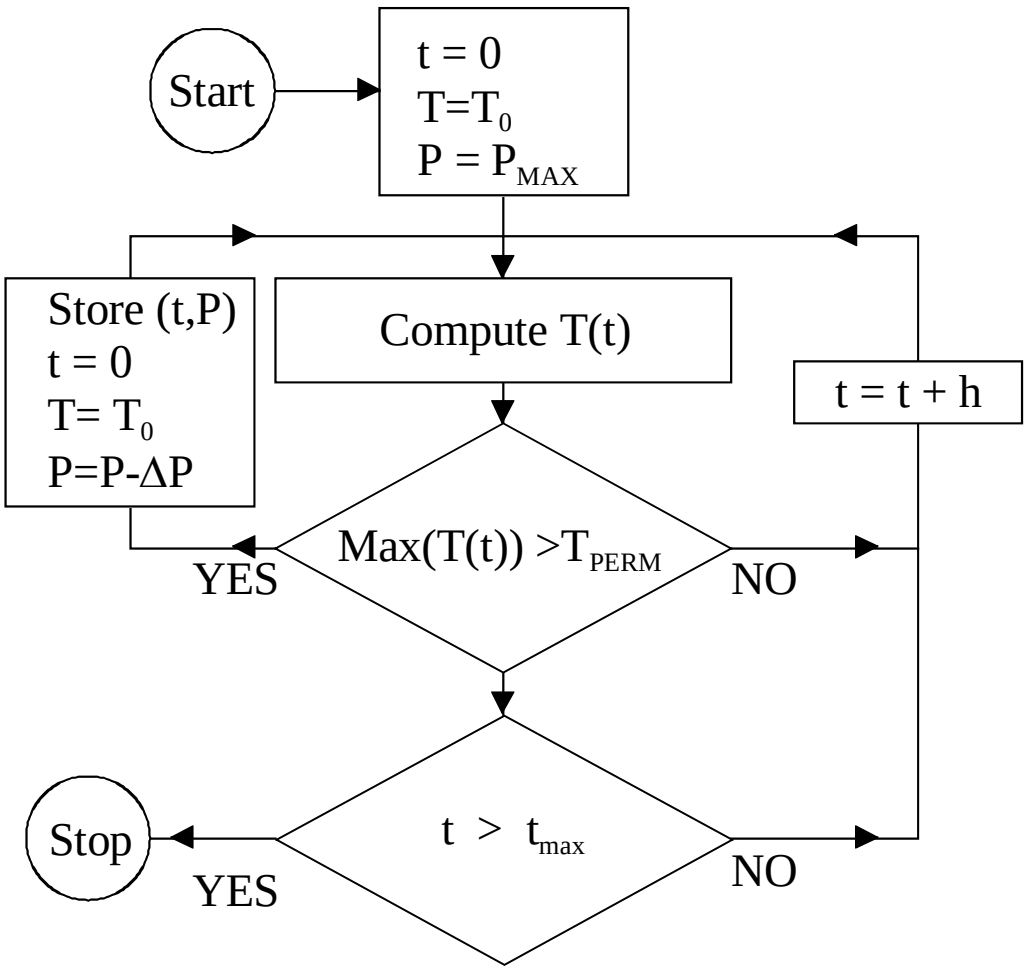

Figure 4.9: Dynamic Loading Algorithm Flow Chart

The overall algorithm for computing the pairs (t,P) is illustrated in Figure 4.5. A series of simulations is performed all starting with initial temperature values (T_0) taken from the present operating conditions of the transformer. Each simulation assumes a different transformer total power, P, within a user selectable range. The transformer terminal voltages and power factor are assumed constant and equal to those voltages and power factor of the present operating

conditions. The terminal currents are computed from the known voltages, power factor and the assumed power P. Then, the heat source vector Q used for the simulations is computed as described in the section 'Real time electro-thermal model' from the transformer terminal voltages and currents.

Each simulation is carried out until the transformer hot-spot temperature reaches the maximum allowable value (T_{PERM}). The maximum allowable hot-spot temperature is a user-specified quantity. The first simulation starts at the maximum power loading P_{MAX} (typically about 2.5 p.u.). Then the power is reduced and the simulation is repeated until a power level is reached where the hot spot temperature is not reached for a certain simulation time limit t_{MAX} (typically 90 minutes). The results of the simulations are presented as a plot of transformer loading versus time to hot-spot temperature limit (as illustrated in Figure 4.6).

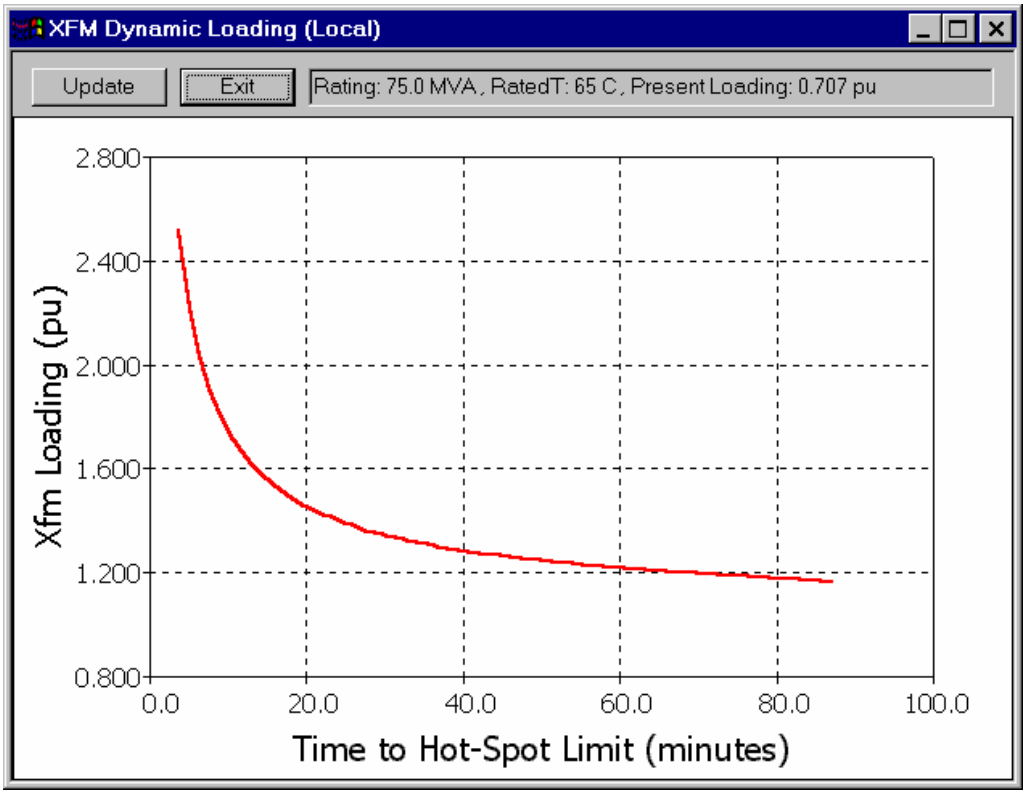

Figure 4.10: Transformer Dynamic Loading Display

4.2.5 Transformer Visualization and Animation

The computed real time electro-thermal model, temperatures and dynamic loading can be visualized. The visualization may be updated as time progresses providing an animated impression of the operation of the system. The visualization of the transformer can be implemented in a variety of ways. We have elected to build a 3D model of the transformer and color code the temperatures of the various parts of the transformer. The 3D model can be rotated, paned, zoomed, etc. so that the user can take as close a view of the operating conditions of the transformer as he/she desires. Figure 4.7 and Figure 4.8 illustrate two stills of the visualization representing different operating conditions of the same transformer. Note that in Figure 4.7 the

temperatures of the various transformer coils are quite different indicating an unbalanced operation. This type of application obviously requires three phase measurements and three phase network solutions. Figure 4.8 illustrates near balanced operating conditions. Figure 4.6 provides the transformer dynamic loading for the condition of the transformer of Figure 4.8. It is important to note that in real time applications (or simulated demonstrations) all visualizations can be displayed simultaneously. It is also important to note that in a real time application, the transformer temperatures do not change very fast. This means that the animation of the transformer conditions may be updated at a relatively low rate.

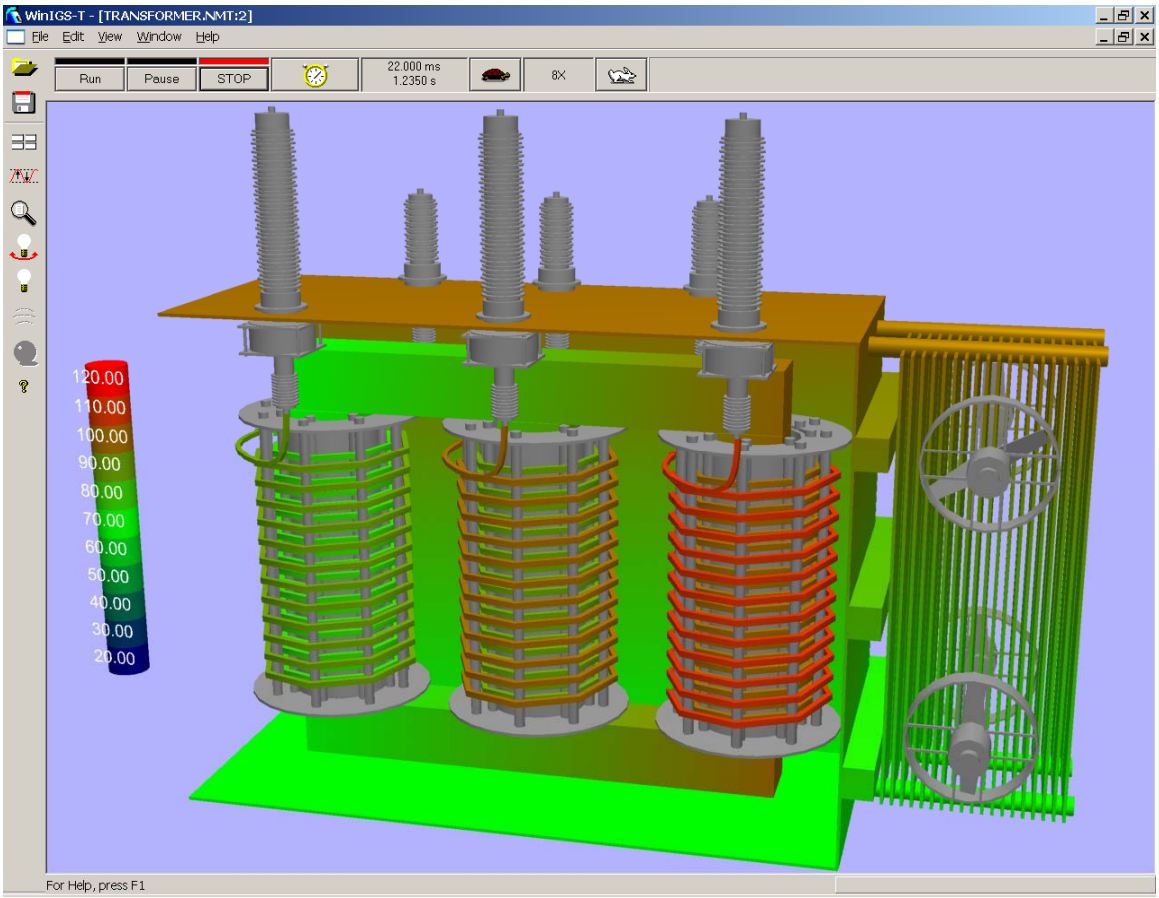

Figure 4.11: Transformer 3D Model View with Color-Coded Temperatures – View 1

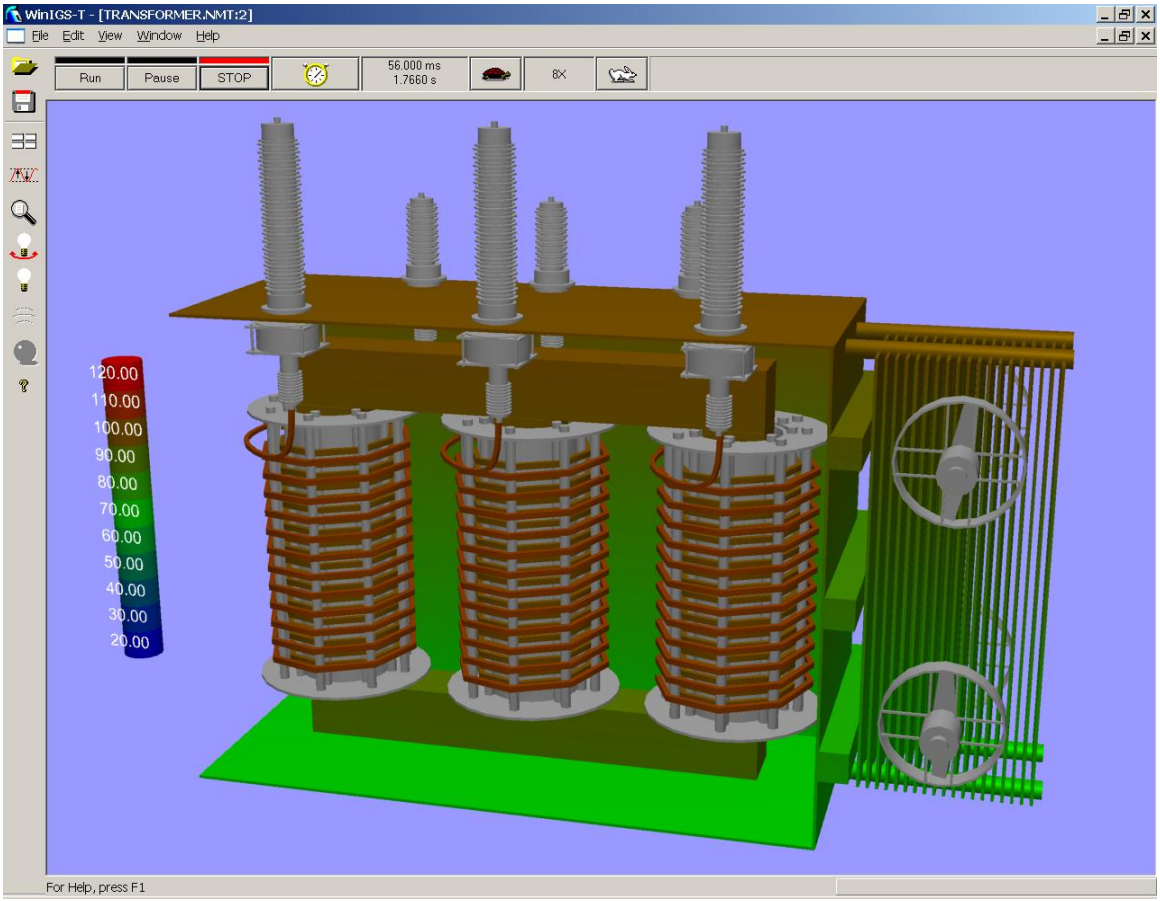

Figure 4.12: Transformer 3D Model View with Color-Coded Temperatures – View 2

4.2.6 Transformer Simulated Demonstration

In order to demonstrate the proposed approach for transformer monitoring and evaluation, we use the 24 bus IEEE RTS. This system is loaded with a time varying electric load. At pre-specified interval, the power flow problem is solved and the results are passed to the transformer monitoring and evaluation system. This system estimates the electro-thermal model of the transformer, computes the transformer temperatures, loss of life, and the dynamic loading of the transformer. The results of these analyses are fed into the transformer visualization module. As time passes, the operation of the transformer is viewed in an animated way. Figure 4.7 andFigure 4.8 present stills of this animation.

5 Human Factors Testing

The last portion of the project focused on the performance of formal human factors experiments to evaluate the effectiveness of the new visualizations developed in Chapters 2 and 3. Overall, four experiments were conducted over the length of the project with each experiment involving undergraduate electrical engineering students recruited from the power systems classes at the University of Illinois at Urbana-Champaign. The first two experiments looked at the impact of motion on power system visualizations while the last two experiments looked at 3D. In all experiments each participant was required to have either completed, or be currently enrolled in, at least one class in the electric power systems area. Therefore, all participants had at least some familiarity with basic power system terminology and the use of one-line system models. The participants worked independently and were paid a nominal amount for their one hour participation in the experiments. This chapter provides the key results for these experiments, with more details provided in the Chapter 7 publications.

5.1 Motion Experiments

The first two experiments focused on the impact of motion (animation) on power system visualization. Many of the results given in this section were presented earlier in [20]. Power engineers have long been concerned with studying how power (real, reactive and complex) flows through the transmission network. As the transmission system models have increased in size, with large models now having tens of thousands of buses and lines, the question of how to represent the results has grown in importance. Numeric fields on one-lines and tabular listings showing the exact power flows and percentage loadings can be crucial. But for medium to large systems such approaches need to be supplemented to give an overall view of the system. More recently, due to the growing popularity of power transfer distribution factors (PTDFs) [21], [22], the flow representation issue has also been expanded to include PTDFs. PTDFs are used extensively in the operation of the North American electric grid.

Several approaches have been suggested in the literature to supplement numeric fields for transmission flow visualization, including dynamic sizing of the transmission line size on the one-line [2], [3], animated flows [23], [24], and dynamically sized pie charts to show the percentage loading of the lines.

A survey of the broader human factors literature is promising, since animated displays have been shown to improve operator performance in other disciplines in a variety of ways [25], [26], [39]. For example, motion can help operators interpret displays by directing their attention to the most important information for a particular task or situation, by helping them extract high-level information that requires integration of multiple display elements, and by enhancing the operator's understanding and knowledge of the current state and behavior of the system. Studies have also shown that people can selectively direct their attention to only the moving items in a display and can quickly find a unique feature among the moving items, such as red arrows among green arrows [27]. They can also quickly find fast-moving elements among slower-moving elements [28], an effect that is enhanced by greater differences in movement speed [29]. In addition, viewers respond faster to the sudden onset of a moving indicator if it is moving faster [30], [31].

Research has demonstrated that the human eye has specialized detectors that differentiate between translating, rotating, expanding and contracting, and deforming motion [32], which

suggests that these patterns could be used in displays to direct a viewer's attention. Expansion and contraction lend themselves well to displaying power flow data because they appear to be moving faster than, and may be detected more easily than, translation at the same real speed [33], [34], [35] and because they are orthogonal motions that can be used to indicate positive and negative values unambiguously. The motion patterns created by multiple moving elements are perceived as a single object when they move at similar speeds and in similar directions [36], [37], an effect called common fate, which can still operate when the elements' trajectories diverge or converge [38] as in expansion and contraction.

Researchers have also stated that motion can aid in understanding of the dynamic behavior of a system. Quoting from [25], "[animated mimic] displays can improve real-time performance by (1) contributing to an individual's ability to assess current system state and the causal factors that underlie that state, (2) illustrating alternative system resources that can be used to avoid or recover from the violation of system goals, and (3) providing immediate feedback regarding the effectiveness of control input" (p. 676). This has been confirmed by studies in computer-based instruction showing that participants performed better on tests of electronic troubleshooting after being instructed with displays showing current flow, circuit device behavior, and troubleshooting procedures with animation rather than with static displays that indicated current flow with arrows or did not indicated current flow at all [39].

However, motion should be used in displays with care, since it may not always improve performance. Motion and dynamic changes in task-irrelevant areas of displays can cause distraction and increase search times, especially if the motion is incoherent, moving in multiple directions or at different speeds [40], [27]. It has been shown that this problem can be reduced if moving distracters can be differentiated from moving targets by some feature, such as color [41]. For instance, overloaded lines can be indicated by both faster moving arrows and by highlighting the arrows with a color that indicates an abnormal condition.

5.1.1 Motion Experiments Overview

This section investigates the use of motion to indicate power flow in power systems displays by presenting results of two human factors experiments. The first experiment examined the usefulness of animation for transmission line flow visualization. The experiment compared line overload detection and resolution performance using a 30-bus system, with the power flow indicated on a one-line by numeric fields, stationary arrows, or moving arrows. Hence, this experiment might mimic, at least to some extent, the task a power system operator may need to perform during an emergency situation of determining the extent of transmission system overloads, and of initiating preventative control.

The second experiment examined the usefulness of animation for PTDF visualization by comparing subject performance in analyzing power transactions. In this experiment, subjects needed to determine buyers and sellers, and a common path between them, utilizing a one-line diagram that indicated the PTDFs using either stationary arrows, arrows that moved at a uniform speed, or arrows that moved at a speed proportional to the PTDF value on each line. Here the experiment seeks to simulate (again to some extent) the task of a power system analyst of determining the impact of proposed power transactions on the grid.

A key difference between the two experiments is the relationship between the flow on elements incident to the same node. With the PTDF experiment, in which power is assumed to be injected into the network at a single location (i.e., the seller) and withdrawn at a single location

(i.e., the buyer), the PTDFs appear to radiate from the buyer to the seller. In contrast, in the first experiment, in which there are a number of sources of power (i.e., the generators) and a number of sinks (i.e., the loads), the line flows appear to be much less ordered. Our supposition is that the PTDF display, with its animated expanding pattern of arrows out from the seller and the contracting pattern of arrows into the buyer, will focus attention on these points. Such patterns, which are known as configural displays, can support both detection and diagnosis tasks due to the ability to direct attention to either the high-level or low-level information [42].

5.1.2 First Motion Experiment Setup and Procedure

The study system used in the first experiment had 30 buses, 43 transmission lines, and 10 generators. A one-line of this system is shown in Figure 5.1. During the experiment, the participants were each presented with a sequence of 29 trials (each received the same contingency sequence). A trial initially started with no transmission line overloads. Then, following a delay of between two and fifteen seconds, a contingency occurred, causing overloads on one or more of the transmission lines. All contingencies were either single or multiple line outages. Following the contingency, overloads were indicated visually on the one-line using one of the six different display types discussed in the next section. Half of these display conditions included transmission line loading pie charts (as shown in Figure 5.1) and half did not. Overloads were also indicated audibly by a continuous, beeping alarm.

After each contingency, the participants acknowledged either the worst power violation, for the displays with pie charts, or every violation, for the displays without pie charts. This was done by clicking on either the appropriate line's numeric display of the line loading, on the line's pie chart, or on the line itself. After acknowledging the violation(s), participants solved each violation by adjusting the MW output of one or more of the generators. This was done by clicking on the up or down arrows in the highlighted generator MW fields shown by each generator (see Figure 5.1). Each trial continued until either all violations were solved, or it timed out after 120 seconds.

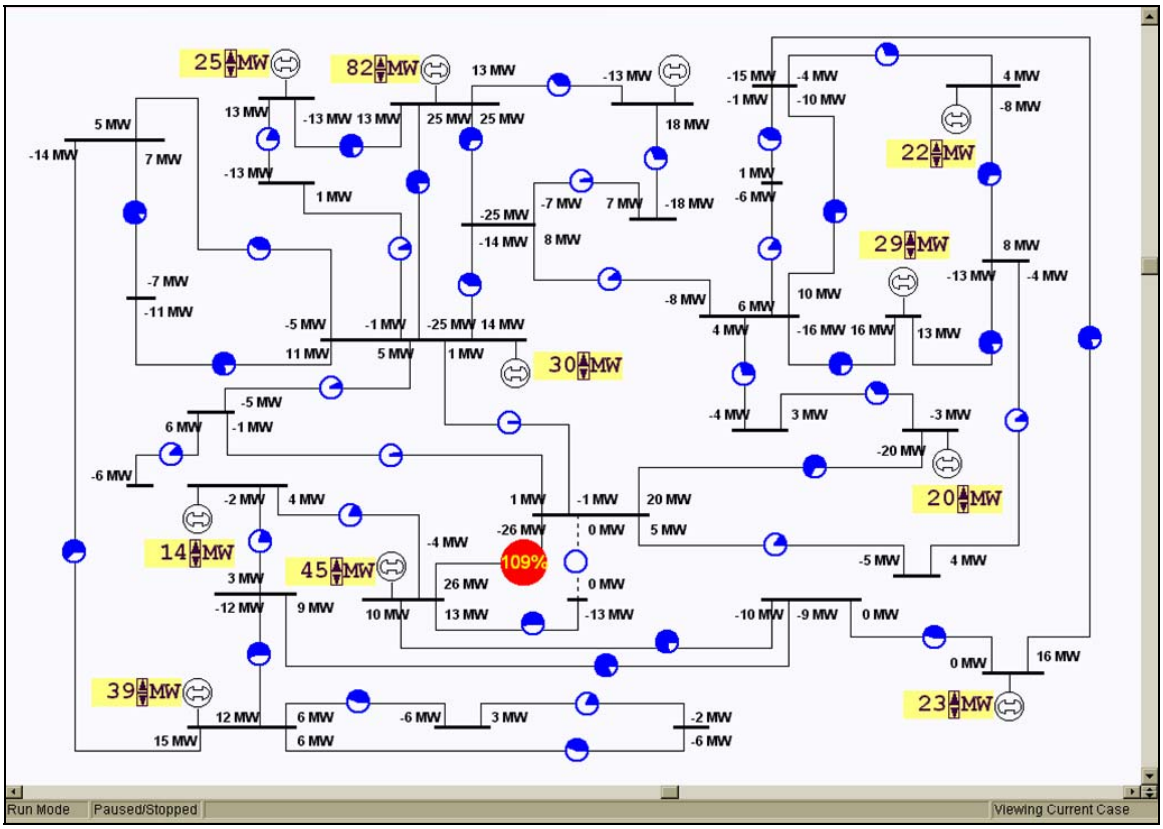

Figure 5.1: First Experiment 30-Bus System

The experiment had 88 participants, 70 men and 18 women, with self-reported normal color vision. All participants either had completed or were currently enrolled in power system classes taught in the Department of Electrical and Computer Engineering (ECE) at the University of Illinois, Urbana-Champaign (UIUC); the gender percentages are roughly proportional to the enrollment in the UIUC ECE power classes. Participants were randomly assigned to one of the six display groups discussed in the next section, except that the 13 participants who had participated in previous electric power systems display experiments were distributed as evenly as possible. Each group had 14, 15 or 16 participants. The experiment consisted of 4 practice trials and 25 experimental trials, which were completed in less than one hour. After the final trial, the participants completed a post-experimental questionnaire, which included the NASA-TLX subjective workload assessment [43].

5.1.3 First Motion Experiment Display Types

Participants completed the experimental tasks using one of six display types, with each display type based upon the 30-bus system shown in Figure 5.1. The display types are (1) the digital-only display, (2) the digital-with-pie-charts display, (3) the stationary-arrows-only display, (4) the stationary-arrows-with-pie-charts display, (5) the moving-arrows-only display, and (6) the moving-arrows-with-pie charts display. The digital-only (Figure 5.2) and digital-with-pie-charts (Figure 5.1) displays indicated power flow with numeric fields (digits) at the end of each line showing the MW flow into the line (negative values indicated flow out of the line into the bus). The stationary-arrows-only (Figure 5.3) and stationary-arrows-with-pie-charts

(Figure 5.4) displays indicated power flow with stationary arrows superimposed on each line, with the arrows pointing in the direction of power flow, having a size proportional to the magnitude of MW flow. Hence, these displays did not use numeric fields to indicate the magnitude of the power flow. The moving-arrows-only (Figure 5.3) and moving-arrows-with-pie-charts (Figure 5.4) displays were identical to the corresponding stationary display types, except that the arrows were animated with the speed of the arrows proportional to the magnitude of the power flow on each line.

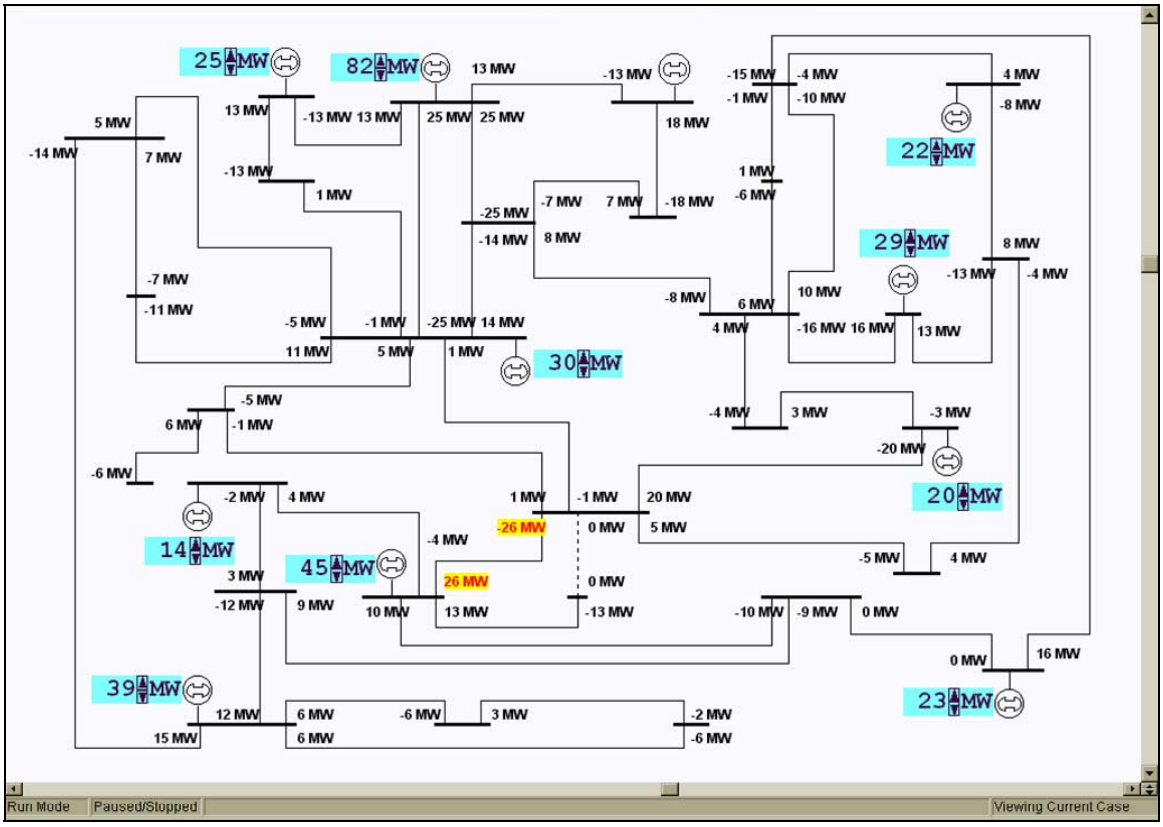

Figure 5.2: Digital-Only One Line

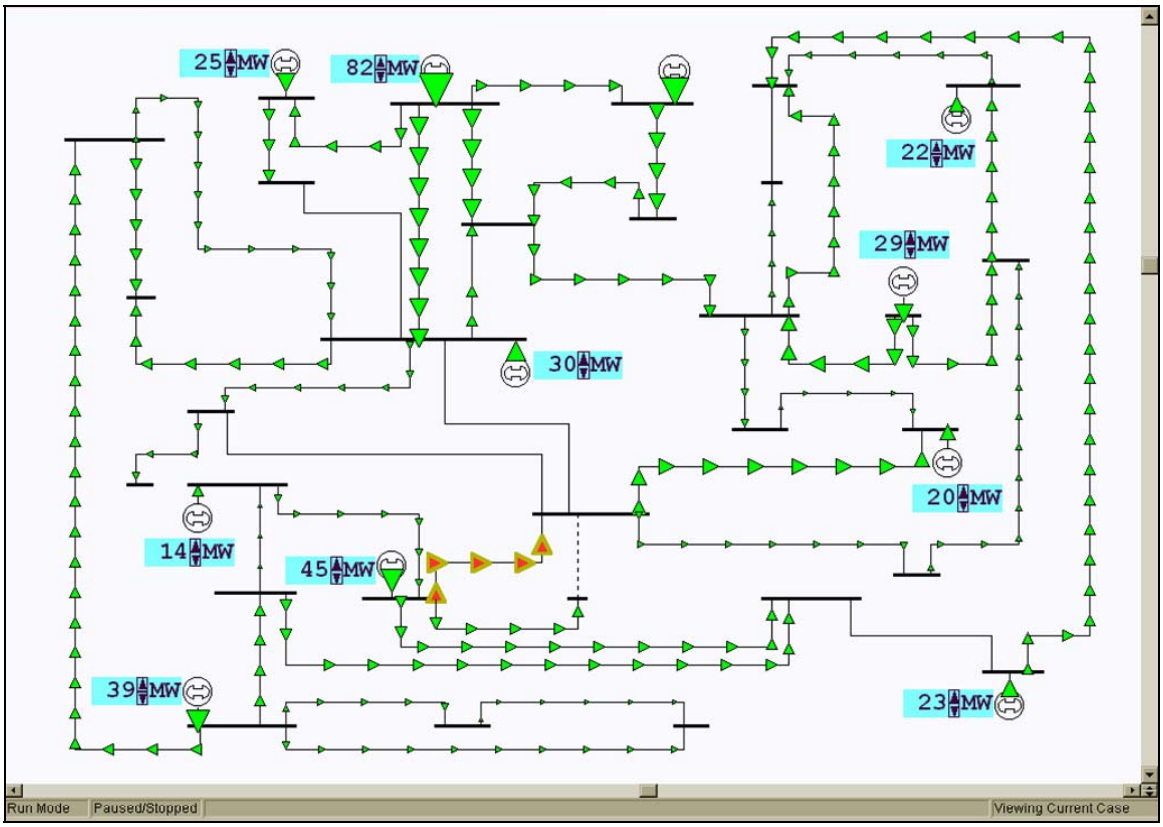

Figure 5.3: Stationary- or Moving-Arrows-Only One-Line

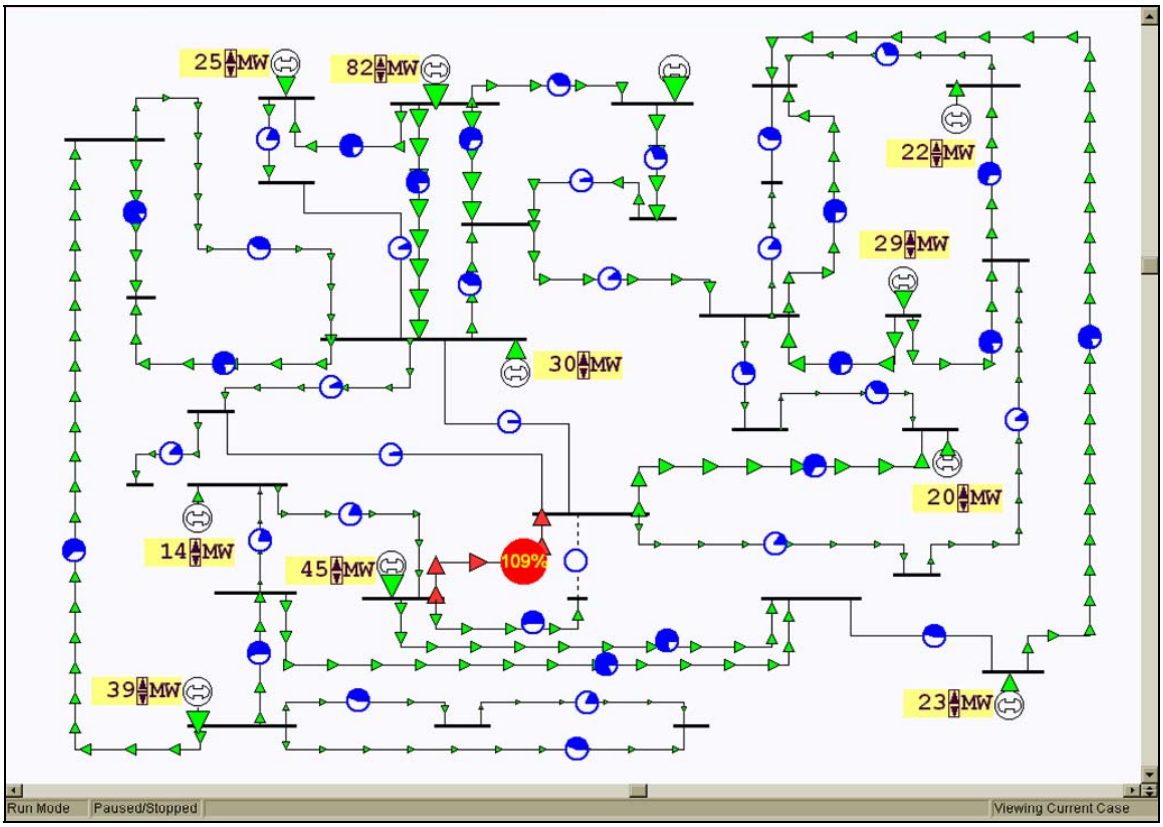

Figure 5.4: Stationary- or Moving-Arrows-with-Pie-Charts One Line

Transmission line overloads were indicated slightly differently on the six displays. In the digital-only display, overloads were indicated when the power flow digits associated with a line turned from black to red with a yellow background. The stationary-arrows-only and moving-arrows-only displays indicated overloads when the arrows associated with overloaded lines changed from green with a thin, black outline to red with a thick, yellow outline. In the three displays with pie charts, the pie charts on overloaded lines enlarged and turned from blue to red with centered yellow digits indicating the loading percentage. In addition, the arrows associated with overloaded lines in the stationary- and moving-arrow displays changed from green to red. The contingent opening of a transmission line was indicated on all six displays by a dashed line, and the pie chart, if present, becoming completely empty.

It is important to note that the size and speed of the arrows in the stationary- and moving-arrow displays were proportional to line's MW flow, not its percentage loading. Hence, a low capacity line could be in violation with much smaller and slower arrows than a high capacity line loaded below its limit. The reason for making the arrows' size and speed proportional to the MW flow was the objective of the experiment, i.e., testing the validity of replacing the MW fields in Figure 5.2 with the arrows – thus, the arrows needed to represent the same information.

5.1.4 First Motion Experiment Results and Discussion

For reporting the results, display types (1) and (2) are grouped as "Digital", (3) and (4) as "Static Arrows", and (5) and (6) as "Moving Arrows". Also, the trials are differentiated based upon whether the contingency caused a single violation or multiple violations (i.e., problem

complexity). Table 5.1 shows the mean solution times per trial by display type and problem complexity. The presence of pie charts did not significantly affect solution times. Solution times were fastest in the moving arrows display groups, followed by the stationary arrows and digital display groups for multiple violation trials. In addition, the increase in solution time as the number of violations increased – from single to multiple – was lowest for the moving arrows display followed by the stationary arrows and digital displays (p = .018).

Table 5.1: Solution time in seconds

Problem Complexity	**Display Type**		
	Digital	Static Arrows	Moving Arrows
Single Violation	8.5	9.8	11.3
Multiple Violations	23.6	21.8	20.4

Table 5.2 shows the mean number of generators used to correct each trial, again as a function of display type and problem complexity. Participants in the moving arrows display groups used fewer generators in multiple violation trials than those in the other groups, and the increase in the number of generators used as the number of violations increased was lowest in the moving arrows display groups (p=0.044). Pie charts, however, as shown in Table 5.3 improved efficiency in multiple violation trials and reduced the difference from single violation trials (p=0.015).

Table 5.2: Number of generators used per trial

Problem Complexity	**Display Type**		
	Digital	Static Arrows	Moving Arrows
Single Violation	1.43	1.52	1.58
Multiple Violations	2.59	2.60	2.42

Table 5.3: Effect of pie charts on number of generators used per trial

Problem Complexity	Without Pie Charts	With Pie Charts
Single Violation	1.48	1.58
Multiple Violations	2.65	2.43

Also, an analysis of the "adjustment error" indicated that participants using pie chart displays made fewer errors (mean of 1.69 per trial) than those using displays without pie charts (3.09 per trial). Here an adjustment error is defined as a generator MW adjustment that increased the load on at least one already overloaded transmission line that did not also decrease the load on any other overloaded lines, or that could have produced those effects in the case of an attempt to adjust a generator already at its minimum or maximum output.

Workload, as assessed subjectively for mental demand, physical demand, temporal demand, performance, effort, and frustration level, by the participants on a scale from 0 to 100, using the NASA Task Load Index (TLX), was affected both by the display type and the presence of pie charts, as shown in Table 5.4. Participants rated workload as lowest with the digital display when pie charts were not present but rated workload as lowest with the moving arrows display when pie charts were present, with the stationary arrows display workload scores falling in the middle of both cases (p = 0.037).

Table 5.4: NASA –TLX workload scores

Pie Charts	Display Type		
	Digital	Static Arrows	Moving Arrows
Without	28.8	36.3	39.8
With	35.6	32.9	29.6

For the more complex trials, the arrows aided the participants in resolving violations by reducing the amount of time required to determine the power flow patterns compared to the digital display, which required mental conversion of the numbers or exploratory generator adjustments to determine power flow directions. Adding motion reduced solution times further and helped the participants determine the best generators to use by displaying power flow directions and magnitudes dynamically, as predicted by [25] and consistent with the results of [39].

The presence of pie charts in the displays improved generator use efficiency and reduced the number of adjustment errors because the digital values indicating the percentage loading on the overloaded lines were more sensitive to generation adjustments than changes in arrow size or speed and were easier to monitor than the digital values in the digital displays, due to their large size and unique shape and coloring. In the displays without pie charts, the participants could have adjusted a generator in the wrong direction, increasing the overloads on lines for many adjustments before realizing that the power flow digits were increasing or that the arrows were increasing in speed and/or size on the overloaded lines, whereas increases in the numbers on the pie charts were easy to detect. In addition, the pie charts provided unique information about the magnitudes of the overloads that was not provided by the arrows or digital power flow values. The overload information allowed the participants to see which violations were most critical and determine which lines were near their upper capacity limit to avoid overloading new lines while adjusting generators.

The presence of pie charts modified the effect of display type on workload. Without pie charts, workload was rated highest for the moving arrow display and lowest with the digital display, perhaps due to distraction caused by the moving arrows throughout the moving arrow display and by the changes in the arrow sizes in the stationary arrow display, as discussed in [41]. Apparently, the pie charts overrode this distraction effect and even made the tasks easier when combined with arrows and motion. This may have been due to the earlier-mentioned fact that the pie charts were more sensitive to the effects of generator adjustments than the arrows and provided information that the arrows did not.

5.1.5 Second Motion Experiment Setup and Procedure

The second experiment also looked at flow animation, but with the focus changed to PTDF visualization. The study system was a 55 node, 148 branch system that was a rough equivalent of much of the electric grid in the eastern part of North America. The nodes corresponded to different operating areas, while the branch reactances approximated the equivalent impedance between the areas; resistive losses were ignored. A one-line diagram of this system is shown in Figure 5.5. Again, during the experiment the participants were presented with a sequence of trials. However, rather than showing actual MW flows, the one-line was used to visualize the PTDFs for transactions between various buyer/seller pairs. Each trial initially started with no transaction. Then, following a delay of between 2 and 12 seconds, a transaction between a

buyer/seller pair was shown on the one-line. The transaction was indicated visually using one of the three different display types discussed in more detail the next section. All display types used magenta colored arrows on the branches to indicate the direction and magnitude of the PTDFs; the display types were differentiated based upon the type of arrow animation.

For each trial, participants were required to perform up to two consecutive tasks. First, they needed to search for and select the buying and selling area (in any order). The buying area was indicated by inbound arrows on all the branches connecting it to other areas, while the selling area was indicated by outbound arrows on all its incident branches. If the buyer and seller were directly connected, the trial ended as soon as both were selected. Otherwise, the participant's second task was to select any set of areas that formed a complete path between the buyer and seller. The participants could select any areas other than the buyer and seller, and the trial ended as soon as any subset of the selected areas formed a complete path.

The experiment included 49 participants, 41 men and 8 women, who were again recruited from UIUC ECE power systems classes. Once again, an entrance questionnaire was used to screen out colorblind participants (two in this experiment). Each participant was randomly assigned to one of the three display types, with either 16 or 17 in each.

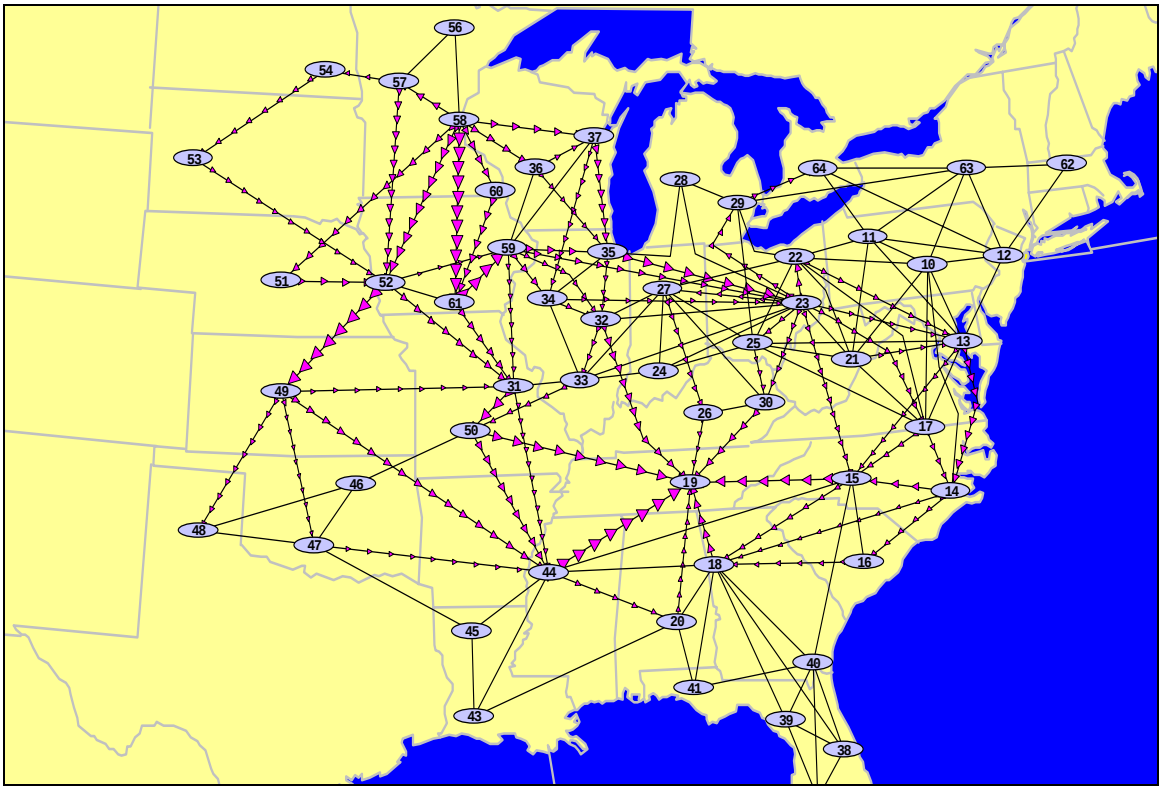

Figure 5.5: The PTDF Display Used in Experiment 2

Each participant was administered 4 practice trials and 50 experimental trials. The 50 experimental trials were divided by buyer-seller connection type into 15 trials where the buyer and seller were directly connected to each other, and 35 trials where the buyer and seller were not directly connected. The trials were identical across the three display types. The participants were allowed a maximum of 60 seconds to complete each trial. When the buyer and seller had

been selected, and, if they were not directly connected, a path connecting them had been selected, or time had run out, the trial ended. After the final trial, the participants completed a post-experimental questionnaire, which included the NASA-TLX subjective workload assessment.

5.1.6 Second Motion Experiment Display Types

Participants completed the experimental task using one of three display types. Each display showed the areas connected by branches with the PTDF magnitude and direction visualized using magenta arrows with the size of each arrow proportional to the PTDF for the branch. For the first display type, no-motion, the arrows were stationary. For the second, uniform-motion, the arrows on all the branches were animated with uniform speed. For the third, proportional-motion, the animation speed for each branch was proportional to the PTDF for that branch.

After an area was selected, it was color-coded to show the participants which areas they had already selected. All areas began as light blue. When selected, the seller's node turned to green, the buyer's node turned to red; prior to the selection of the buyer and seller the other areas did not change color if they were selected. After being selected, the buyer and seller remained red and green, respectively, throughout the remainder of the trial. During the path selection task, each selected area turned from light blue to white and remained white until the completion of the trial. An example is shown in Figure 5.6, with area 37 the seller, area 32 the buyer, and area 35 the selected path element.

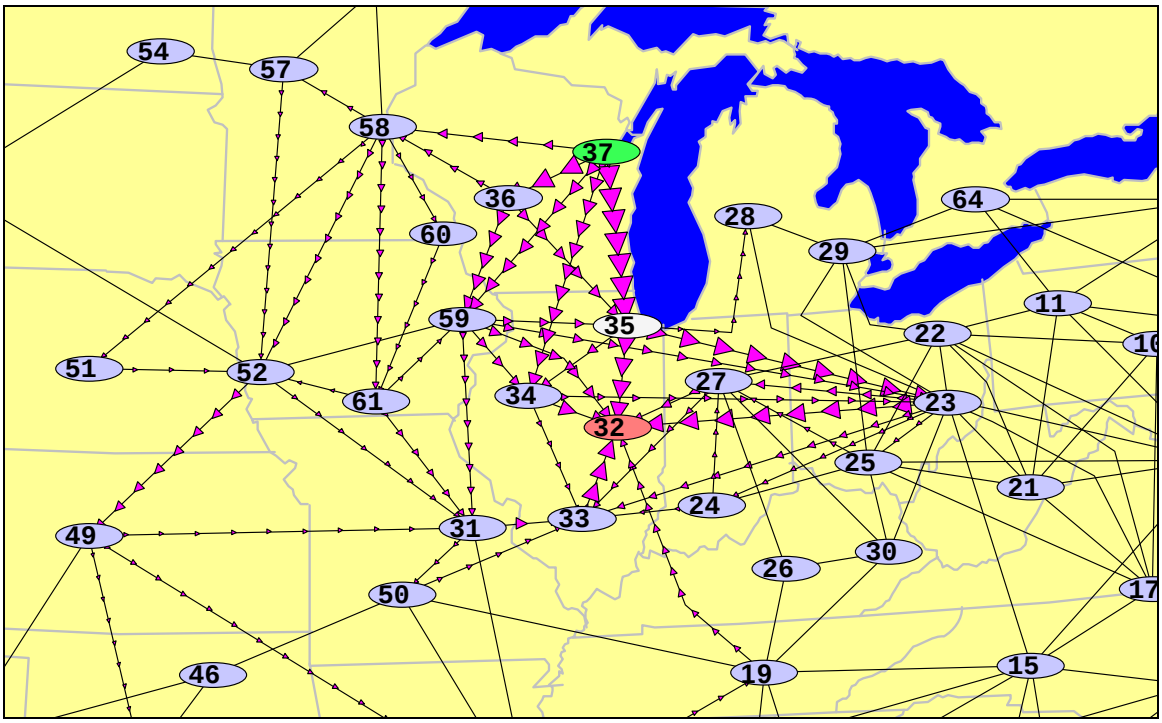

Figure 5.6: Close-Up Showing the Completion of Practice Trial Two

5.1.7 Second Motion Experiment Results and Discussion

The mean times for participants to select both the buyer and the seller are shown in Table 5.5. The results show a clear advantage for the motion displays over the no-motion display, especially in indirect connection trials (p = 0.011). However, the differences between the two motion displays were not significant (p = 0.417, direct; p = 0.249, indirect). In addition, we measured the time required to select the path between the buyer and seller in indirect trials and counted the number of nodes in each path, but did not find significant differences among the display groups for either measure (p = 0.788, time; p = 0.716, number of nodes).

Table 5.5: Mean buyer-seller selection times in seconds

Connection Type	Type of Motion (Display Type)		
	None	Uniform	Proportional
Direct	6.75	4.54	4.14
Indirect	10.42	6.88	6.08

Table 5.6 shows that participants also committed fewer errors, defined as attempted selections of areas that were neither the buyer nor the seller, while using the motion displays than with the no-motion display, an effect that was marginally enhanced in the indirect connection trials (p = 0.075). As for selection times, the differences between the two motion displays were not significant (p = 0.794, direct; p = 0.258, indirect).

Table 5.6: Mean errors per trial

Connection Type	Type of Motion (Display Type)		
	None	Uniform	Proportional
Direct	0.40	0.08	0.07
Indirect	1.26	0.58	0.35

The participants' reported mental workload, assessed with the NASA-TLX, is shown in Figure 5.7 and Figure 5.8. The workload rating was lowest for the proportional-motion display group followed by the uniform-motion and no-motion groups (p = 0.103). Only the individual difference between the no-motion and proportional-motion display groups was significant (p= 0.043). As shown in Figure 5.8, the temporal and mental demand were the most significant contributors to overall workload, receiving scores higher than effort and performance (p = 0.076).

Motion apparently aided the participants in finding the buyer and seller by directing attention to the most relevant areas of the displays. The larger—and faster, in the case of the proportional-motion display—arrows tended to be located near and flowed between the buyer and seller in both motion displays, perhaps leading the participant's attention from the seller to the buyer. The arrows were configured uniquely for the buyer and seller, since they were the only nodes in the displays where all arrows flowed either in or out. Motion probably increased the visibility of these configurations significantly, since humans are sensitive to expanding and contracting patterns [33], perceive those patterns to be moving faster than linear motion [34], [35], and can perceive the pattern as a single object [36], [27], [38], [37]. That error rates followed a pattern very similar to selection times indicates that the participants were not trading accuracy for speed with the motion displays but were truly able to perform faster and more accurately.

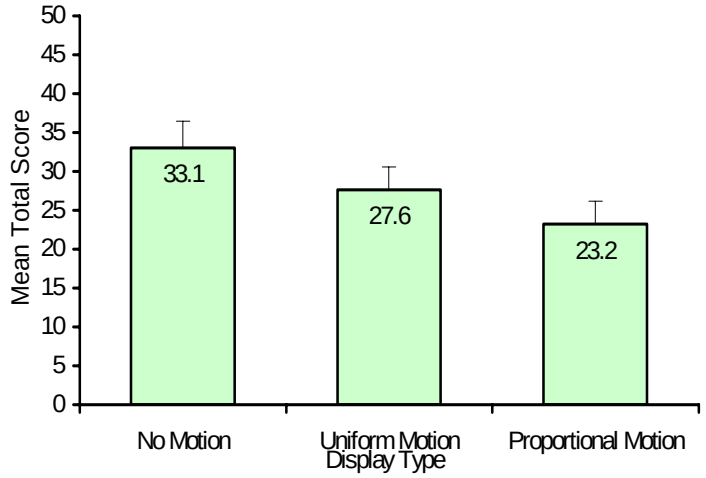

Figure 5.7: NASA-TLX as a Function of Display Type

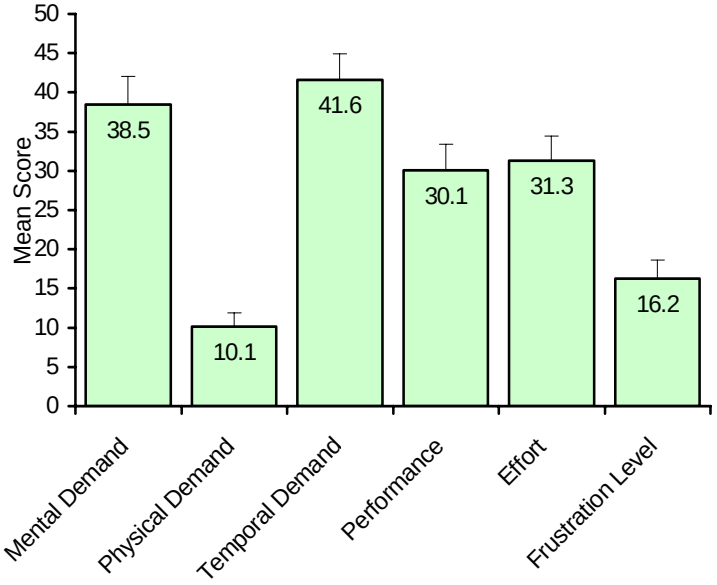

Figure 5.8: NASA-TLX as a Function of Workload Dimension

Motion may also have aided the participants' understanding of the behavior of the power network. This effect might improve users' performance in a task such as the path selection task in helping them detect power flow patterns with less mental conversion than required with the no-motion display, as shown in [39]. The unstructured nature of the path selection task, however, may be the primary reason for the lack of significant differences among the displays for that task. Participants were instructed to choose any path, rather than choose an optimum path, making the task simple. We might have seen effects had the correct path been more difficult to determine and dependent on finding a pattern in PTDF magnitude and direction of flow, which the motion information would have directly supported.

For all display groups combined, the seller was selected first in a significant proportion of trials (p = 0.010). For individual display groups, the proportion of trials in which the seller was

selected first was significantly greater than chance only for the no-motion group ($p = 0.019$) and the proportional-motion group ($p = 0.016$), though the trend was in favor of selecting the seller first in the uniform-motion group as well, as shown in Table 5.7. That this preference was present with the no-motion display suggests that the participants may have consciously looked for the seller first but happened to see and select the buyer while searching for the seller on some trials. It is unclear why this preference effect was significant with the no-motion and proportional-motion displays but not with the uniform-motion display. A possible explanation is that the expansion and contraction surrounding the seller and buyer in each trial were easiest to find in the uniform-motion display, in which motion was most coherent, so that even though participants may have preferred to search for the seller first, the buyer may have popped out during search for the seller more frequently than participants happened to see it in the no-motion display and more frequently than it popped out with the less-coherent contracting motion in the proportional-motion display.

Table 5.7: Percentage of trial in which selected first

	Type of Motion (Display Type)		
	None	Uniform	Proportional
Buyer	44%	48%	39%
Seller	56%	52%	61%

5.1.8 Motion Experiment Conclusion

Motion can be used successfully in displays to aid understanding of the behavior of systems and aid search if the display is configured so that motion provides information that is directly relevant to the user's tasks and draws the user's attention to the areas most relevant to the current task. Task-relevant areas of displays can be highlighted with higher-speed motion or moving elements that configure themselves into moving patterns that are easily grouped together and separated from the rest of the display, such as expansion, contraction, rotation, and deformation. This result was most clearly shown in experiment 2 in which the PTDF motion displays had a clear advantage in terms of speed, accuracy, and reduced mental workload. Proportional motion was also slightly better than uniform motion for such displays.

However, our results do not show a clear advantage for encoding real power flow with motion speed, suggesting that care should be taken to ensure that the resulting incoherence of the motion will not overpower the advantage of highlighting with motion and will not weaken the perception of patterns in the flow. In addition, there may be no advantage to incorporating motion in displays to support tasks requiring integration of information when the integration task is simple.

In displays similar to one-lines, where the user monitors power flows and resolves contingencies affecting flow patterns, it appears that indicating flows graphically with arrows that move at a speed proportional to power flow can reduce contingency resolution times and increase efficiency in terms of the number of resources used, compared to displays without motion or arrows. For displays where the user must analyze flows to determine the locations of flow sources and sinks, such as in PTDF analysis, it appears that the best configuration is to use arrows that move at a uniform speed, reducing search times, error rates, and workload compared to displays with non-moving arrows. We expect that these differences will be even more pronounced for larger networks and contingencies that affect more components, as could be the case in real systems.

Last, this study underscores the need for further usability and human factors research to test the effectiveness of power system-specific visualization techniques, in addition to motion. With the ongoing advances in computer visualization hardware and software, the visualizations that can be performed on the power system data sets are (almost) limited only by the human imagination. However, the development of new visualization techniques must proceed hand-in-hand with usability assessment and human-factors research. Further experiments are needed using both academic participants, such as was presented here, and practicing power system operators and engineers.

5.2 3D Experiment Introduction

The third and fourth experiments looked at the impact of 3D on power system visualization. In the third experiment two different display conditions were tested. However, a review of this work by some human factor colleagues indicated a need to test a third display condition. This was done in the fourth experiment. This section describes those results, with the results presented as though it were a single experiment.

Power system analysis and operations requires the consideration of a large amount of multivariate data. For example, even in a simple power flow application data of interest includes a potentially large number of independent and dependent variables, such as transmission lines flows, bus voltages, generator real/reactive outputs and reserves, transformer tap positions, flowgate values, and scheduled versus actual power transactions. With systems containing tens of thousands of buses, a key challenge is to present this data in a form so one can assess the state of the system in a quick and intuitive manner.

The information associated with power systems has usually been presented using a 2D display space, often consisting of either a one-line diagram or tabular list displays. However, over the last several years this pattern has begun to change as new visualization techniques are developed and integrated into both power system analysis software and utility control centers. One such technique, made possible by recent increases in computing power, is the interactive 3D visualization of power system information. An early application of 3D for power system information visualization is [44] in which simple 3D graphics are used to show power system voltage security. A few years later the use of 3D is presented for plant and substation operator training in [45], [46], [47]. More recently, [48] and [49] mention the use of interactive 3D techniques for power system information visualization in a control center context, while [18] describes potential applications of 3D in power system analysis packages.

However, just because interactive 3D visualizations are now computationally possible does not imply that they are the best approach. Indeed, reference [50] states, “because it is so inexpensive to display data in an interactive 3D visual space, people are doing it – often for the wrong reasons” (p. 259). Rather, interactive 3D should only be used if it is better, at least in some way, than the existing 2D approaches at helping people understand the power system information and/or perform a desired task. Of course effective visualizations, like beauty, are to some extent “in the eye of the beholder.” Nevertheless, empirical research can be helpful in providing guidance as to what works and what doesn’t. Currently there are no results in the power system literature evaluating the effective of 3D visualization of power system information. The purpose of this section is to present the results of human factor experiments comparing 2D versus 3D power system one-line visualizations.

5.2.1 3D Experiment Overview

Overall, the experiment compared line overload detection and resolution performance using a 67 bus, 15 generator system with the three different one-line visualizations shown in Figure 5.9 to Figure 5.11. Each of the visualizations showed the loading of the transmission system with pie charts and animated arrows [24], and the actual MW output of each generator using yellow text fields. The main differences between the displays were 1) the visualization of the generator capacity and reserves, and 2) the use of 3D visualization with Figure 5.11.

Figure 5.9 showed each generator's MW capacity with a magenta field immediately below the yellow MW field; the generator's MW reserves (capacity minus actual output) were not shown. Figure 5.10 showed the generator capacity and reserves using a gauge [3], in which the height of the gauge was proportional to the generator's capacity. With this approach the height of the lower, gray portion of the gauge was proportional to the generator's actual output, while the height of the top, magenta portion of the thermometer was proportional to the generator's reserves. Figure 5.9 and Figure 5.10 both had a strictly 2D representation.

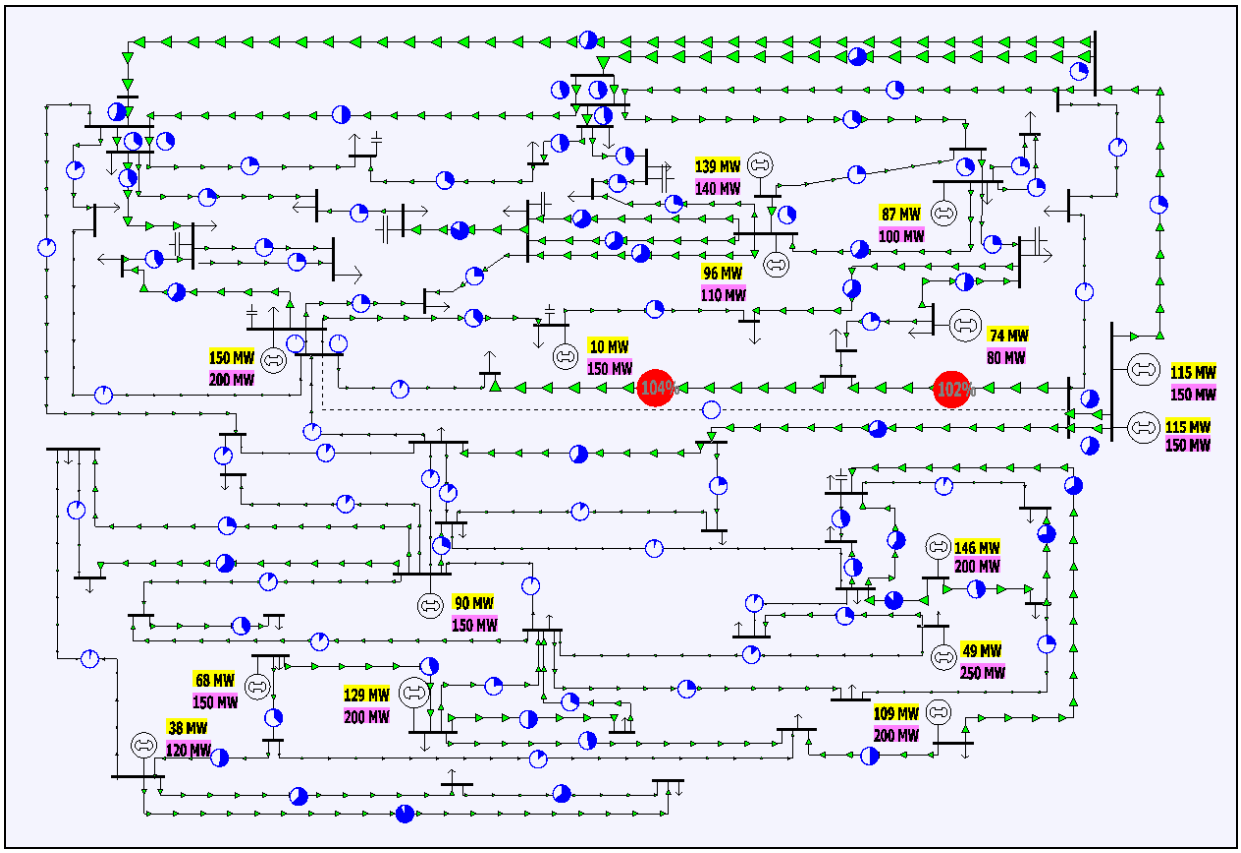

Figure 5.9: 67 Bus System Using a 2D Representation with Numeric Fields

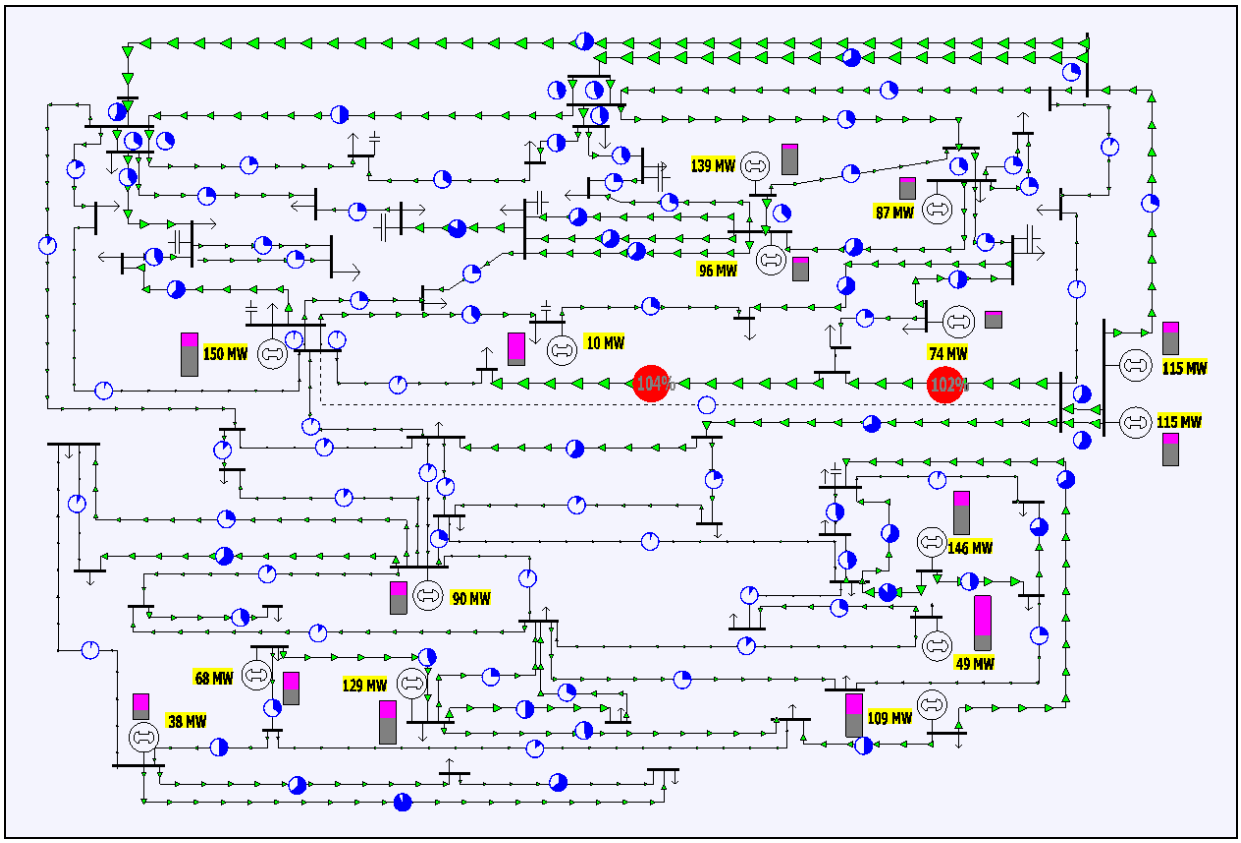

Figure 5.10: 67 Bus System Using a 2D Representation with Numeric Fields and Themometers

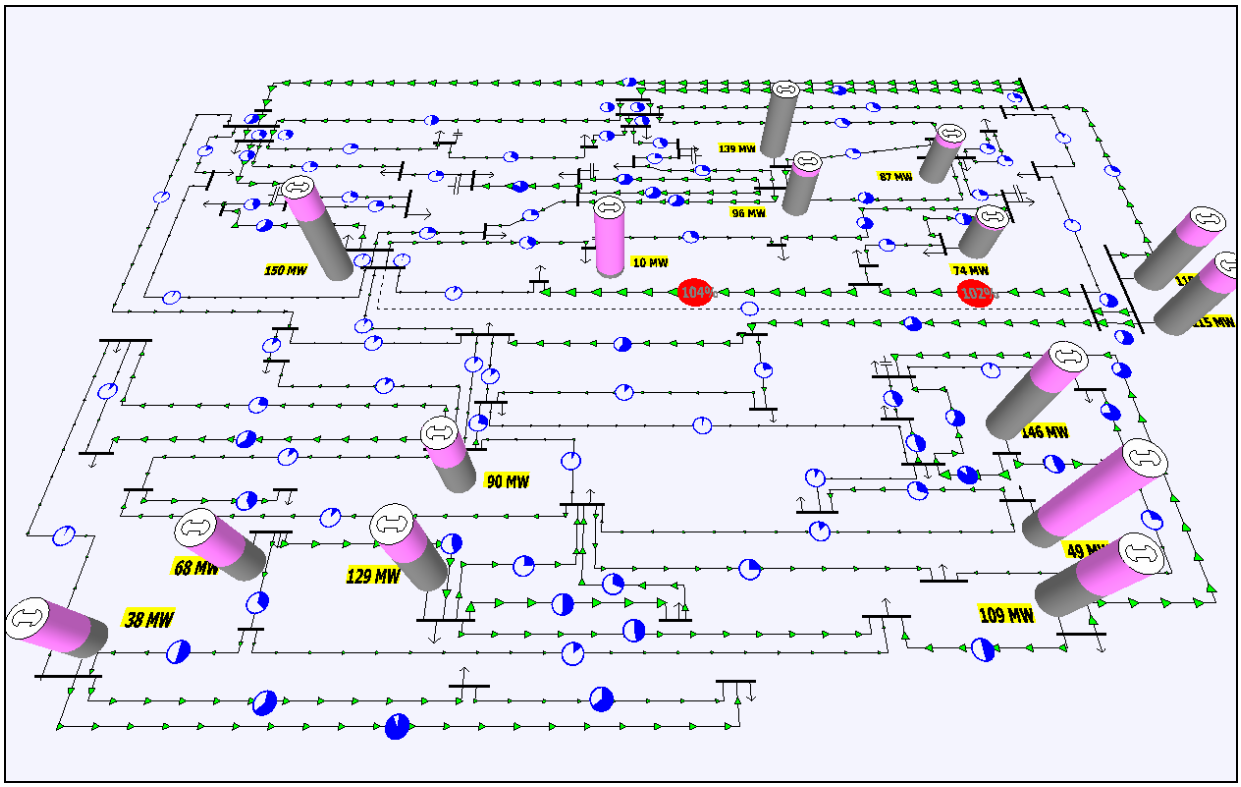

Figure 5.11: 67 Bus System Using a 3D One-Line Representation

In contrast, Figure 5.11 showed the one-line using a 3D perspective view in which objects closer to the display's frame of reference appear larger (a display's frame of reference refers to the viewpoint from which the graphical information is shown). The information shown in Figure 5.11 is identical to that shown in Figure 5.10 – what is different is how it is displayed. The gauges have been replaced by 3D cylinders with the height of each cylinder proportional to the generator's MW capacity. Shading of the cylinder was identical to the shading used with the Figure 5.10 gauges. That is, the height of the lower, gray portion was proportional to the generator's actual output, while the top, magenta portion was again proportional to the generator's reserve. Note, with the 3D display the numeric generator MW output fields were sometimes blocked by the generator's 3D cylinder.

5.2.2 Advantages and Disadvantages of 3D

Before discussing the experimental results it is useful to briefly mention some of the expected advantages and disadvantages of 3D versus 2D visualizations. While relatively new to the power system arena, interactive 3D displays have been used and studied in other industries such as aviation. Certainly the strongest argument for 3D visualizations is we live in a 3D world and our brains are designed to recognize and interact with 3D [8].

A great deal of research indicates that performance of tasks requiring divided attention, information integration, or mental model development, improve with 3D displays compared to their 2D counterparts. For example, [53] found that both 3D line graph and bar chart formats required less time to use compared to 2D line formats for the estimation of global trends, a task requiring mental integration. Reference [51] discovered that performance with 3D scatter plot

displays exceeded that with 2D plots for tasks involving information integration, which was attributed to the 3D plots providing superior visual depictions of the intricate shapes of the 3D surfaces.

Of course, there are some potential disadvantages to using 3D visualization, such as perceptual ambiguities of depth, size, and distance, which inevitably occur when the 3D world is graphically depicted on a 2D display [52]. Reference [53] found a performance decrement for participants making relative magnitude estimations with 3D line graphs compared to their 2D counterparts. Reference [54] performed experiments with terrain stimuli and determined that while 3D perspective views enhanced performance on tasks requiring shape understanding, 2D views were superior for precise judgments of angle, distance, and relative position. Research has also indicated that 3D displays are often ineffective visualizations for focused attention tasks, such as determining the precise value of a single variable [53], [55]. In these cases, depth cues in the 3D displays impeded precise judgments of size, distance, and other exact measurements.

Overall, however, the potential advantages of 3D graphic displays over 2D numeric displays are significant. The added dimension and pictorial enhancements will often increase the amount of information (e.g., non-distance quantities) that can be presented on standard display screens, allow for graphic representations of alphanumerics, increase the operator's sense of presence within the display environment, assist in navigation and search activities, aid in tasks requiring information integration through the creation of emergent properties, enable the separation of targets and distractors at varying depths, and facilitate more accurate mental models of the systems being manipulated.

Although 2D displays supplemented with graphics may share some of the aforementioned benefits (e.g., graphical representation of alphanumerics, enhanced information integration), limiting displays to two dimensions will eliminate many others (e.g., mental integration and divided attention) and may increase clutter. Indeed, the abundance evidence suggests that 3D displays may be an effective visualization technique in the domain of power systems monitoring, control, and analysis. This section of the report presents quantitative experimental results testing the applicability of 3D power system one-line visualizations. In particular, the use of 3D to present generator MW reserves is examined.

5.2.3 3D Experiment Setup and Procedure

Overall the experiment compared line overload detection and resolution performance using a 67 bus, 15 generator, 103 line system, with generator MW output and capacity (reserves) indicated on a one-line by either numeric fields, 2D bars, or 3D cylinders. This experiment might mimic, at least to some extent, the task a power system operator may need to perform during an emergency situation of determining the extent of transmission system overloads, the resources available to resolve them, and of initiating preventative control.

Before beginning the experiment our hypothesis was that solution times would be faster for the 2D bar and 3D cylinder displays compared to the 2D numeric display because their graphical depiction would aid mental integration of multiple information sources, such as present generator MW output, maximum generator MW output, and available MW reserves. In addition, the salient illustration of generator reserves in the 2D bar and 3D cylinder displays was expected to expedite fault resolution by quickly drawing attention to the generator(s) with the greatest reserves. We further expected that resolution times would be faster with the 3D cylinder display than with the

2D bar display because the nature of the displays allows the 3D cylinders to be sized larger than the 2D bars, making them easier to find and more noticeably indicating changes in output levels.

During the experiment, the participants were each presented with a sequence of 40 trials, with each participant receiving the same trial sequence. A trial initially started with no transmission line overloads. Then, following a delay of between 2 and 12 seconds, a contingency occurred, causing overloads on one or more of the transmission lines. All contingencies were either single or multiple line outages. Following the contingency, overloads were indicated visually on the one-line using one of the three different display types shown in Figure 5.9 to Figure 5.11. Overloads were also indicated audibly by a continuous, beeping alarm.

After each contingency, any line overloads were indicated on all three display types by the pie charts for the overloaded lines enlarging and their background fill color changing from blue to red with centered gray digits indicating the loading percentage. Any open transmission line was indicated by its one-line representation changing from a solid line to a dashed line, and their pie chart becoming completely empty.

After the contingency participants acknowledged each line overload by clicking on either the appropriate line's pie chart or the line itself. After acknowledging the violation(s), participants solved each violation by adjusting the MW output of one or more of the generators. This was done by left-clicking on the generator symbol, the generator output numeric field, or the bar/column indicating output and reserves in the two graphical displays to increase the MW output or right-clicking to decrease the MW output. The MW output was changed by 2 MW per click. Each trial continued until all violations were solved, or it timed out after 120 seconds.

The experiment had 52 participants, 40 men and 12 women, all with self-reported normal color vision. All participants either had completed or were currently enrolled in power system classes taught in the Department of Electrical and Computer Engineering (ECE) at the University of Illinois, Urbana-Champaign (UIUC). Participants were randomly assigned to one of three display groups: (1) 2D Numerical, whose members used the Figure 5.9 display, (2) 2D Graphical, whose members used the Figure 5.10 display, and (3) 3D whose members used the Figure 5.11 display. Hence each group had either 17 or 18 participants. The experiment consisted of 4 practice trials and 40 experimental trials, which were completed in less than one hour. After the final trial, the participants completed a post-experimental questionnaire, which included the NASA-TLX subjective workload assessment [43]. As an example, Figure 5.9 to Figure 5.11 depict the system after the first practice trial, a single line outage contingency.

5.2.4 3D Experiment Results

For reporting the results, the trials are sometimes differentiated based upon whether the contingency caused a single violation or multiple violations (i.e., problem complexity). Figure 5.12 shows the mean response time per trial by display type and task. Note, these results are not differentiated by problem complexity because it did not have a significant effect on response time. Acknowledgment time was significantly faster than solution time ($p < 0.001$). Display type did not significantly affect acknowledgment time, but solution times were significantly faster with the 3D display than with the two 2D displays ($p = 0.001$).

To further investigate this important result, the solution task times were further differentiated into two categories, (1) the first adjustment time, defined as the time from the acknowledgment of all initial violations until the first generator adjustment, and (2) the adjustment interval, defined as the mean time between generator adjustments following the first generator

adjustment. Hence the values in the first category indicate the time it took the participant to figure out which generator to move first.

Figure 5.13 shows the mean first adjustment time by display type and problem complexity. As was the case with the total solution time, the first adjustment times were significantly faster with the 3D display compared to the 2D displays (p = 0.001). First adjustment times were also significantly faster for multiple violation trials compared with the single violation trials (p = 0.001). In addition, the difference in first adjustment times between single and multiple violation trials was least for the 3D display, followed by the 2D graphical display, and greatest for the 2D numerical display (p = 0.013).

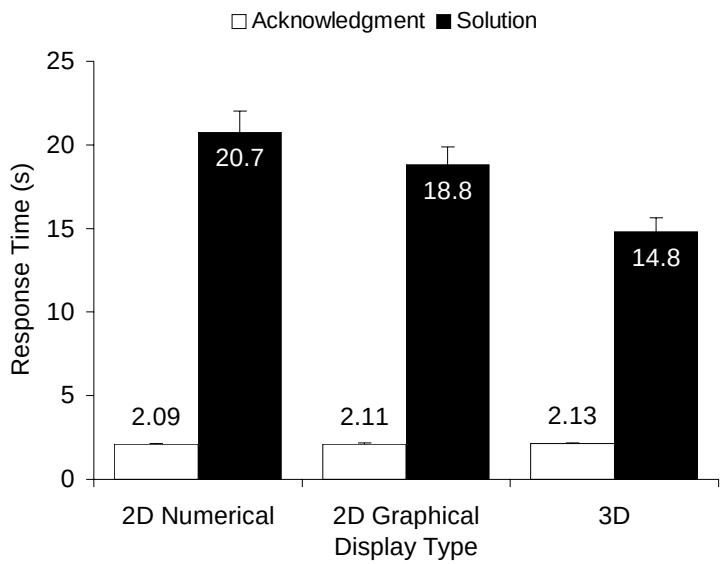

Figure 5.12: Response Time in Seconds

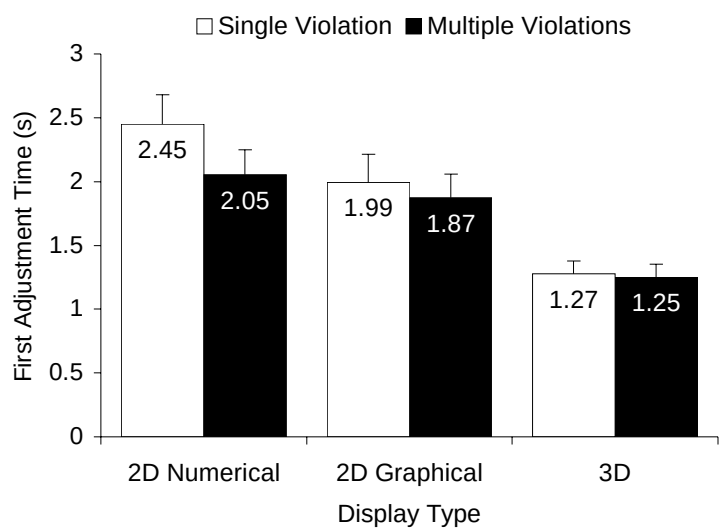

Figure 5.13: First Adjustment Time in Seconds

Figure 5.14 shows the mean adjustment interval per trial by display type and problem complexity. The adjustment interval was significantly shorter in the 2D graphical and 3D displays than in the 2D numerical display ($p = 0.039$). Opposite the effect for first adjustment time, the adjustment interval was significantly shorter for single violation trials than for multiple violation trials ($p < 0.001$). Also, the increase in adjustment interval as problem complexity increased – from single to multiple – was significantly less with the 3D and 2D graphical displays than with the 2D numerical display ($p = 0.001$).

Figure 5.15 shows the mean upper limit of errors per trial, where an error is defined here as the number of sequences of one or more generator output increases when a generator was already operating at its maximum capacity. There were significantly fewer upper limit errors with the 3D display than with the 2D displays ($p < 0.001$). In addition, the increase in upper limit errors as problem complexity increased was less with the 3D display than with the 2D graphical and 2D numerical displays ($p = 0.003$). There were no significant differences among the display types for the number of generator adjustments in the wrong direction or the number of sequences of one or more generator decreases when a generator was already operating at zero output.

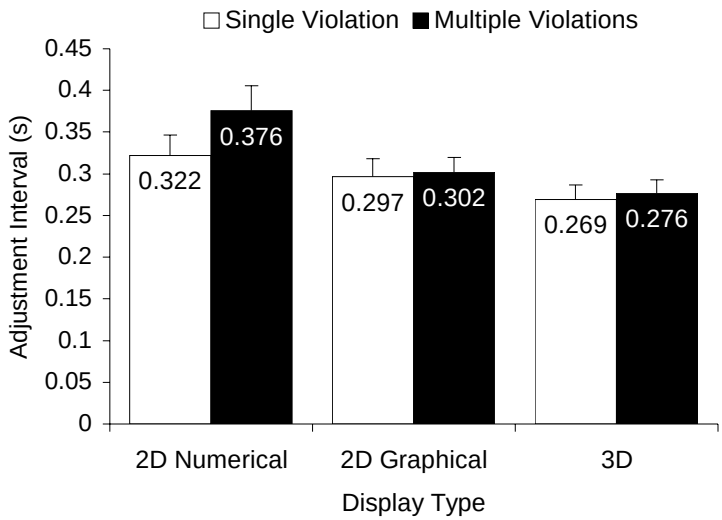

Figure 5.14: Adjustment Interval in Seconds

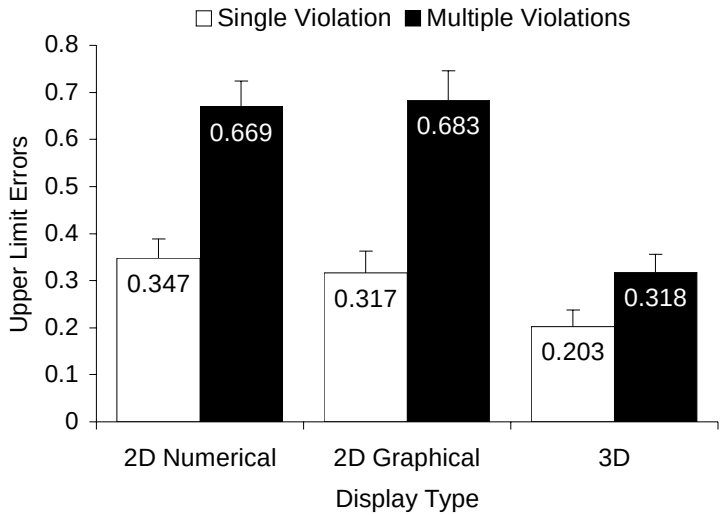

Figure 5.15: Upper Limit Errors Per Trial

At the conclusion of the computer simulations the participants' reported mental workload was assessed with the NASA-TLX with the results shown in Figure 5.16. Display type did not have a significant effect on workload scores. However, differences among the six dimensions on which workload was scored indicated that performance, temporal demand, mental demand, and effort were the most significant contributors to overall workload, in order of decreasing mean score ($p < 0.001$).

5.2.5 3D Experiment Discussion

Overall the 3D display supported the fastest solution times, followed by the 2D graphical display. This is partly because the 3D and 2D graphical displays integrated output, capacity, and reserve into a single object for each generator, which supported the divided attention and parallel mental processing required for the solution task, as predicted by [53], [51], and [56] and consistent with the results of [57]. Because precise judgments were not explicitly required to solve the line flow violations, the 2D numerical display, which would normally improve performance in this type of task, was of lesser value. Another advantage of the graphical displays in the solution task is that generators with large reserves stood out due to the large magenta portions of their bars or cylinders, making them much easier to find than in the numerical display, which required mental subtraction of the output field from the maximum capacity field, consistent with the results of [58].

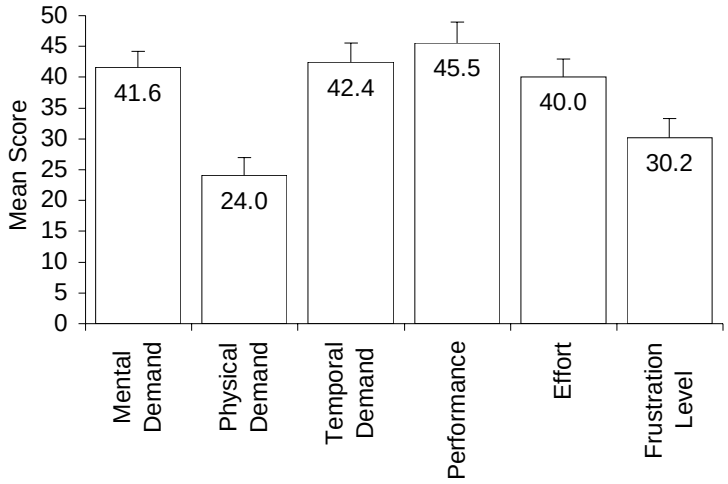

Figure 5.16: NASA-TLX as a Function of Workload Dimension

The advantage of the 3D display with respect to the 2D graphical display was likely due to the increased size and salience of the cylindrical generator representations in the 3D display compared to the 2D bars in the 2D graphical display, coupled with a reduced level of clutter in the 3D displays and the perception that the generator cylinders projected out of the one-line diagram, rather than being embedded within it. In addition, the larger size of the generator cylinders in the 3D group made dynamic changes in power outputs and reserves easier to see, enabling operators to better see the effects of individual generator adjustments on the entire system.

Breaking the solution task into subcomponents of first adjustment time and mean adjustment interval revealed that the 3D display was advantageous with respect to both the thinking/searching time before beginning the generator adjustments and the thinking/searching time while adjusting. Both measures showed reduced effects of complexity for the 3D display with respect to the 2D numerical display, and first adjustment time showed a reduced effect with respect to the 2D graphical display, as well. Another interesting effect is that multiple violation trials had faster first adjustment times overall but longer adjustment intervals. A possible explanation is that as the number of violations increased, a greater proportion of the generators could help solve the problem, thus requiring less initial search time to find an appropriate generator to adjust, compared to single violation trials. Therefore, although participants acted faster following acknowledgment to begin adjusting generators in complex trials, solution times were still dominated by participants spending, on average, more time between generator adjustments.

Reduction of upper limit errors also contributed to faster solution times in the 3D display. Because the 3D display clearly showed when a generator reached its capacity, less time was wasted trying to increase the outputs of generators already operating at capacity. Note that, due to a problem in the 2D graphical display, a generator operating at capacity was still shown with a thin magenta line at the top of its graphical bar, possibly explaining the lack of a significant difference in upper limit errors from the 2D numerical display. The smaller size of the 2D bars compared with the 3D cylinders probably also significantly contributed to the greater number of upper limit errors in the 2D graphical display.

5.2.6 3D Experiment Conclusion

The advantages of 3D displays over their 2D counterparts can be quite significant. As this study has indicated, the added dimension can allow non-distance information previously confined to alphanumerics to be presented graphically on standard display screens, aid in tasks requiring information integration, facilitate a more accurate mental model of the system being manipulated, and allow for a better understanding of the interconnected nature and structure of a complex system such as an electrical power grid. However, we cannot conclude that there is an advantage for 3D displays in terms of accuracy. Although our results indicated an advantage in reducing upper limit errors for the 3D displays over both 2D displays, this was the only accuracy measurement that was significant across display types and is not a comprehensive measure of solution accuracy. We predict, though, that 3D displays will improve accuracy in terms of choosing the best generator(s) to resolve a contingency, especially in large networks with many generators, due to their graphical depiction of reserves, reduced clutter, and the perception of the cylinders as rising out of the network.

While more studies are certainly needed, the results of this experiment indicate that 3D displays could be valuable tools in the power system visualization, particularly with the tasks of monitoring and controlling sets of interrelated variables. Specifically, they should improve the speed of high-level judgments of current operating levels in relation to upper and lower limits for parameters such as real and reactive generation, voltage magnitude, and perhaps other reactive power controls such as switched shunts and LTC transformers. With the appropriate software environment power system display designers could use such techniques to explicitly present information in ways that were previously impossible with 2D formats.

6 Conclusion

Restructuring in the electricity industry is resulting in a need for innovative new methods for representing large amounts of system data. Visualization can also play a crucial role in reducing the risk of future blackouts by helping operators to quickly assess a potentially rapidly changing system state, and by helping them to formulate corrective control actions. This research project has developed several new methods that could be quite useful for the representation of this data both at a system level and at a component level, performed formal human factors experiments to test the effectiveness of several of these techniques, and assisted in the actual implementation of research results in various control centers. Nevertheless, significant challenges remain. Key challenges include the problem of wide-area visualization of all pertinent system quantities, the incorporation of new system measurements into the visualizations such as those from phasor measurement units and substation IEDs (intelligent electronic devices), the visualization of time-varying system information, the integration of enhanced visualization into existing EMS applications such as alarming, and further work on component level visualization. Hence while we believe we have made significant progress over the course of this research project, more research is certainly needed to develop better methods for visualizing this data, performing human factors assessments on these new techniques, and rapidly transferring the results to industry.

Project Publications

A. R.K. Klump, W. Wu, G. Dooley, "Displaying Aggregate Data, Interrelated Quantities, and Data Trends in Electric Power Systems," accepted for presentation at 36th Hawaii International Conference on System Sciences, Kona, HI, January 2003.

B. T. J. Overbye, "Estimating the actual cost of transmission system congestion," accepted for presentation at 36th Hawaii International Conference on System Sciences, Kona, HI, January 2003.

C. T.J. Overbye, D.A. Wiegmann, A.M. Rich, Y. Sun, "Human Factors Aspects of Power System Voltage Contour Visualizations", *IEEE Trans. on Power Systems*, vol. PWRS-18, pp. 76-82, February 2003.

D. Y. Sun, T.J. Overbye, "Visualizations for power system contingency analysis transmission element loading data," *Proc. 35th North American Power Symposium*, Rolla, MO, pp. 629-635, October 2003.

E. Y. Sun, T.J. Overbye, "Three dimensional visualizations for power system contingency analysis voltage data," P*roc. 6th International Conference on Advances in Power System Control, Operation and Management (APSCOM)*, Hong Kong, November 2003.

F. T.J. Overbye, Y. Sun, R.P. Klump, J.D. Weber, "Interactive 3D visualization of power system information," *Electric Power Components & Systems*, pp. 1205-1215, December 2003.

G. T.J. Overbye, X. Cheng, Y. Sun, "A comparison of the ac and dc power flow models for LMP calculations," *Proc. 37th Hawaii International Conference on System Sciences*, Kona, HI, January 2004.

H. A.P.S. Meliopoulos, G.J. Cokkinides, T.J. Overbye, "Component monitoring and dynamic loading visualization for real time power flow model data," *Proc. 37th Hawaii International Conference on System Sciences,* Kona, HI, January 2004.

I. Y. Sun, T.J. Overbye, "Visualizations for power system contingency analysis data," *IEEE Trans. on Power Systems*, vol. PWRS-19, pp. 1859-1866, November 2004.

J. T.J. Overbye, D.A. Wiegmann, "Reducing the risk of major blackouts through improved power system visualization," *Proc. 2005 Power Systems Computational Conference* (PSCC), Liege, Belgium, August 2005.

K. D.A. Wiegmann, G.R. Essenberg, T.J. Overbye, Y. Sun, "Human factor aspects of power system flow animation," *IEEE Trans. on Power Systems*, vol. PWRS-20, pp. 1233-1240, August 2005.

L. T.J. Overbye, "Power system visualization," *Automation of Electric Power Systems*, vol. 29, no. 16, August 2005.

M. A. P. Sakis Meliopoulos and G. J. Cokkinides, Mike Ingram, Sandra Bell, Sherica Matthews, "Visualization and Animation of State Estimation Performance", *Proceedings of the 38st Annual Hawaii International Conference on System Sciences*, Big Island, Hawaii, January 3-6, 2005.

References

[1] Y. Sun, T.J. Overbye, "Visualizations for power system contingency analysis data," *IEEE Trans. on Power Systems*, vol. PWRS-19, pp. 1859-1866, November 2004.

[2] P.M. Mahadev, R.D. Christie, "Envisioning Power System Data: Concepts and a Prototype System State Representation," *IEEE Trans. Power Syst.*, Vol. 8, No. 3, pp. 1084-1090, Aug. 1993

[3] EPRI, Visualizing Power System Data, EPRI Project RP8010-25, EPRI, Palo Alto, CA, April 1994.

[4] Y. Liu, J. Qiu, "Visualization of Power System Static Security Assessment Based on GIS," in *Proc. Int. Conf. on Power System Technology*, Aug. 1998, Vol. 2, pp. 1266-1270.

[5] A.J. Hauser, "Visualization of Global Power System States in a Compact and Task Oriented Way," in *Proc. 13th Power Systems Computation Conf.*, Trondheim Norway, June 1999, pp. 413-419.

[6] A.J. Hauser, J.F. Verstege, "Seeing Global Power System States with Compact Visualization Techniques," in *Proc. IEEE Power Tech '99*, Budapest, Hungary, Aug. 29 – Sept. 2, 1999, pp. 118-123.

[7] Ming Ni, J.D. McCalley, V. Vittal, S. Greene, Chee-Wooi Ten, V. Sudhakar, T. Tayyib, "Software Implementation of Online Risk-based Security Assessment," *IEEE Trans. Power Syst.*, Vol. 18, No. 3, pp.1165-1172, Aug. 2003

[8] A. Thiyagarajah, B. Carlson, J. Bann, M. Mirheydar, S. Mokhtari, "Seeing Results in a Full Graphics Environment," *IEEE Computer Applications in Power*, Vol. 66, pp. 33-38, July 1993.

[9] R. Bacher, "Graphical Interaction and Visualization for the Analysis and Interpretation of Contingency Analysis Results," in *Proc. IEEE Power Industry Computer Application Conf.*, Salt Lake City, UT, May 1995, pp. 128-134.

[10] C.N. Lu, M. Unum, "Interactive Simulation of Branch Outages with Remedial Action on a Personal Computer for the Study of Security Analysis," *IEEE Trans. Power Syst.*, Vol. 6, No. 3, pp. 1266-1271, Aug. 1991.

[11] S.L. Clark, J. Steventon, and R.D. Masiello, "Full-Graphics Man-Machine Interface for Power System Control Centers," *IEEE Computer Applications in Power*, Vol.1, No. 3, pp.27-32, 1998.

[12] T.J. Overbye, D.A. Wiegmann, R.J. Thomas, "Visualization of Power Systems," PSERC Final Report, Oct. 2002, pp. 22-25.

[13] J.D. Weber, T.J. Overbye, "Voltage Contours for Power System Visualization," *IEEE Trans. Power Syst.*, Vol. 15, No. 1, pp. 404-409, Feb. 2000.

[14] T.J. Overbye, D.R. Hale, T. Leckey, J.D. Weber, "Assessment of Transmission Constraint Costs: Northeast U.S. Case Study," in *Proc. IEEE PES 2000 Winter Meeting*, Singapore, Jan. 2000, Vol. 2, pp. 903-908.

[15] T.J. Overbye, J.D. Weber, M.J. Laufenberg, "Visualization of Flows and Transfer Capability in Electric Networks," in *Proc. 13th Power Systems Computation Conf.*, Trondheim Norway, June 1999, pp. 420-426.

[16] G. M. Nielson, H. Hagen, H. Muller, *Scientific Visualization: Overviews, Methodologies, and Techniques*. Los Alamitos, CA: IEEE computer society press, 1997, pp. 204-205.

[17] Colin Ware, *Information Visualization: Perception for Design.* San Diego: Academic Press, 2000, pp. 188-194.
[18] T.J. Overbye, Y. Sun, R.P. Klump, J.D. Weber, "Interactive 3D Visualization of Power System Information," *Electric Power System Components and Systems*, vol. 31, pp. 1205-1215, December 2003.
[19] G.P. de Azevedo, C.S. de Souza, B. Feijo, "Enhancing the Human-Computer Interface of Power System Applications," *IEEE Trans. Power Syst.*, Vol.11, No. 2, May 1996, pp. 646-653.
[20] D.A. Wiegmann, G.R. Essenberg, T.J. Overbye, Y. Sun, "Human factor aspects of power system flow animation," *IEEE Trans. on Power Systems*, vol. PWRS-20, pp. 1233-1240, August 2005.
[21] P.W. Sauer, "On the formulation of power distribution factors for linear load flow methods," *IEEE Trans. on Power App. And Syst.*, vol. 100, pp. 1001-1005, March 1981.
[22] *Transmission Transfer Capability*, North American Reliability Council (NERC), pp. A-9, May 1995.
[23] F.L. Alvarado, "Visualizing power system security with Matlab," *EPRI Workshop on Visualization Methods for Electric Power Industry Applications*, Palo Alto, CA, Oct., 1993.
[24] T.J. Overbye, et. al., "A simulation tool for analysis of alternative paradigms for the new electricity business," *Proc.30th Hawaii International Conf. on System Sciences*, Maui, HI, pp. v634-v640, Jan. 1997.
[25] K.B. Bennett, "Encoding apparent motion in animated mimic displays," *Human Factors*, vol. 35, pp. 673–691, 1993.
[26] J.D. Hollan, E.L. Hutchins, T.P. McCandless, M. Rosenstein, L. Weitzman, "Graphic interfaces for simulation," *Advances in Man-Machine Systems Research*, vol. 3, pp. 129–163, 1987.
[27] P. McLeod, J. Driver, Z. Dienes, J. Crisp, "Filtering by movement in visual search," *Journal of Experimental Psychology: Human Perception and Performance*, vol. 17, pp. 55–64, 1991.
[28] R.B. Ivry, A. Cohen, "Asymmetry in visual search for targets defined by differences in movement speed," *Journal of Experimental Psychology: Human Perception and Performance*, vol. 18, pp. 1045–1057, 1992.
[29] R. Rosenholtz, "A simple saliency model predicts a number of motion popout phenomena," *Vision Research*, vol. 39, pp. 3157–3163, 1999.
[30] J. Hohnsbein, S. Mateef, "The relation between the velocity of visual motion and the reaction time to motion onset and offset," *Vision Research*, *32*, vol. 32, pp. 1789–1791, 1992.
[31] C. Ware, J. Bonner, W. Knight, R. Cater, "Moving icons as a human interrupt," *International Journal of Human-Computer Interaction*, vol. 4, pp. 341–348, 1992.
[32] T.S. Meese, M.G. Harris, "Independent detectors for expansion and rotation, and for orthogonal components of deformation," *Perception*, vol. 30, pp. 1189–1202, 2001.
[33] T.C.A. Freeman, M.G. Harris, "Human sensitivity to expanding and rotating motion: Effects of complementary masking and directional structure," *Vision Research*, vol. 32, pp. 81–87, 1992.

[34] P.J. Bex, W. Makous, "Radial motion looks faster," *Vision Research*, vol. 37, pp. 3399-3405, 1997.
[35] B.J. Geesaman, N. Qian, "The effect of complex motion pattern on speed perception," *Vision Research*, vol. 38, pp. 1223–1231, 1998.
[36] J. Driver, G.C. Baylis, "Movement and visual attention: The spotlight metaphor breaks down," *Journal of Experimental Psychology: Human Perception and Performance*, vol. 15, pp. 448–456, 1989.
[37] M. Valdes-Sosa, A. Cobo, T. Pinilla, "Transparent motion and object-based attention," *Cognition*, vol. 66, pp. B13–B23, 1998.
[38] W.R. Uttal, L. Spillman, F. Stürzel, A.B. Sekuler, "Motion and shape in common fate," *Vision Research*, vol. 40, pp. 301–310, 2000.
[39] O. Park, S.S. Gittelman, "Dynamic characteristics of mental models and dynamic visual displays," *Instructional Science*, vol. 23, pp. 303–320, 1995.
[40] J. Driver, P. McLeod, Z. Dienes, "Motion coherence and conjunction search: Implications for guided search theory," *Perception and Psychophysics*, vol. 51(1), pp. 79–85, 1992.
[41] D.G. Watson, G.W. Humphreys, "Visual marking of moving objects: A role for top-down feature-based inhibition in selection," *Journal of Experimental Psychology: Human Perception and Performance*, vol. 24, pp. 946–962, 1998.
[42] K.B. Bennett, J.M. Flach, "Graphical displays: Implications for divided attention, focused attention, and problem solving," *Human Factors*, vol. 34, pp. 513–533, 1992.
[43] S. Hart and L. Staveland, "Development of NASA-TLX (Task Load Index): Results of empirical and theoretical research," in *Human Mental Workload*, North Holland B.V. Amsterdam, pp. 139-183, 1988.
[44] F. L. Alvarado, Y. Hu, C. Rinzin, and R. Adapa, "Visualization of Spatially Differentiated Security Margins," Proc. *11th Power Systems Computation Conference (PSCC)*, Avignon, France, August 1993.
[45] P.T. Breen Jr. and W.G. Scott, "Virtual reality applications in T&D engineering," *Proc. Rural Electric Power Conference*, May 1995, pp. B5/1-6.
[46] A.O. Veh, et. al., "Design and Operation of a Virtual Reality Operator-Training System, *IEEE. Trans. on Power Systems*, vol. 11, pp. 1585-1591, August 1996.
[47]E.K. Tam, et. al., "A Low-Cost PC-Oriented Virtual Environment for Operator Training, *IEEE. Trans. on Power Systems*, vol. 13, pp. 829-835, August 1998.
[48] R.P. Klump, D. Schooley, and T.J. Overbye, "An advanced visualization platform for real-time power system operations," *Proc. of the 14th Power Systems Computation Conference* (PSCC), Seville, Spain, June 2002.
[49] R.P. Klump, W. Wu, G. Dooley, "Displaying aggregate data, interrelated quantities, and data trends in electric power systems," *Proc. Hawaii International Conference on System Sciences*, Waikoloa, HI, January 2003.
[50] C. Ware, *Information Visualization* (2nd Ed.), Morgan Kaufmann Publishers, San Francisco, CA, 2004.
[51] C.D. Wickens, D.H. Merwin, and E.L. Lin, "Implications of graphics enhancements for the visualization of scientific data: Dimensional integrality, stereopsis, motion, and mesh," *Human Factors*, vol. 36, pp. 44-61, 1994.
[52] R.L. Gregory, *The Intelligent Eye*, Great Britain: McGraw-Hill, 1970.

[53] C.M. Carswell, S. Frankenberger, and D. Bernhard, "Graphing in depth: Perspectives on the use of three-dimensional graphs to represent lower-dimensional data," *Behaviour and Information Technology,* vol. 10, no. 6, pp. 459-474, 1991.

[54] M. St. John, H.S. Smallman, and M.B. Cowen, "Designing for the task: Sometimes 2D is just plane better," *Proc. IEA 2000/HFES 2000 Congress,* San Diego, CA, pp. 407-410, 2000.

[55] I.D. Haskell and C.D. Wickens, "Two- and three-dimensional displays for aviation: A theoretical and empirical comparison," *International Journal of Aviation Psychology,* vol. 3, pp. 87-109, 1993.

[56] C.D. Wickens and C.M. Carswell, "The proximity compatibility principle: Its psychological foundation and relevance to display design," *Human Factors*, vol. 37, pp. 473-494, 1995.

[57] T.J. Overbye, D.A. Wiegmann, A.M. Rich, and Y. Sun, "Human factors analysis of power system visualizations," *Proc. Hawaii International Conference on System Sciences,* Maui, HI, pp. 647-652, January 2001.

[58] S. Yantis and A.P. Hillstrom, "Stimulus-driven attentional capture: Evidence from equiluminant visual objects," *Journal of Experimental Psychology: Human Perception and Performance,* vol. 20, pp. 95-107, 1994.

[59] A. P. Sakis Meliopoulos and George J. Cokkinides, "Substation Lightning Shielding and Risk Assessment", *European Transactions on Electrical Power (ETEP),* Vol. 13, No. 6, pp. 407-412, November/December 2003.

[60] A. P. Sakis Meliopoulos and George J. Cokkinides, "A Virtual Environment for Protective Relaying Evaluation and Testing", *IEEE Transactions of Power Systems,* Vol. 19, No. 1, pp. 104-111, February, 2004.

[61] A. P. Sakis Meliopoulos, "Operational Tools for Large RTOs: Assessment and Needs", Proceedings of the 2004 IEEE PES Power Systems Confernce & Exposition, New York, NY, October 10-13, 2004.

[62] A. P. Sakis Meliopoulos, Sun Wook Kang, and G. J. Cokkinides, "Animation and Visualization of Spot Prices via Quadratized Power Flow Analysis", *Proceedings of the 36st Annual Hawaii International Conference on System Sciences*, p. 49 (pp. 1-7), Big Island, Hawaii, January 6-9, 2003.

[63] A. P. Sakis Meliopoulos and G. J. Cokkinides, "Visualization and Animation of Instrumentation Channel Effects on DFR Data Accuaracy", Proceedings of the 2002 Georgia Tech Fault and Disturbance Analysis Conference, Atlanta, Georgia, April 29-30, 2002